Title
Design, fabrication, and dynamic gait control for a novel buoyancy assisted bipedal robot

Author
Ghassemi, Sepehr

Publication Date
2023

Peer reviewed|Thesis/dissertation

UNIVERSITY OF CALIFORNIA

Los Angeles

Design, fabrication, and dynamic gait control for a novel buoyancy assisted bipedal robot

A dissertation submitted in partial satisfaction

of the requirements for the degree

Doctor of Philosophy in Mechanical Engineering

by

Sepehr Ghassemi

2023

ABSTRACT OF THE DISSERTATION

Invention, design, fabrication, testing, and motion analysis of a novel bipedal humanoid robot

by

Sepehr Ghassemi

Doctor of Philosophy in Mechanical Engineering

University of California, Los Angeles, 2023

Professor Dennis W. Hong, Chair

The advancement of the humanoid robotics field shows significant potential and progress, however humanoids still have many limitations. This is due to the complexities, cost, danger, and the functional limitations associated with the current state of this technology.

This dissertation presents a new type of humanoid bipedal robot. It includes the invention, detailed design, software modeling, fabrication, testing, control, and motion analysis done on the robotic platform BALLU. Buoyancy Assisted Lightweight Legged Unit, or BALLU, is a safe, low cost, simple bipedal robot that uses a helium filled upper body, along with two thin carbon fiber legs. Due to the new architecture and buoyancy force, this robotic platform never falls down and is intrinsically stable. The main prototype version discussed is comparable in size to an adult human, and uses cable driven actuated knee joints for locomotion. The actuation components and the majority of the robot's weight are located on the feet. Even though each leg has only one active

degree of freedom, BALLU can walk forwards and backwards, jump, turn, climb and descend stairs, and go over obstacles and rough terrain. Understanding its non-intuitive dynamics, along with correct actuation and timing and control of the knee joints is the key factor for these types of locomotion.

Although BALLU's leg architecture is inspired and is reminiscent of traditional humanoids and human legs, this novel approach to humanoid design behaves drastically differently and is not modeled using traditional robotic locomotion methods. This dissertation includes the foundational understanding and categorization of this platform's behavior. The platform's physics, control, and locomotion strategies are specifically analyzed and explained in detail. This robotic platform is not intended to replace traditional humanoid robots, rather to introduce new possibilities and present an ultra-safe, low-cost, light-weight alternative tuned for specific applications. The main contribution of this thesis is organization and classification of behavior understanding, and proposing novel unique methods of movement and locomotion for a buoyancy assisted biped robot

The dissertation of Sepehr Ghassemi is approved.

Jonathan Hopkins

Jacob Rosen

Vijay Gupta

Dennis W. Hong, Committee Chair

University of California, Los Angeles

2023

to family stars trees

TABLE OF CONTENTS

LIST OF FIGURES

LIST OF TABLES

ACKNOWLEDGEMENTS

I would like to thank and express my gratitude to everyone and everything that has supported the advancement of science, thinking, and human evolution. Specifically those who have directly and positively impacted my PhD journey.

I would like to thank my advisor, Dr. Dennis Hong for giving me the opportunity to pursue creative research. I would like to thank him for presenting a model to observe and learn from, and specifically appreciate his honesty in discussions regarding science, tech, philosophy, and life. I would like to express my gratitude to my current and past committee members, Dr. Hopkins, Dr. Rosen, Dr. Gupta, Dr. Tsao, and Professor Allen for their valuable guidance, experience, and knowledge. Their insight and wisdom has impacted my progress significantly.

I would like to express my intangible gratitude to my family. Additionally I'd like to thank my great friends, colleagues, staff, media and the rest of the people whom I have interacted with and worked with along this journey.

Lastly, I note and remind myself about my inability to put in-formation and into words my appreciation of the gargantuan blessing that is the experience of life in this wild beautiful universe. About the love of the known, unknown, and the unknown unknowns, and of the ecstasy of unwrapping the present.

CURRICULUM VITAE

2011 - 2014	B.S. in Mechanical Engineering and in Industrial Design, at Virginia Tech
2014 - 2017	M.S. in Mechanical Engineering, at UCLA
2014 - Present	Ph.D. in Mechanical Engineering, at UCLA

SELECT PUBLICATIONS

Ghassemi, Sepehr, and Dennis Hong. "Dynamic Locomotion Strategies for a Bipedal Buoyancy Assisted Humanoid Robot. " *2023 IEEE-ICRA International Conference on Robotics and Automation (ICRA)*. IEEE, 2023. *Submission in progress*

Ghassemi, Sepehr, and Dennis Hong. "Modeling and analysis of a Single Leg Single Actuator Buoyancy Assisted Humanoid Robot with Walking and Hopping Capabilities. " *2023 SCR Southern California Robotics Symposium (SCR)*. 2023.

Ghassemi, Sepehr, and Dennis Hong. "Feasibility study of a novel robotic system BALLU: Buoyancy assisted lightweight legged unit." *2016 IEEE-RAS 16th International Conference on Humanoid Robots (Humanoids)*. IEEE, 2016.

Ghassemi, Sepehr, and Dennis Hong. "Investigation of a novel continuously rotating knee mechanism for legged robots." In *2018 15th International Conference on Ubiquitous Robots (UR)*, pp. 130-135. IEEE, 2018.

Ghassemi, Sepehr, Jeffrey Yu, Joshua Hooks, and Dennis Hong. "Feasibility study of a novel biped NABiRoS: Non anthropomorphic bipedal robotic system." In *2016 IEEE-RAS 16th International Conference on Humanoid Robots (Humanoids)*, pp. 145-145. IEEE, 2016.

Lin, Xuan, Gabriel Fernandez, Sepehr Ghassemi, and Dennis W. Hong. "Feasibility Study of an Aerial Lifting Device Using Aerodynamic Drag for Ascent." In *International Design Engineering Technical Conferences and Computers and Information in Engineering Conference*, vol. 59247, p. V05BT07A016. American Society of Mechanical Engineers, 2019.

Yu, Jeffrey, Joshua Hooks, Sepehr Ghassemi, and Dennis Hong. "Exploration of turning strategies for an unconventional non-anthropomorphic bipedal robot." In *International Design Engineering Technical Conferences and Computers and Information in Engineering Conference*, vol. 58189, p. V05BT08A021. American Society of Mechanical Engineers, 2017.

Yu, Jeffrey, Joshua Hooks, Sepehr Ghassemi, Alexandra Pogue, and Dennis Hong. "Investigation of a non-anthropomorphic bipedal robot with stability, agility, and simplicity." In *2016 13th International Conference on Ubiquitous Robots and Ambient Intelligence (URAI)*, pp. 11-15. IEEE, 2016.

SELECT PATENTS

GHASSEMI, Sepehr. HONG, Dennis. "Systems and Methods for Implementing Humanoid Balloon Robots." U.S. Patent Application 15/777,515, filed December 27, 2018.

GHASSEMI, Sepehr. HONG, Dennis. "Continuous Robotic Knee Joint System" WO, WO2017201184A1, Patent Application PCT/US2017/033140, filed NOVEMBER 23, 2017.

GHASSEMI, Sepehr. HONG, Dennis. "Systems and Methods for Using Atmospheric Resistance to Accelerate a Payload and Ascend, Jump, or Dampen Descents and Falls" Provisional filed.

CHAPTER 1

Introduction

1.1 Motivation

Ideas paired with action change the world. Ideas are thoughts. Software is a string of thought capable of causing action. Robots allow us to use software in the physical domain. Limbs and tools such as robots, are our way to edit this reality and reorganize it as we desire. To take our observations, and put them in formation.

It's been a long-standing desire of humanity to replicate human capability and build functional, practical humanoid robots. Current bipedal robots often have stability limitations. A high center of mass, combined with multiple degrees of freedom, makes bipedal walking and balancing among the most complex and difficult tasks in robotics. Present solutions depend on intricate dynamic systems that utilize detailed control algorithms and precise sensors. One radical approach to this problem would be to design a system that negates the downward pull of gravity. While this is currently impossible, the presence of atmospheric pressure means using a gas that's lighter than air to create an upward pull may be a possible solution. The buoyancy force from a lightweight gas such as helium, could theoretically assist a robot by opposing the gravitational force acting on its structure. However, contemporary robots are too heavy making this approach impractical for the current architecture of bipedal robots. Buoyancy force depends on gas volume and density. The amount of this force is relatively small. For example, a conventional helium party balloon can only lift a mass of 5 to 10 grams. A very large volume of helium would be needed to help assist a heavy humanoid robot in balancing. A practical buoyancy assisted robot must be extremely lightweight to really benefit from the effects of this force. It's worth noting that the robot's posture is desired

to be maintained balanced and upright by buoyancy. Parts such as the feet may be heavier as they remain grounded while the body is uprighted and in a balanced state.

Figure 1.1: Inspirations. Images shown have inspired and contributed to improvements in BALLU.

Buoyancy Assisted Lightweight Legged Unit (BALLU) is a robot that utilizes buoyancy to remain upright. Its body is constructed from helium balloons and its legs are made of thin, rigid, lightweight carbon fiber tubes. The robot's feet are the heavier component and house the actuators, batteries, and circuitry. While the robot isn't lighter than air, it cannot fall and its intrinsic stability ensures the robot's balanced upright equilibrium state.. This feature renders this robot especially safe for human interaction. Moreover, with only two actuated degrees of freedom (one in each knee joint), the robot is capable of performing a multitude of motions such walking, hopping, and

turning. The robot can even navigate and go over obstacles, climb stair, and walk on rough terrain, and in some cases even walk on a slackline and on water.

Figure 1.2: A visual render of the BALLU concept. A safe bipedal robot interacting with humans.

1.2 Background

1.2.1 Humanoid Robot Research Progress

The desire to recreate life and expand human capability has been with us since the start of time. Throughout history, humans have constantly further enabled themselves through tool making. They have entangled their minds with possibility, and pursued those dreams to bring them into fruition and physical reality. One of these desires and seductive visions has been creating artificial humans and human organs. A mechanical manifestation of this vision could be referred to as a humanoid robot. As early as 250 BC, a humanoid “automaton” was described by philosopher Lie Yukou [change numbers later 1]. In 50 AD a concept of “automata” machine was introduced by a Greek mathematician to automate some tasks [2]. Of the most famous examples is Leonardo da Vinci’s humanoid design commonly referred to as Leonardo’s robot. A cable driven geared

humanoid robot designed within a metal suit of armor [3]. Another robot he envisioned was an entertainment purpose full sized humanoid drummer (Fig. 1.3 a). This pursuit has continued and Isac Asimove writes about three laws of robotics in his books in 1941 [4].

The dream continued but the practicality of this technology remained far fetched till recent times. The most popular examples are the humanoid WABOT project (first full size humanoid to walk) at Waseda university [5], and Marc Raibert's Leg Lab at MIT [6,7] which paved the way for modern robot legged locomotion and was the precursor to his company Boston Dynamics the maker of the famous highly dynamic humanoids PETMAN and ATLAS [8,9]. Development of humanoids only accelerated since. Some notable robots (up to 2012) include Honda ASIMO [10], Nao[11], DARwIn-OP[12], Robonaut[13], Hubo[14],and CHARLI[15].

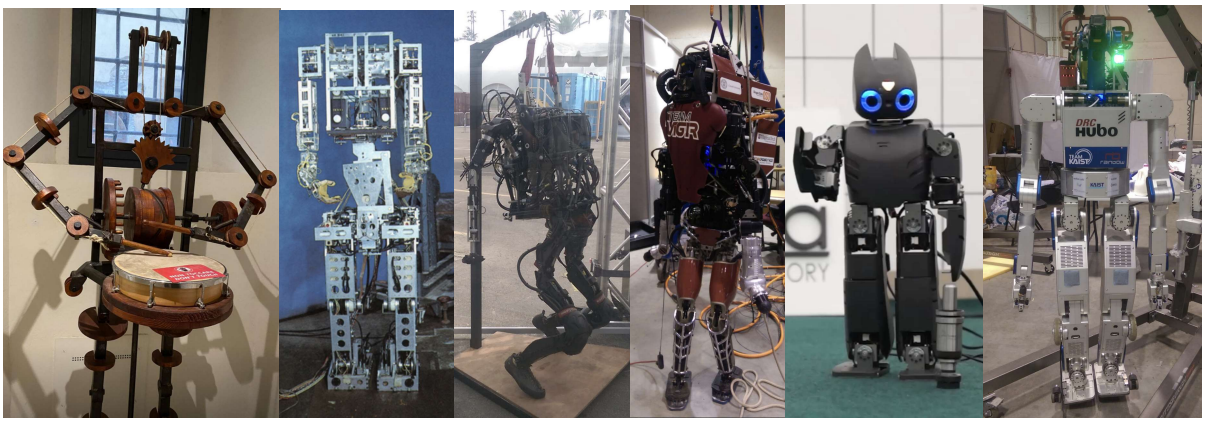

Figure 1.3: Humanoid robots in history. Left to right. (all photos by Ghassemi except b.)

a. Drummer prototype at Da Vinci museum, Florence Italy.

b. WABOT robot. From (https://www.humanoid.waseda.ac.jp/booklet/kato_2.html)

c. PETMAN robot by boston dynamics at DRC, California USA.

d. ATLAS robot by boston dynamics at DRC, California USA.

e. DARWIn-OP at RoMeLa at UCLA.

f. Hubo robot by KAIST at DRC, California USA.

A major catalyst for the advancement of the humanoid robotics field was the DRC (DARPA Robotics Challenge) held in 2015. Teams from across the world competed and as a result, many shortcomings, and many capabilities of humanoids became apparent[16,17,18]. This led to major improvements in the field in the years 2015-2020.

The concept of BALLU didn't originate as an independent project; it evolved from research in traditional humanoid robotics. In 2013, Ghassemi worked at RoMeLa (Robotics and Mechanisms Laboratory) on building testbeds and support platforms for the humanoid robot THOR (Tactical Hazardous Operations Robot). These tools and environments were developed in preparation for the DRC (Darpa Robotics Challenge) trials. THOR is a humanoid robot that employs linear series elastic actuators and full-body momentum control [19]. Despite the technology being promising, the robot was intricate and heavy. Consequently, even the gantries and support systems had to be sophisticated. In the subsequent year, Ghassemi continued his work on humanoid robots, specifically THOR and a similar platform SAFFIR (Shipboard Autonomous Fire Fighting Robot)[20], assisting the team by fabricating components, designing subsystems, writing code, and conducting experiments.

The components were intricate, and testing necessitated extensive planning. Owing to these constraints, a simpler humanoid was deployed at the DRC final competition. THOR-OP utilized an older position-controlled actuator architecture and prioritized reliability over dynamic capability. By the conclusion of the DRC, it was evident that while humanoids hold promise, they also possess significant limitations and shortcomings. They are highly complex systems that demand the flawless operation of each subsystem for proper functionality.

A few months later, a simplified version of the robot was employed to compete in, and subsequently win first place at, the RoboCup humanoid soccer competition. Even though the tasks

performed were not as complex as those at the DRC, simplicity demonstrated its strength in ensuring reliability and functionality.

Figure 1.4: Robots THOR and THOR-OP at RoMeLa (2014).

1.2.2 Non-Anthropomorphic Humanoids

Drawing insights from the DRC and RoboCup competitions; with the goal of simplicity and practicality, Ghassemi, along with the team at RoMeLa, designed and constructed a new two-legged robot. NABi (Non-Anthropomorphic Biped). A humanoid with a unique twist: its two legs were still similar in form to a humanoid, yet the hip configuration was aligned in the sagittal plane, deviating from the typical human form [21,22]. This simplified the mechanics, making Nabi much simpler to control. Testing performed on multiple prototypes showed improved operation reliability and practicality.

Figure 1.5: Nabi. a. Left is the robot's configuration compared to a traditional humanoid configuration. The sagittal place is shown for clarity. b. Right is the fabricated prototype of NABi.

Some versions of Nabi used entirely new subsystems, which opened the door for completely new possibilities. Examples include a continuously rotating knee mechanism[24] that can navigate obstacles and stairs elegantly. And new momentum based turning strategies [23].

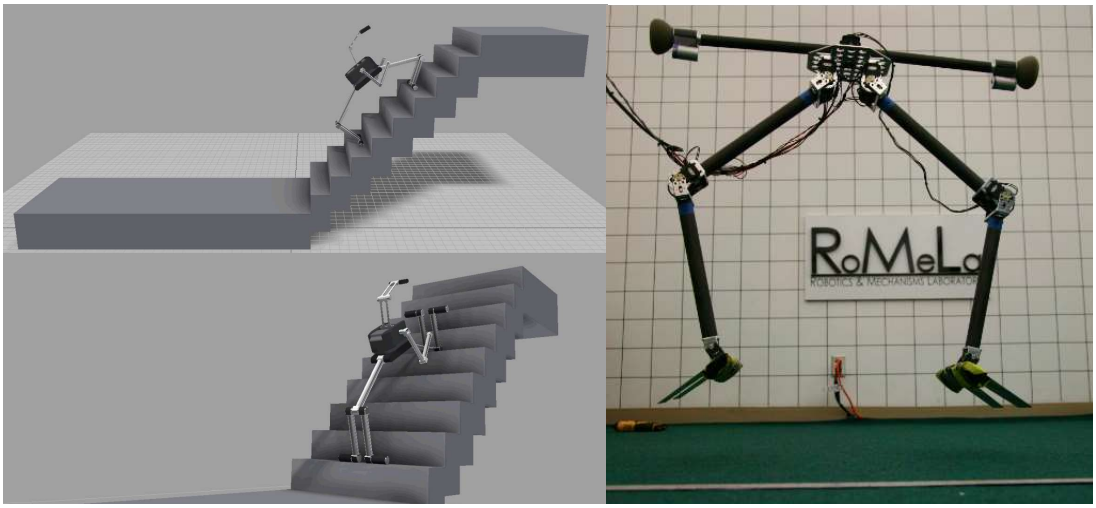

Figure 1.6: Novel approaches. a. Left is a simulation of a robot ascending stairs using a rotating knee. b. Right is a prototype of NABi performing a mid air turning action by controlling a rotating arm.

The fruition of suh approaches, paved the way towards the ideation and conception of BALLU.

1.2.3 Buoyancy Assisted Robots

Robots are tools designed to extend and expand human capabilities. To enhance their utilization, we must overcome limitations and explore possibilities. For instance, imagine a world where robots couldn't fall. Or one where we could reverse the direction of gravity. Although it might seem impractical at first, consider a simple helium balloon: it doesn't fall. It rises. But what is the cause of this behavior? When generally dealing with gravity, we assume everything falls down and is pulled to earth with the acceleration g. But in reality, the force is a function dependent on the mass of objects, and in space, the direction is variable based on these mass differences. Observed gravity is a result of object densities and their placement in space. Without knowing the details of gravitational waves and inter atomic communications, and by simply knowing that objects with more mass and density attract each other more. We can logically conclude the opposite as well. That, if left to go to equilibrium, denser heavier bodies come toward each other effectively pushing away the less dense object occupying that space. Helium is only rising because we have a heavier atmosphere made of air. Wood falls down on earth but rises in water. It is important to clarify how buoyancy and gravity are not different, rather the different classifications of one phenomena.

Buoyancy assisted robots are not common. First, using gasses such as helium can only generate a small amount of force, and secondly, bringing in fluid mechanics of atmospheric ambient conditions may introduce more issues for mechanical robotic systems. BALLU’s inspiration started by pondering the use of the upward buoyancy force from a gas lighter than air to aid a robot in maintaining its balance. Given the weight of actuators and robotic components, this seemed unattainable. That was until we envisioned a new configuration. A unique design to reorganize the

architecture: what if the robot's body posture remains upright due to buoyancy, while the feet, containing the majority of the mass, are drawn to the ground? The entire robot wouldn't be lighter than air, and the joint coils could be actuated using a cable-driven system, with the actuators situated in the feet. Thus investigation started, and so did the error intensive task of fabricating a working new robotic hardware system.

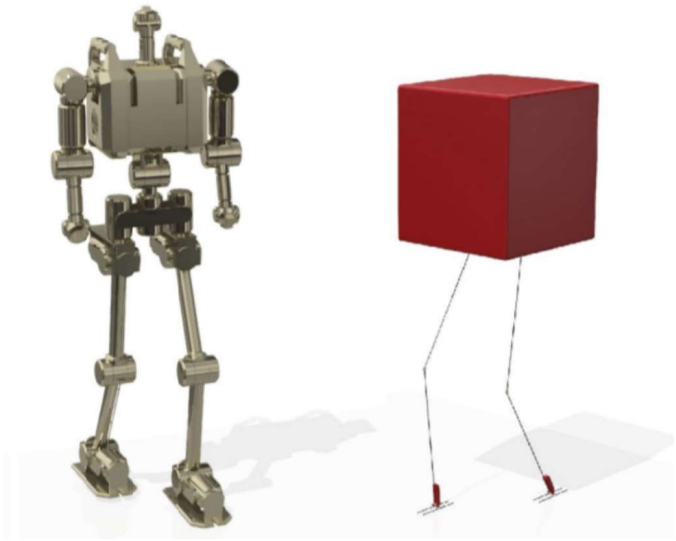

Figure 1.7: BALLU (right) compared to the traditional humanoid system (left).

Assuming this system would balance, would fabrication, actuation, and locomotion even be possible? Answers and more questions are discussed in the next chapters with their order explained in the organization section 1.3. These questions became the sparks and challenges that initiated the investigation of details of such a system we know so little about. From this curiosity and vision, BALLU (Buoyancy Assisted Lightweight Legged Unit) was conceived; an intrinsically stable lightweight humanoid that simply cannot fall.

1.3 Organization

This dissertation encompasses BALLU's conception, design, fabrication, modeling, testing, and the identification of its overall system behavior. **Chapter 1** delves into the genesis of the idea, discussing how and why it came to formation. **Chapter 2** details the design and fabrication of prototypes. **Chapter 3** presents a comprehensive model of the system, discussing its various components in depth. And **Chapter 4** introduces the diverse potential configurations of this robotic platform in an orderly method.

In **Chapter 5**, we deeply explore the physics and dynamic behavior of this non-intuitive system. This chapter examines all the forces in play, their dynamic behaviors, and the consequent effects. Building on the foundation laid in Chapter 5, **Chapter 6** delves into a comprehensive analysis of potential motions including jumping, turning, and walking for both single and double-legged robot architectures. We investigate the impacts of alterations in various variables on these motions, and present new findings in system behavior. The robot's motion is observed through various physics models, simulations, and hands-on experiments. It is digested, simplified and categorized into a system best fit for understanding, using, and discussing this new type of humanoid robotic platform.

At last, **Chapter 7** summarizes our findings and provides insights into our current progress. We discuss BALLU's potential and limitations and consider various possible modifications. We present BALLU’s impact and spinoff technologies. Finally, this chapter sets the stage for the next evolution of this endeavor, suggesting avenues for future research and development.

CHAPTER 2

Design

2.1 Design Origin

Initial calculations and simulations confirmed that constructing such a system is theoretically feasible. However, the size and design constraints determine the final structure of the robot. Our ambition was to develop a bipedal robot similar in size to a human. Given this size requirement, the buoyancy force we could implement was significantly limited. To illustrate, a cube with each side measuring 0.5 meters and filled with helium can lift a mass of only 136 grams under standard conditions. A minimalist design approach would entail a body composed of a helium balloon, complemented by two basic legs. Considering the weight of the balloon itself, we would be left with only a few grams to allocate for the rest of the robot. This is not an easy task. The joints and links cannot be flimsy or weak or the robot will not be properly controlled and become prone to every possible disturbance. Given that the balloon's primary role is to keep the robot upright and the robot is not lighter than air, the logical strategy is to house all actuation, energy storage, and communication systems within the feet, keeping the legs. This is done by selecting lightweight components that can be interfaced together in the most simple way. Even small screws would be a design consideration when dealing with grams. Designing rigid yet lightweight actuated links and joints became a unique challenge. Their design, material selection, fabrication, and assembly is further discussed in the next sections.

2.2 Robot Components

2.2.1 General Components

The legs were designed to mirror the size and structure of a typical humanoid. This design choice was made since the robot is intended to operate in human-made environments designed for humans. Examples include standard dimensions stairs and steps Moreover, this humanoid resemblance endows the robot with an anthropomorphic geometry, which is advantageous for human-robot interactions and collaborations. Each leg is composed of two main links (femur and tibia) and three main joints (hip, knee, foot). Additionally, the legs have a tendon driven actuation system and elastic knee element. The last component besides the balloon would be a simple link connecting the two legs together through the hip joints and also with the balloon.

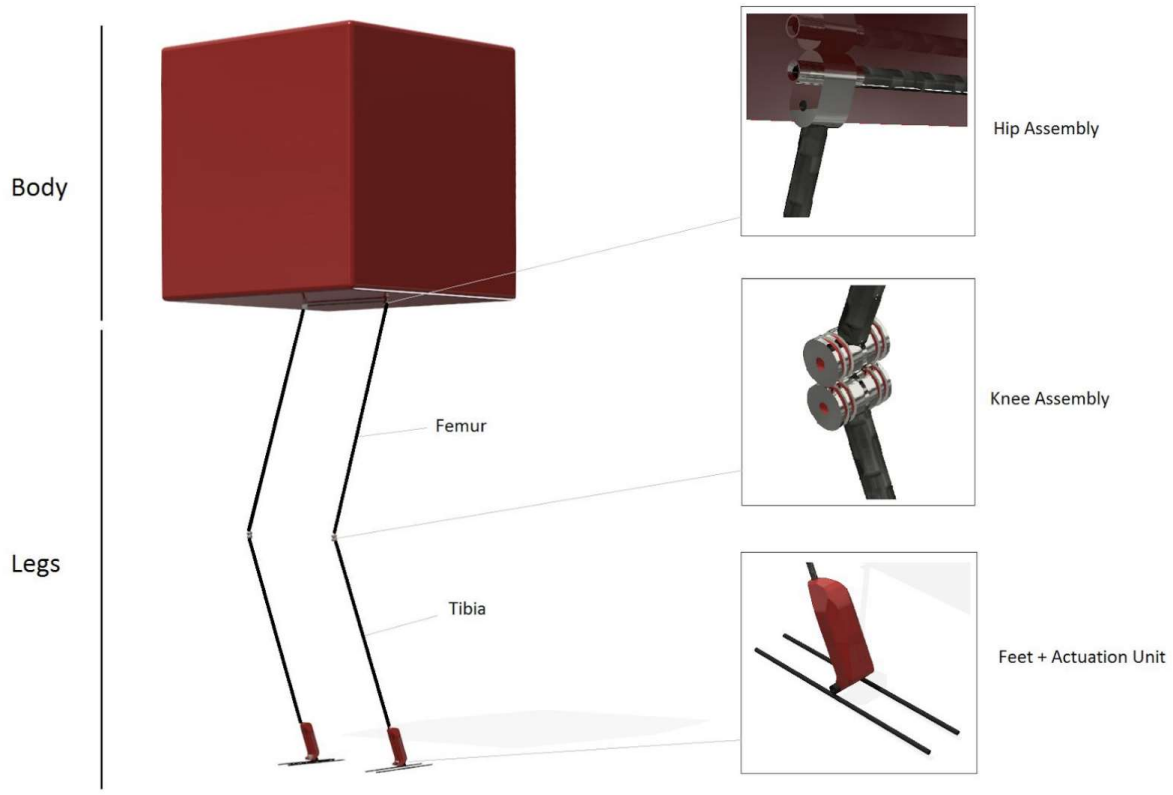

Figure 2.1: BALLU general components

The legs links need to be stiff enough not to deform under operation, and lightweight enough to be lifted by the body. Plastic, aluminum, and carbon fiber tubes were tested. The cable driven actuation system discussed in the future sections puts a high loading in the links and high stiffness against buckling and bending was required. The optimum material selection was thin carbon fiber tubes. Link lengths are 50 cm in length with the tube outer and inner diameters of 3.2 and 1.6mm respectively.

2.2.2 Balloons and Body

The body or buoyant component of the robot is made of helium filled balloons. Thin Mylar balloons were used as the optimum material. Mylar balloons hold helium longer than rubber balloons (~4 days vs. ~1 day). Three smaller cylindrical off the shelves Mylar balloons were connected and used together as the body of the robot. Later prototypes may use balloons of different shapes and sizes.

The balloons , when filled with helium, can lift a mass of 5-20 grams each based on size. On average, the balloons used in our testing lift a mass of 10-20 grams each when filled with helium. Due to pressure variability and gas leaks, this force is measured every time when performing tests. To correct for variations in this force, a small magnet is attached to the hip; to which we can add or remove small washers and keep the balloon lift force at our desirable constant. This tuning is only done for slight weight adjustments, since even though it doesn't directly affect lift, it affects inertial forces. The body, made of multiple balloons, is taped to a small carbon fiber tube (same diameter used in all links) and attached to the legs using the ABS hip joints. The joint is attached to the femur link by a simple press fit connection.

2.2.3 Dimensions

Overall, our bipedal prototype is 185 cm tall when upright with a maximum width of 50 cm. The legs are 1m tall when upright with a hip offset of 18cm. Figure 2.2 shows these dimensions. Detailed dimension tables are provided in the parameters section.

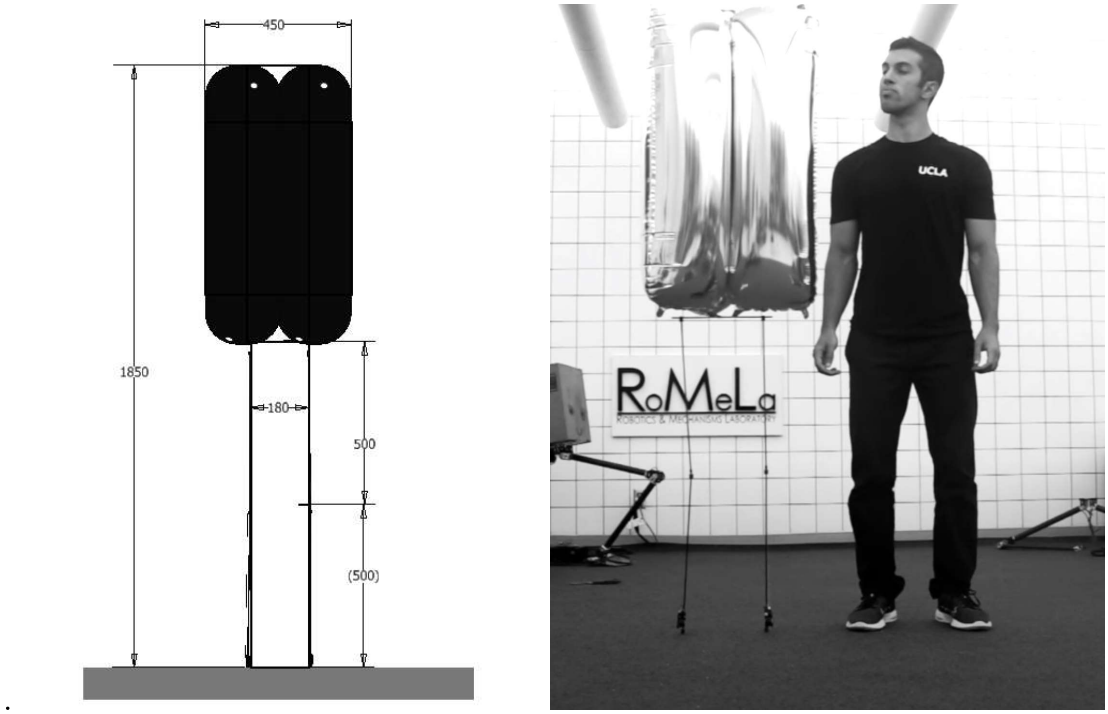

Figure 2.2: a.BALLU bipedal dimensions (mm). b. Prototype standing next to a 175cm tall human.

2.2.4 Joint Fabrication

Robot joints are often made of metals such as aluminum, although due to the weight requirements of BALLU, plastic joints are used. The initial testing used ABS living hinges as the joints, however the joints could easily twist in unwanted directions given small unwanted force and torque inputs . Making them thicker would fix the issue, yet it would increase the mass and render them ineffective. Thus custom designed plastic joints were machined from ABS and PEEK (PolyEther Ether Ketone).

Each foot used a small machined casing (made from ABS, Acrylonitrile Butadiene Styrene plastic) to house a battery, a motor, and the circuit. Initially, the feet used small parts for ground placement and friction increase. Although they were later changed to a point contact design to allow new motion behavior. For the foot casing, a later prototype replaced the case and used machined brackets similar to ones found in the hips. The hip and ankle use a simple passive rotary joint made of ABS plastic. A small bracket connects the links through a press fit connection. The small precision machined joint components keep the movements limited to the desired rotation axis. Due to the lightweight nature. Any inaccuracy in fabrication, will magnify the possibility of system hardware malfunction and imperfections.

Figure 2.3: Fabricated parts compared to computer models.

2.2.5 Knee Joint Design

The knee joint is actuated and more complex. The main holding structure is machined from PEEK, which makes them stiff and lightweight. Additionally, PEEK has bearing quality properties which allow two brackets to easily slide on eachother. That said, they do not slide or contact each other. They have grooves filled with high grade woven fishing line. This string is knotted around the knee in an infinity pattern (better shown in figure) to allow for multiple uses.

One; hold the brackets together. Two; prevent knee unwanted twist. Three; prevent sliding. And fourth; to allow the joint to roll on them without any sliding. This minimal, simple, yet highly functional configuration has proven extremely durable. A single knee has been used on the robot through thousands of testing and demo sessions from 2016 to 2023. The robot has been kicked, tested, taken to the pool, and even thrown off buildings for testing purposes. This mechanism is inspired by the human anatomical knee. Living hinges did not constrain the motion properly, metal joints were too heavy, and a single axis rotary joint made of plastic could easily wear out and have high friction due to components rubbing against each other. Instead, the final design uses a double jointed rolling mechanism constrained by tendon and ligament like strings. This also allows for 360 degree knee range of motion. It also does not require the fabrication of an axis or hinge. Even though the knee is actuated, there is no motor connected to the knee brackets. The motor in the feet pulls a tendon-like string which causes the knee to close. Additionally, an elastic element in front of the knee is used to let the knee extend again after contraction. Details on the behavior and force exertion of tendon and spring are discussed in the forces section.

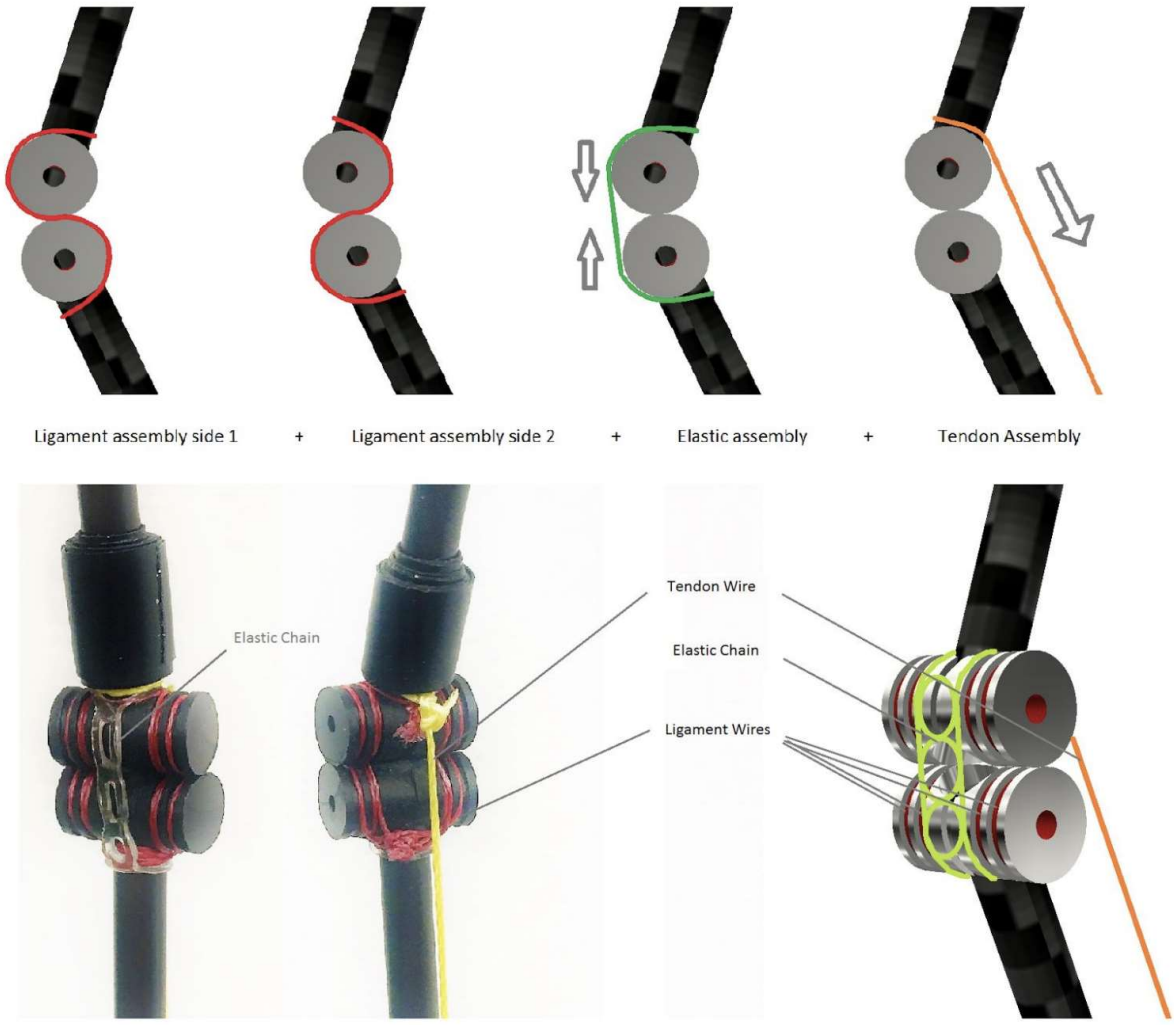

Figure 2.4: BALLU knee joint assembly.

As shown in the figure, the ligament wires wrap around the bracket to allow the two brackets to roll on each other providing the needed motion, and keeping the knee together (Red). The elastic (Green) pulls the knee back after actuation by the tendon wire (Orange). Setup levels (Top), CAD assembly (Lower Right), and assembled prototype (Lower Left) are shown.

2.2.6 Tendon and Ligament Material Selection

To make this minimal knee mechanism effective, material selection was done meticulously. The elastic component is made of orthodontics power chains which provide constant elasticity over long durations. Their elastic force can be adjusted based on the length of material used in the knee. The ligament mimicking strings is made of 50lb grade braided high strength fishing lines. O-rings were tested initially, yet failed after repeated testing. Kevlar wires were strong and reliable yet introduced manufacturing difficulties due to their porous structure. Steel and tungsten cables were also neglected due to their weight. The braided fishing line did not fail and showed minimal to no elongation in use over time. A 100lb grade braided fishing line is used for the tendon that connects the knee to the motor shaft. Note that normal fishing wire is elastic while braided fishing lines are not elastic. The tendon wire is directly attached to a small lever connected to the motor on the foot. Note that an initial design used small pulleys to allow the tendon to travel through the inside of the tibia as opposed to a simpler design having the tendon simply go from the outside, yet proved too complex and inefficient.The various components are assembled together using press fit joints, knots, and minimal adhesives.

2.2.7 Electronic Components

Each package includes one 30 RPM 3.7V electric dc motor with a 100/1 gear box, an aluminum machined lever attaching the output shaft to the tendon (1cm long), the controlling circuit and IR receiver, along with rechargeable lithium ion batteries. The electronic chip on the feet is harvested from RC toy helicopters and is extremely lightweight. The circuit is then connected to the electric motor gearbox assembly. The overall foot assembly, along with the knee and one full leg, only weighs 35 grams (included in spec tables). For communication, the initial prototypes

used the same controller from the toys for wireless IR communication with the robot, the next prototype had a three step setup. Where first, code was run on MATLAB (where majority of our code runs) and transferred by the computer to an arduino uno. The arduino controlled the voltage output to a basic circuit with control LEDs and potentiometers. Third, the circuit was directly wire connected to the same manual IR controller, hacking it to be used with the same IRsignals, but controlled by code instead of manual.

CHAPTER 3

Configurations

3.1 Balloon Link System

As discussed in the fabrication and materials section, the legs are simple carbon fiber tubes with plastic minimally designed joints and a tendon driven actuation architecture. Using this system, various different robot configurations are possible, the main configurations explored are single and double leg robots with a human-style knee system. Other configurations such as inverted knees, more links, and fully rotating joints are possible and will be explored as future work.

3.2 1 Leg Robot

This configuration includes the balloon alongside one leg.

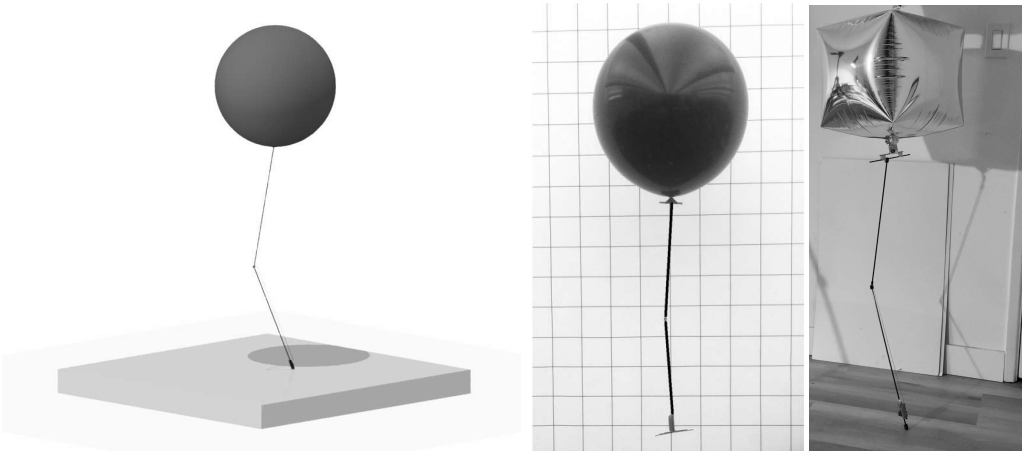

Figure 3.1: BALLU single leg configuration. a. CAD model (left) b. Fabricated prototype 1 (right)

With a single DOF, this version can hop and take steps. Further analyzed in motion planning.

3.3 2 Leg Robot

Similar to the single leg, but with two legs and with a hip offset.

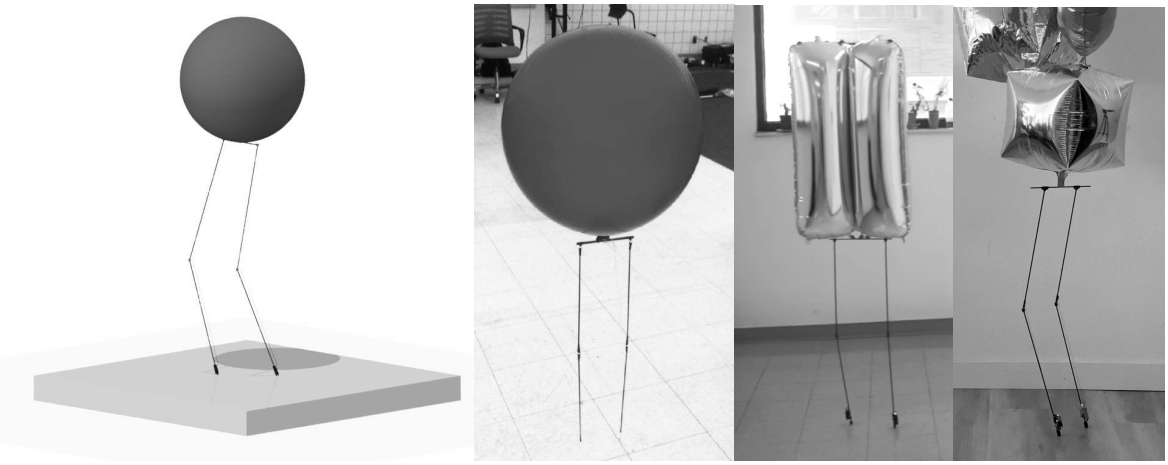

Figure 3.2: BALLU double leg configuration (left to right). a. CAD model. b. Fabricated prototype 1. c. Fabricated prototype 2. d. fabricated prototype 3.

The change in balloon shape from 2 to 3 is only due to balloon availability and not functionality. Not that even though it's not visible, model 3 has software control, and better joints and connections. This two leg version uses two actuated DOF (1 per leg) to move, hop, dance, walk and turn. All further analyzed in motion planning.

3.4 Multi Leg Robot

Multiple units may be attached and controlled in tandem to create a larger multi link robot.

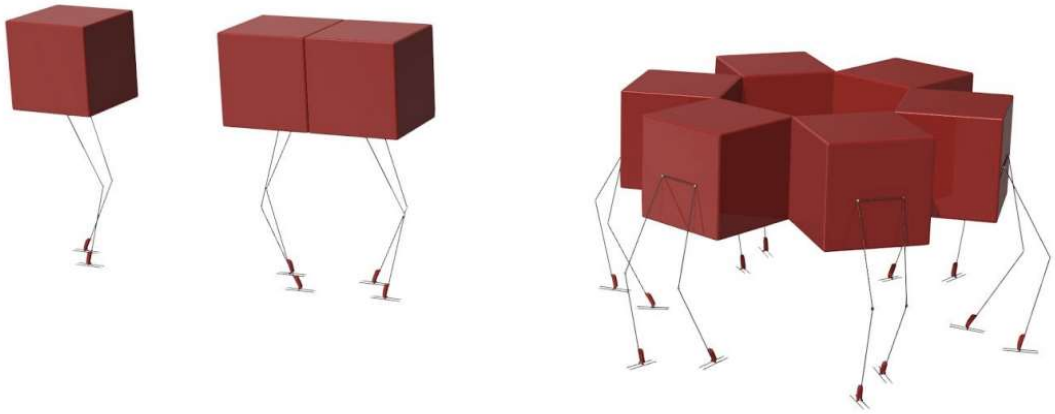

Figure 3.3: BALLU platform potential and modularity.

3.5 Robot Specifications

3.5.1 Parameters

Tables below summarizes the initial variables associated with the 1 and 2 leg robotic systems.

Table 3.1: Robot geometric parameters

variable	***value***	***units***	***comment***
scale	*1*	-	*Scale multiplier variable*
numleg	*1*	-	*number of legs for 1 leg robot*
numleg2	*2*	-	*number of legs for 2 leg robot*
pi	*3.14159*	-	*Pi constant*

Table 3.2: Robot dimension parameters

variable	***value***	***units***	***comment***
Brad	*.25*scale*	*m*	*spherical balloon radius*
Brad2	*.5*scale*	*m*	*larger balloon radius*
Bvol	*4/3*pi*Brad^3*	*m^3*	*spherical balloon volume*
Bvol2	*4/3*pi*Brad2^3*	*m^3*	*larger balloon volume*
femur	*.5*scale*	*m*	*femur length*
tibia	*.5*scale*	*m*	*tibia length*
Frad	*.03*scale*	*m*	*spherical foot radius*
Fconrad	*.005*scale*	*m*	*circular foot contact*

Table 3.3: Robot environment parameters

variable	***value***	***units***	***comment***
Envgas	*air*	*-*	*environment gas type*
densityair	*1.292*	*kg/m^3*	*at 25 deg density of air*
Bgas	*helium*	*-*	*balloon gas type*
densityhelium	*0.164*	*kg/m^3*	*at 25 deg density of helium*
g	*9.81*	*m/ss*	*gravity*
gravity	*[0 0 -g]*	*m/ss*	*gravity 3d*
Z0	*0*	*m*	*ground z position*

Table 3.4: Robot friction parameters

variable	***value***	***units***	***comment***
hfric	*0*	*-*	*hip joint friction*
kfric	*0*	*-*	*knee joint friction*
mius	*1*	*-*	*foot-ground coefficient rubber-concrete static*
miuk	*.8*	*-*	*foot-ground coefficient rubber-concrete dynamic*

Other parameters are discussed in their respective sections.

3.5.2 Range of Motion and Workspace

The table shows the range of motion for the leg units for both single and double leg systems.

Table 3.5: Robot link range of motion parameters

Joint angle	***min***	***max***
Hip theta	*0*	*pi*
Knee theta	*-pi*	*0*
Actuator linkage	*0*	*pi*

The schematics show this range along with potential link workpace. Legs have similar ranges.

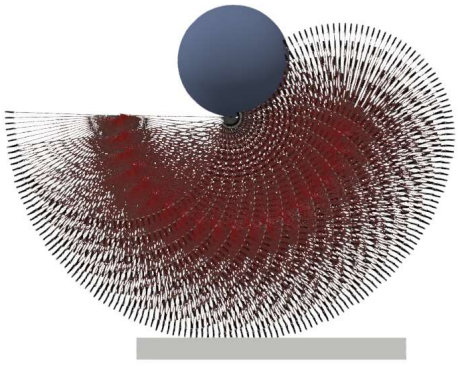

Figure 3.4: Leg possible motion range considering fixed balloon and in 2D side view.

Even though figure 3.4 shows the possible states of one leg swinging, it does not include an exact representation of possible foot placements. Factoring that in,

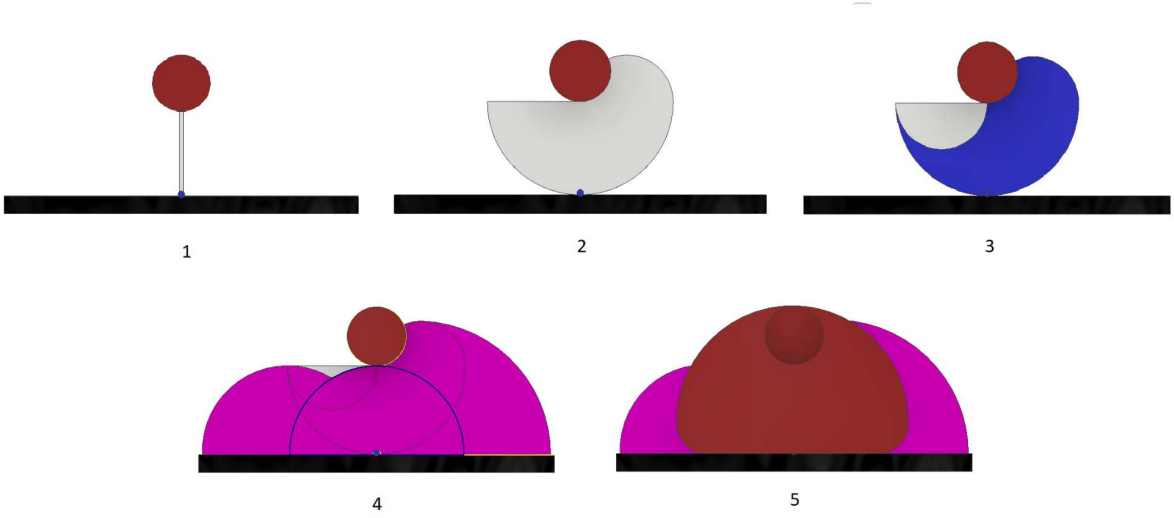

Figure 3.5: 1. BALLU biped side view range of motion cases.

The figure Shows the side view of a bipedal BALLU. 2. Is the possible range of motion of one leg considering stationary support leg and balloon. 3. Considering the angle limits, blue is that leg's foot range of motion in that plane. 4. Shows the case where now the balloon may move too but the support legs foot stays at one point pivoting. While the support leg may move in the half circle shown by the black curve, the swinging foot can reach any point in the pink area. 5. Shows case 4 with the balloons possible motion drawn as well. These cases include maximum possible range and are only limited to that single plane of view, the 3d case is a volume and within normal operating conditions, these limits may never be reached due to force and motion requirements associated.

3.6 Forces

Forces acting on the system are calculated and shown in this chart. These forces are discussed in detail in the following subsections.

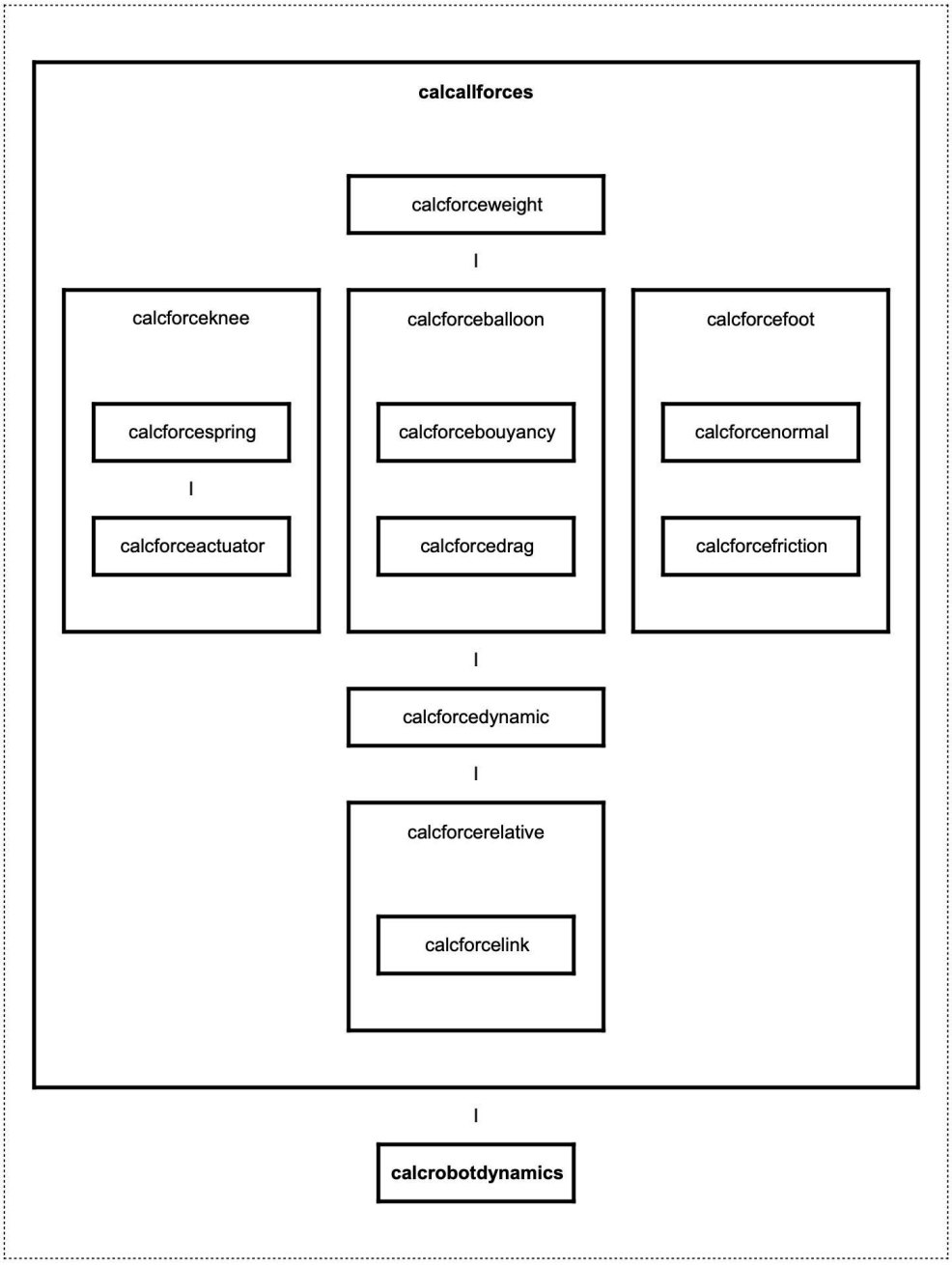

Figure 3.6: Flowchart of all force calculations required to model the system.

3.6.1 Weight

The weight forces are calculated using the simple equation:

$$F = ma \tag{3.1}$$

$$W = m\,g \tag{3.2}$$

where the acceleration is g due to gravity of [0 0 -9.81] and the masses include the balloon mass (Bm), helium mass (hemass), robot foot assembly mass (footm), and total robot mass (robot1m).the helium mass is factored into the buoyancy equation. Given the hip and knee joints have very small masses, their weight

calculations are omitted. This results in three main weight forces. W1, or total balloon mass is Bm with center of mass at the cob (center of buoyancy). Note that for momentum calculations we also factor in the air mass of the balloon. W2 is the foot mass centered on the feet, and lastly W4 is total mass with center at com (robot center of mass).

3.6.2 Buoyancy

The buoyancy forces are calculated using the equation:

$$Fbo = Bvol\ g\ (densityair\text{-}densityhelium) \tag{3.3}$$

$$Fbouyancy = [0\ 0\ Fbo] \tag{3.4}$$

The buoyancy force acts upward in the z direction. Where Bvol is the volume of the gas in the balloon. Acceleration is g due to gravity of [0 0 -9.81]. We use the density difference between balloon gas (Helium) and atmospheric gas (Air).

3.6.3 Drag

The air resistance drag force acting on the balloon is calculated using the equation:

$$Fdrag = (.5)*densityair*v^2*Cd*A \quad (3.5)$$

The velocity of the balloon is calculated based on its motion and dynamics and varies with position, behavior and time. Cd is 0.5, the drag coefficient of the sphere (spherical balloon). A is the cross sectional area of sphere (balloon) calculated by the equation:

$$A = (3.1415)*Brad^2 \quad (3.6)$$

where Brad is 0.25 m, the spherical balloon radius The cross sectional area stay constant regardless of the direction of motion given the spherical shape of the balloon. The direction of the drag force acts opposite to the direction of balloon velocity passing through the cob (center of buoyancy). Given the legs are made of very thin links, the air resistance force exerted on the legs is omitted. In these calculations, we do not take into consideration the drag caused by non translational rotations on the balloon and the effects of air friction itself.

3.6.4 Normal

The normal force exerted on the foot upward is calculated using the equation:

$$f=ma \quad (3.7)$$

$$Fn = robot1m * foot\ acceleration \quad (3.8)$$

$$Fnormal = [0\ 0\ Fn] \tag{3.9}$$

The normal force is 0 when the foot is not in contact with ground and is directly opposite to the sum of the downward forces exerted by the foot on the ground. This includes the force due to robots weight and any dynamic downward forces.

3.6.5 Ground Friction

The friction force is exerted on the foot contact point between feet and ground and is calculated by the equation:

$$Ffriction = miu*Fnormal \tag{3.10}$$

where Fnormal is the normal force acting on the feet by ground, and miu is the coefficient of friction. miu equals mius (static coefficient of friction) when static, and it equals miuk(kinetic coefficient of friction) when the foor has a velocity and is sliding. The values for coefficient of friction are used based on rubber feet and concrete ground and are; mius = 1 (foot-ground coeffcient rubber-concrete static), and miuk = .8 (foot-ground coeffcient rubber-concrete dynamic). Some experiments are done on carpet or ceramic ground, however it is observed for the foot to have minimal to no sliding given the rubber coating. In the simulation, we have three cases considered; accurate friction value, no friction , and max friction with no sliding.

3.6.6 Joint Friction

The rotary joint frictions on the hip and knee joint do not play significant roles. The hip joint has a very smooth rotary contact that is designed to have minimal friction. While the knee joint is

rolling and dominated by spring and tendon forces. These joints also have very small radii and roll contact which further minimizes friction force and torque effects.

3.6.7 Momentum

The momentum or described dynamic force is the force resulting from the momentum of an object and the change in velocity given a specific timeframe. It is calculated using the equation below.

$$f=ma \tag{3.11}$$

$$f = m\ dv/dt \tag{3.12}$$

$$f = m\ (v\text{-}v0)/dt \tag{3.13}$$

For our system, the equation becomes

$$Fdynamic(tc,:,i) = masses(i,:)*(velocities(tc,:,i)-velocities(tp,:,i))/dt \tag{3.14}$$

$$Tdynamic(tc,:,i) = sumI(i,:)*(avelocities(tc,:,i)-avelocities(tp,:,i))/dt \tag{3.15}$$

where i represents the joint number (hip i =1, knee i =2, foot, i=3, cor i = 4). Tc is timecount and dt is the time difference. The variable tp is simply the time of tc -dt. For the center of rotation the equation becomes

$$Fdynamic(tc,:,4) = masses(i,:)*(corv(tc,:,1)-corv(tp,:,1))/dt \tag{3.16}$$

$$Tdynamic(tc,:,4) = sumIc(3,:)*(acorv(tc,:,i)-acorv(tp,:,i))/dt \tag{3.17}$$

Note that even though the masses are constant, for calculations of moments of inertia, we need to first find the joint distances for every joint. This force is specially important in a dynamic system involving impact, collisions and significance of momentum control effect of the leg swings.

3.6.8 Actuation

The actuator torque and torque exerted on the knee joint by the actuators are fully discussed in section 5.1.1. In short, this torque is calculated as follows when the tendon is engaged.

$$Ftt(act,tc) = acttor(act,tc)*Mll*sin(actpos(act,tc)) \quad (3.18)$$

$$ktoract(act,tc) = Ftt(act,tc)*(sin(-1*thetak(tc))/Tll) \quad (3.19)$$

3.6.9 Elasticity

The spring and elastic forces and set up are further discussed in other chapters. The forces are calculated as follows.

$$Fs(act,tc) = k*Sdis; \% spring\ force \quad (3.20)$$

$$kjreq = 2*Jrad; \% knee\ joint\ equivalent\ radius \quad (3.21)$$

$$ktorspring(act,tc) = Fs*kjreq \% torque\ on\ knee\ by\ spring \quad (3.22)$$

Where Fs is the spring force as a function of knee angle, Jrad is simplified rotary knee joint equivalent radius, and ktorspring is the torque input from spring on knee at the given instant and state.

3.6.10 Complex Knee Torque

The knee input torque is a combination of the actuator and elastic element input torques.

$$kitortotal(act,tc) = ktorspring(act,tc) + ktoract(act,tc) \quad (3.23)$$

Note this is simply the input torque, the total torque acting on the knee is different as is impacted by many other dynamic and input forces. The plot below compares the input actuation force, angle dependent spring force, and possible total knee force input.

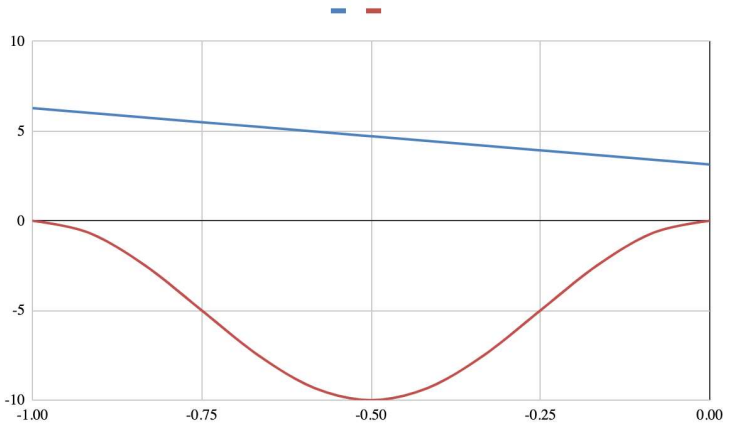

Figure 3.7: Forces of the spring and actuator are compared to knee angle. x axis is knee joint angle from fully closed to straight and the y axis is relative torque generation.

As observed, the behavior of the knee is based on input, though highly dependable on posture. The input torque creates a force on the hip and foot joints with a magnitude of

$$kiforknee\ (tc,:,j) = kitortotal(act,tc)/linklength \quad (3.24)$$

The direction of this force is orthogonal to the link in the plane of the knee joint rotation. This is our main input variable into the robot to control the system. But using it at various timing and postures creates a vast array of possibilities.

3.7 Mass Properties

3.7.1 Masses

Mass variables are summarized in the table below.

Table 3.6: Masses

variable	***value***	***units***	***comment***
Bm	*.01*scale^3*	*kg*	*Balloon mass*
femurm	*.0004*	*kg*	*Femur mass*
tibiam	*.0004*	*kg*	*Tibia mass*
hipm	*.0001*	*kg*	*Hip mass*
kneem	*.0001*	*kg*	*Knee mass*
footm	*0.03*	*kg*	*Foot mass*
Hem	*Bvol*densityhelium*	*kg*	*helium mass*
Hipmeffectiv	*Bm+Hem+hipm*	*kg*	*effective hip balloon mass*
robot1m	*Bm+footm+Hem*	*kg*	*robot1 mass*
robot2m	*Bm+2*footm+Hem*	*kg*	*robot2 mass*

3.7.2 Moments of Inertia

Moments of inertia are needed for all torque and rotation calculations. The moments of inertia for each point is calculated by the equation:

$$I=m\ r^2 \qquad (3.25)$$

Where I is inertia, m is mass, and r is the distance between the rotation axis and revolving mass. The moment of inertia about each point is calculated as the sum of inertia by all masses revolving.

calculation details are found in calcinertia script. The specific calculations are presented below.

$$Inertia(j,jj) = masses(jj,1)*jd(jj,j)^2 \quad (3.26)$$

Where j is the rotation axis joint, and jj is the joint revolving around that axis. Jd is joint distances. We use the same method to calculate the inertia around center of mass points (further discussed in the next section)

$$Inertiac(j,jj) = masses(jj,1)*jdc(jj,j)^2 \quad (3.27)$$

Inertia with respect to com cor cob. Note thatJd is the joint distances, and jdc is distances to the calculated center of buoyancy, mass, and rotation points.

$$sumI(j,:) = (Inertia(j,1)+Inertia(j,2)+Inertia(j,3)) \quad (3.28)$$

$$sumIc(j,:) = (Inertiac(j,1)+Inertiac(j,2)+Inertiac(j,3)) \quad (3.29)$$

As shown in the equations above, to find the total inertia around each axis at every instance, sums of the inertia of all point masses are calculated . Note that we treat our masses as point mass along their respective centers of mass for calculation simplification.

Joint distances are separately calculated at each instance. Note that even though the links are constant, the rotations and motion cause the rest of the distances to vary.

$$deltpos(tc,:) = positions(tc,:,j) - positions(tc,:,jj) \quad (3.30)$$

$$jd = sqrt(deltpos(tc,1)^2 + deltpos(tc,2)^2 + deltpos(tc,3)^2) \quad (3.31)$$

Deltpos measures the difference in position of two points and jd uses the x,y,z coordinates of this difference to calculate the distance magnitude. For center of mass, buoyancy, and rotation points, their positions are used instead of joint positions.

3.7.3 Center of Buoyancy

For the case of Ballu, the COM (center of mass) alone is not sufficient. This is due to the environmental effect and presence of buoyancy forces. To properly perform calculations, we also measure the center of buoyancy and use that to apply the buoyant forces facing upward. Given we have a spherical balloon in the model, the center of buoyancy is simply the center of the sphere.

$$cob(tc,:) = balloonpos(tc,:,1) \quad (3.32)$$

Where we find balloon position using the dh and transform matrices associated with its line and use that to find COB(center of buoyancy). This method is applied for both single and double leg versions of the robot (for the bipedal version, the hip center position is different from the two hip joint positions and that is factored into the calculations).

3.7.4 Center of Mass

In legged animals and traditional robots, center of mass and component centers of mass is one of the most important calculation metrics. COM is calculated using the mass ratio with disregard to

buoyancy and helium mass. Note that there are two main calculated points of masses on the robot. The top balloon section and the feet section. It is important to factor in the helium gas mass as well, however, the calculations will be wrong if we use that and not the environment mass effects. This makes COM confusing and impractical for this system if used alone. For a single leg robot, the COM is calculated using the equations below.

$$rotrat1 = Bm/(Bm+footm) \tag{3.33}$$

Where this ratio is the balloon mass over total robot1 mass (masses(4,1))....fix

$$footmpos = real(positions(tc,:,3)) \tag{3.34}$$

Foot position or the foot mass assembly position is set at joint 3.

$$cdd(tc,:) = cob(tc,:) - footmpos \tag{3.35}$$

Cdd is the distance between the top mass center (which happens to be COB) and the foot position. To avoid calculation issues, we set cdd as 0 if the distance is closer than +- .001 m.]

$$com(tc,:) = footmpos + cdd(tc,:) * rotrat1 \tag{3.36}$$

Thus, we calculate COM based on the mass ratios of the two points. The ratio remains constant although the position changes based on posture and especially knee angle changes which alter the distance of the foot and hip joint. This is best seen in the schematic presented in the COR section. We could alternatively use the moments of inertia and use moment to find this point, although the methods only differ in calculation path and are effectively identical.

Note that the above equations only apply to the single leg version. For the double leg, we have three main points of mass interacting in. For the bipedal version we calculate COM as presented below. Since the two feet masses are identical, we can first find their midpoint.

$$feetdelta = positionfoot1 - positionfoot2 \quad (3.37)$$

$$feetmidpoint = positionfoot2 + feetdelta/2 \quad (3.38)$$

This is calculated by knowing the position of both feet. Next, the rest of the steps are similar to 1 leg case with the difference of using feet midpoint and a new mass ratio factoring both feet masses.

$$rotrat12leg = Bm/(Bm+2*footm) \quad (3.39)$$

$$cob(tc,:) = balloonpos(tc,:,1) \quad (3.40)$$

$$cdd(tc,:) = cob(tc,:) - feetmidpoint \quad (3.41)$$

$$com(tc,:) = feetmidpoint + cdd(tc,:) * rotrat12leg \quad (3.42)$$

By calculating COB and COM we can now start to observe why none are sufficient alone. To have a proper singular point of reference, we define a new point called COR (center of rotation).

3.7.5 Center of Rotation

As discussed in the previous sections, our calculated COM does not take buoyancy into account. And by calculating COB and COM separately, we have two separate points of reference that do

not properly address the behavior of the system and its motion and rotation about a singular point of reference. Thus, we use a method often used in ship engineering. We define a new point called COR(center of rotation) . This new reference point is the rotation caused by the various forces acting on COB and COM about a new point. The next schematic shows the presence of COB and COM along with some basic forces for a simple 1 leg robot in a given state.

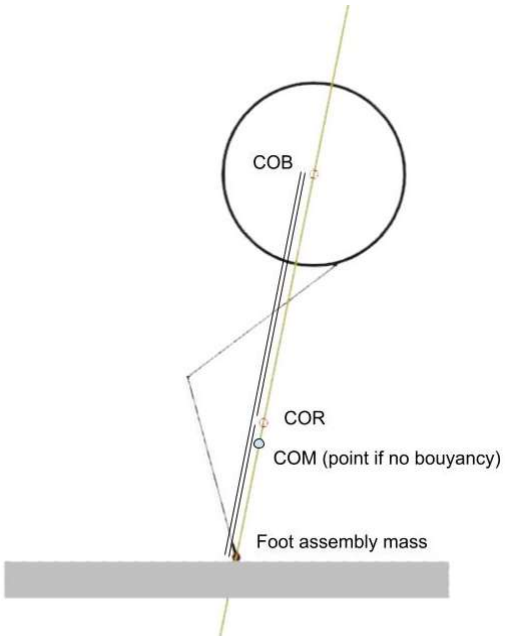

Figure 3.8: Points are labeled on an arbitrary axis. The parallel lines signify distance ratios.

The opposing force of buoyancy and foot weight between the buoyant top component and heavier bottom component not only creates a net force, but also a net rotation. The point at which this rotation happens is defined as COR. This is our main reference point regarding the motion of Ballu models.

The schematic shows the parallel and orthogonal forces about a hypothetical line between COB and COM. The orthogonal components cause a moment acting on a point associated with the mass ratio of these two components. The net force shifts the whole body. Note that this point is not identical to COM, since it does factor all the masses including moving gas mass. Note that

we could not do this from the start due to environmental impact. But with this method, we have taken into account all the air resistance and buoyancy force and have a clear observation of all interacting forces independent of environment. That is unless the feet directly contact the ground, at which point the friction and normal forces change the behavior and not COR. This is because COR is also at a constant ratio between the COB and foot position (1 leg) or feetmidpoint (2 leg). Calculations of COR are done using the following equations for the single leg model.

$$hipmeffectiv = Bm+Hem+hipm \tag{3.43}$$

$$rotrat2 = hipmeffectiv/(hipmeffectiv+footm) \tag{3.44}$$

$$cor(tc,:) = footmpos + cdd(tc,:) * rotrat2 \tag{3.45}$$

The repeating variables are identical as the ones used to measure COM for the single leg model. Calculations of COR are done using the following equations for the double leg model.

$$rotrat22leg = (hipmeffectiv+hipm)/(hipmeffectiv+hipm+2*footm) \tag{3.46}$$

$$cor(tc,:) = feetmidpoint + cdd(tc,:) * rotrat22leg \tag{3.47}$$

Hipmeffectiv stays constant and the repeating variables are identical as the ones used to measure COM for the double leg model. This last schematic shows a geometric representation of some of the discussed points, dimensions, and calculations.

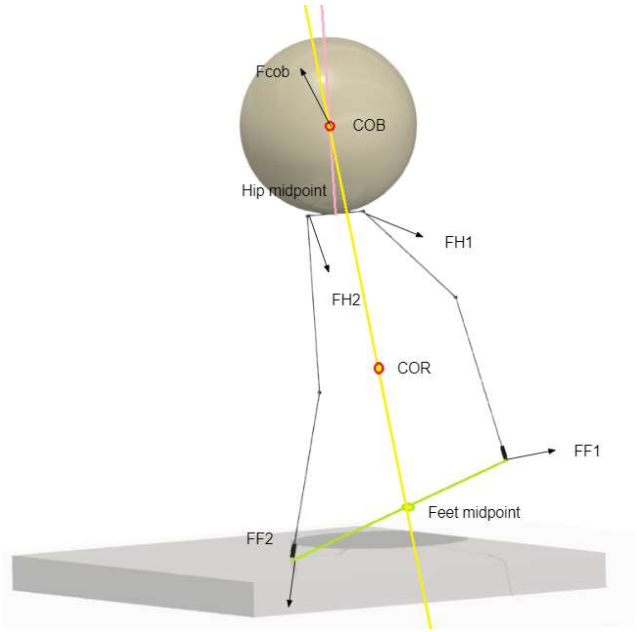

Figure 3.9: Schematic of 3d robot with discussed points labeled

A 3d version is shown for biped. Midpoints and balance lines are labeled. The unknown total forces acting on points of interest are also labeled. Due to the hip offset, new torques and forces will act on the system.

3.8 FBD

With the identification and analysis of all these forces and reference points, a FBD (free body diagram) is best to show the location and geometry of the acting forces and their location.

This table acts as a legend for the free body diagrams:

Table 3.7: Acting forces

Forces on cob	**Forces on hip**	**Forces on knee**	**Forces on foot**	**Forces on cor**
Fb (buoyancy)	Tdh (torque momentum)	Tdk (torque momentum	Fn (normal)	AFrobot Acting Total
Fwb (weight)	Minimal weight	Minimal weight	Fwf (weight)	ATrobot Acting total
Fdb (momentum)	Minimal Fd momentum	Minimal Fd momentum	Ff (friction)	
Fr (air resistance)		Tki (knee input)	Fdf (momentum)	
ATo (acting other)	ATo (acting other)	Ftl (link)	Ftl (link)	
AFo (acting other)	AFo (acting other)	Tkis (spring component)	AFo (acting other)	
		Tkia (actuator component)		

AF and AT are acting force and toques and not input forces.

$$Tki = Tkis+Tkia \tag{3.48}$$

The schematics below show the approximate forces acting on each joint and point of interest. The exact values are calculated for every instance along with every acting force on all the other joints and points.

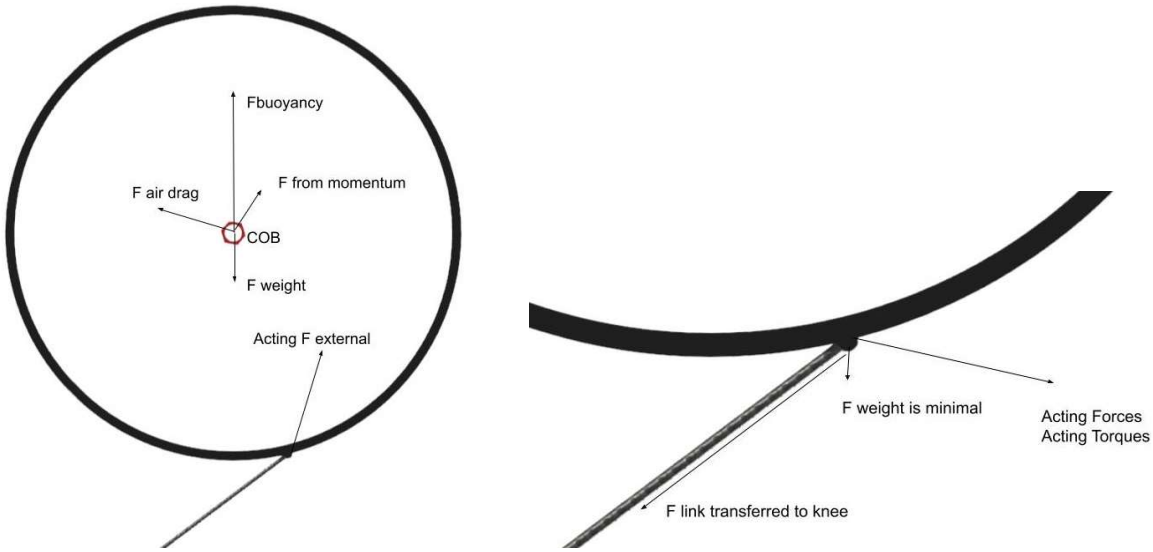

Figure 3.10: Schematic of balloon and hip with some forces shown.

3.8.1 Balloon Link System

Starting from a simpler system, FBD of a single link mass and buoyant balloon system is shown in the next figure in two positions in and off contact.

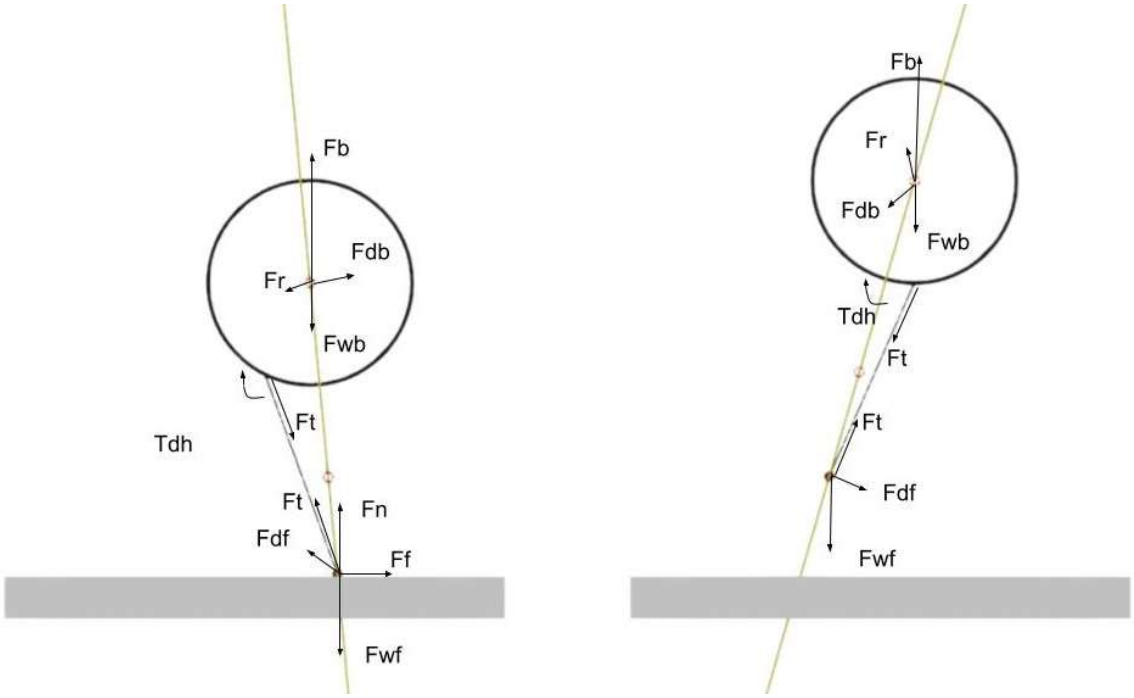

Figure 3.11: Schematic of balloon link system with forces shown.

3.8.2 1 Leg Robot

For the single leg model, the FBD is presented for no ground contact, and ground contact cases.

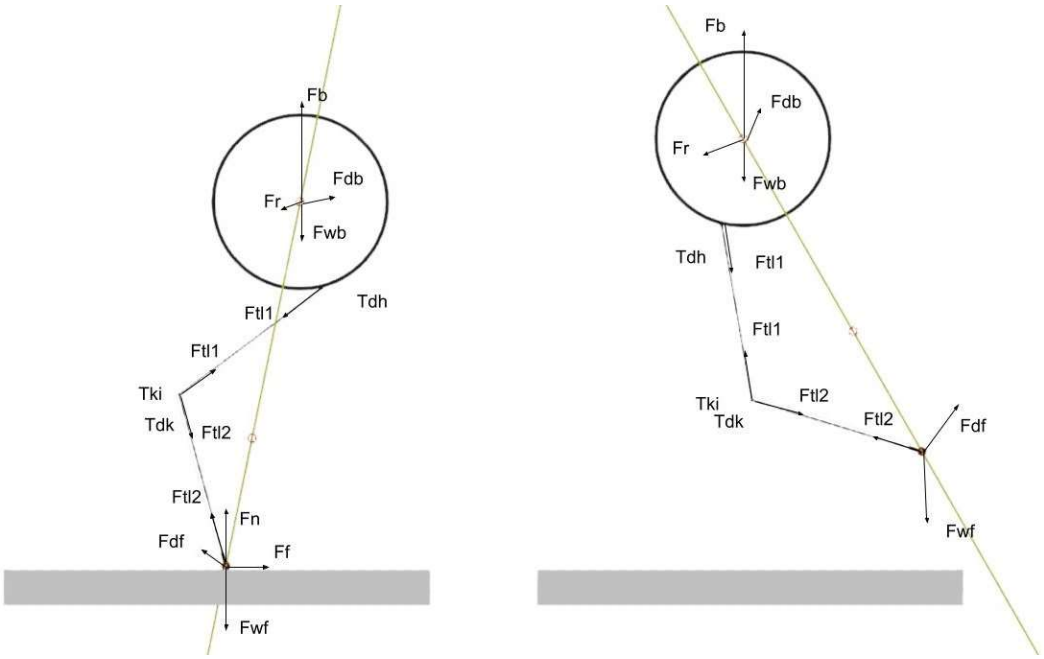

Figure 3.12: Schematic of robot with forces shown.

The simulation and code used their own force calculations and generated FBD plots.

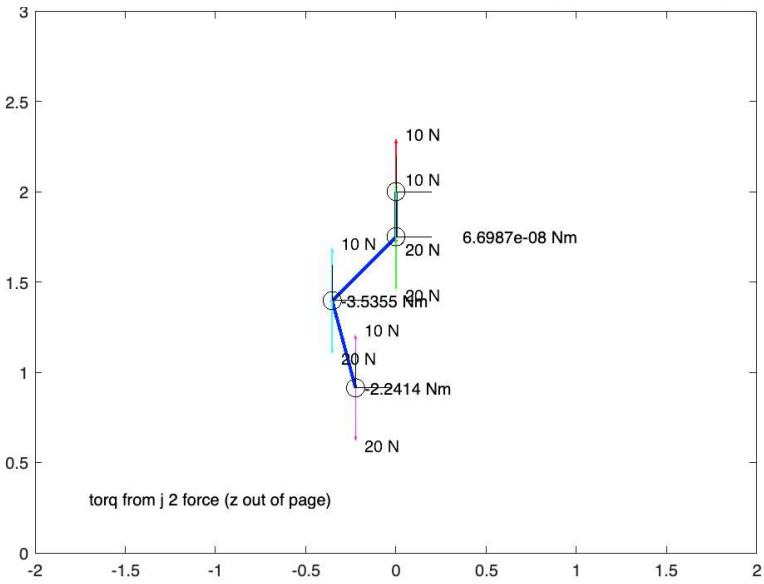

Figure 3.13: MATLAB plot of robot with some forces labeled in 2D space (x and y in meters).

For an extremely simplified sequence of explaining the robots configuration and setup, the figures below are presented.

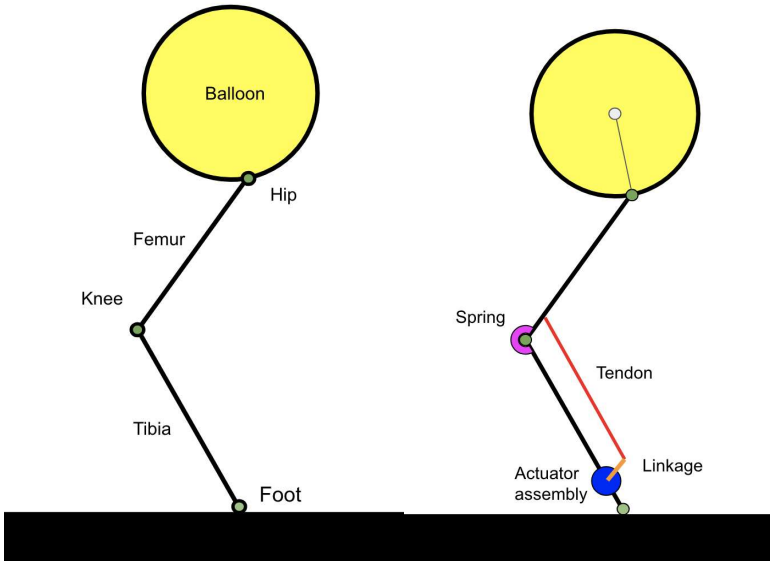

Figure 3.14: Simplified robot configuration.

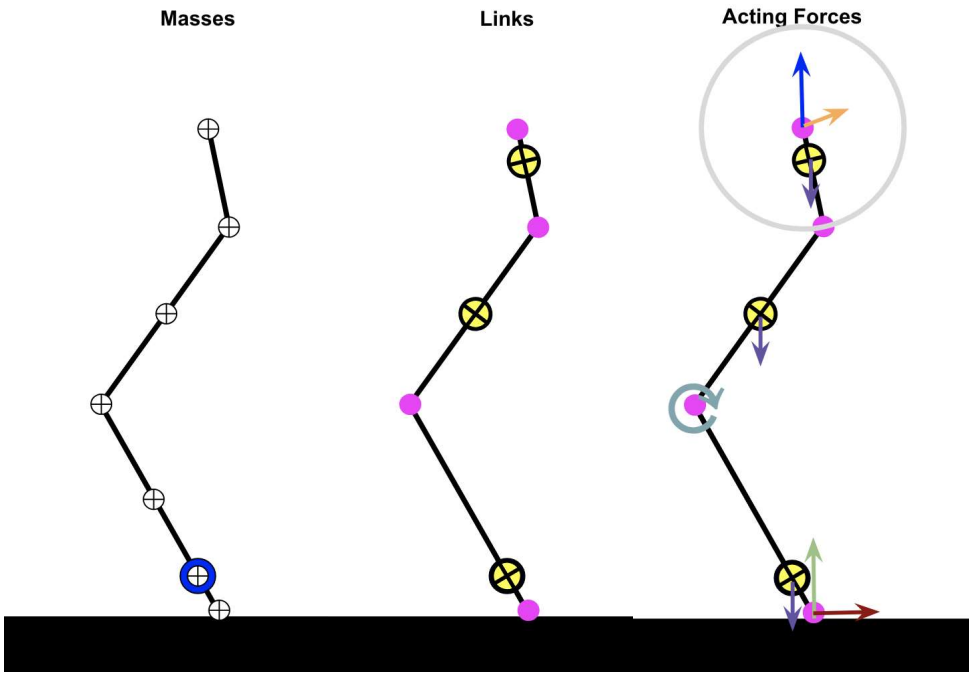

Figure 3.15: Simplified link and force configuration.

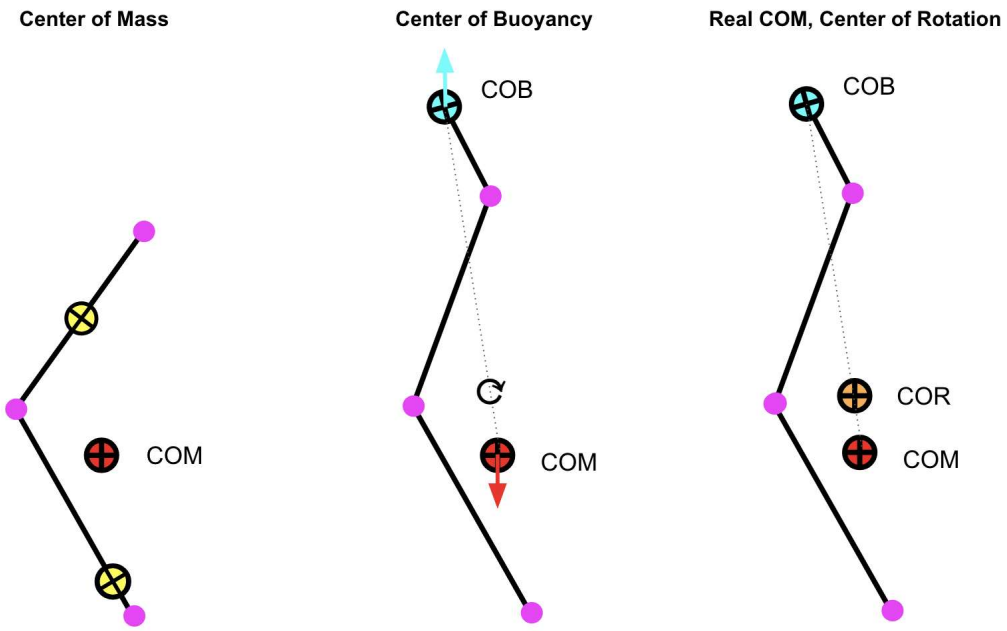

Figure 3.16: Simplified COM,COB,COR configuration.

3.8.3 2 Leg Robot

For the double leg model, the FBD for each leg at each contact case is similar to the one leg robot. The main difference is the placement of the forces and the change caused by the hip link and offset. Refer to the 3d figure in the center of rotation section section.

CHAPTER 4

System Modeling

4.1 Software

To understand and model this system, various simulations and codes were used. The initial approach involved a cad model along with a full cad simulation. This resulted in initial observations of feasibility and practicality of the model. However, due to the many dynamic forces involved, and differences between ideal cad environment and the real prototype, and specially the many variables involved, it wasn't clear if they behaved similar to the real world. One issue here was the lack of a conceive model that could be used for both robotics forces, solid mechanics forces, and atmospheric fluid mechanics forces. And if there was, the systems are very general and need lots of coding. Additionally, the lack of a proper control method meant we cannot rely on human operation for motion repeatability and accuracy.

Thus, a full detailed mathematical code was written in matlab to model the robot along all its forces. This model consists of the code and mathematics to calculate all necessary forces. Note that our code can supplement other software and work alongside them in tandem. For example, a great way to simulate is to use the analytical data from our code and feed it into the expansive and capable simulation space of autodesk.

4.2 CAD

BALLU does not have very complex parts and assemblies that require lots of design work in CAD, instead it has complex dynamics which can also be understood and optimized using proper

software. The initial cad model shown below showed promising results on the possibility of bipedal walking with this system. Following this model walking in simulation, the prototyping began. The model only used buoyancy , gravity, and motor torque to walk.

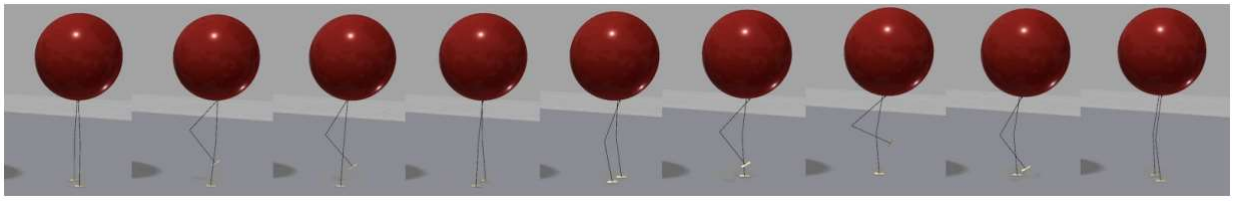

Figure 4.1: The elementary and initial simple simulation model for BALLU in Autodesk Inventor

Even though the model showed walking, this simulation was as beneficial as it was harmful to the progression of the project. The gate looks like human walking, but the forces are entirely different. This is the main reason why the dynamics are so non intuitive.

Next, from the simulation results, detailed models and experimentation started. The model later evolved alongside our own code to simulate, and generate our data including point motion paths. Force plots, solutions of state variables and all other desired calculations and data. Below is a screenshot showing the versatility of our setup and how we can get live data simultaneously along with a data intensive 3d real physics simulation.

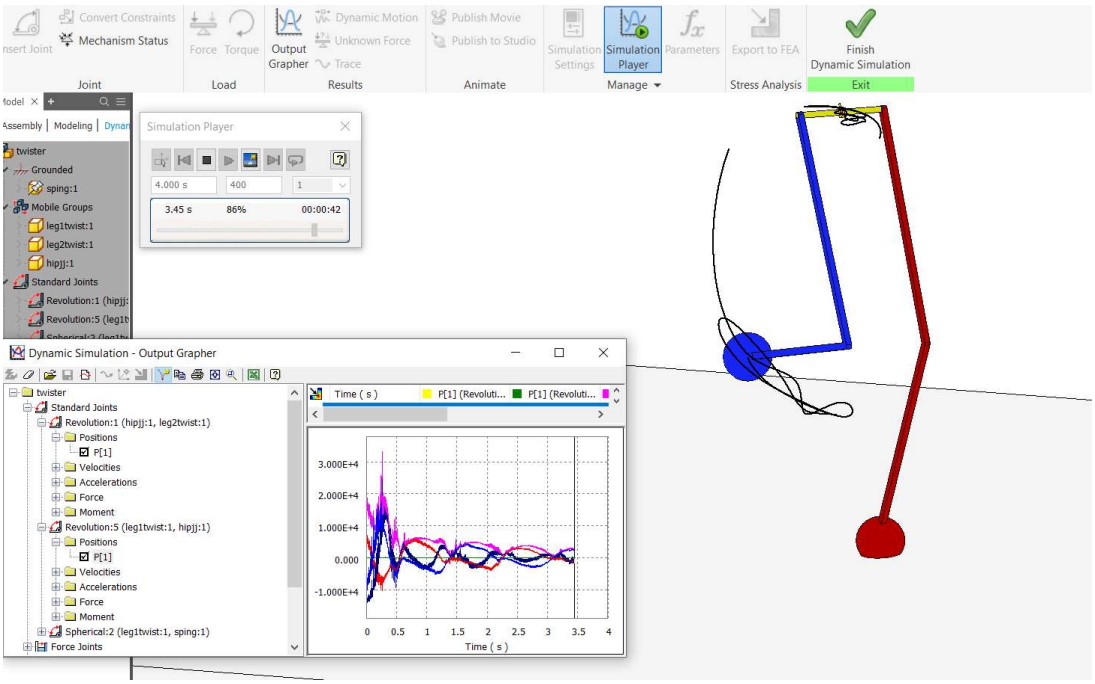

Figure 4.2: Simulation and data collection set up in CAD (used in tandem with other code).

Calculations and data may be collected using any code, however, the ability to observe data collection in real time along with full physics simulation and 3d viewpoint control is very beneficial when trying to understand new behaviors of a novel system. We can only perform so many real world tests and without this setup, accurate locomotion and motion classification would not be possible. Even very complex motion and error cases may be observed and reviewed. In order to make our simulations as realistic as possible, we used a combination of experimental data, math models, and physics calculations to set the constants and adjust for dynamic variables. It is not always the case where simulation is wrong, in some cases it was observed that book values and chart constants were off and the materials simply did not behave that way. Simple examples include friction constants, spring constants.

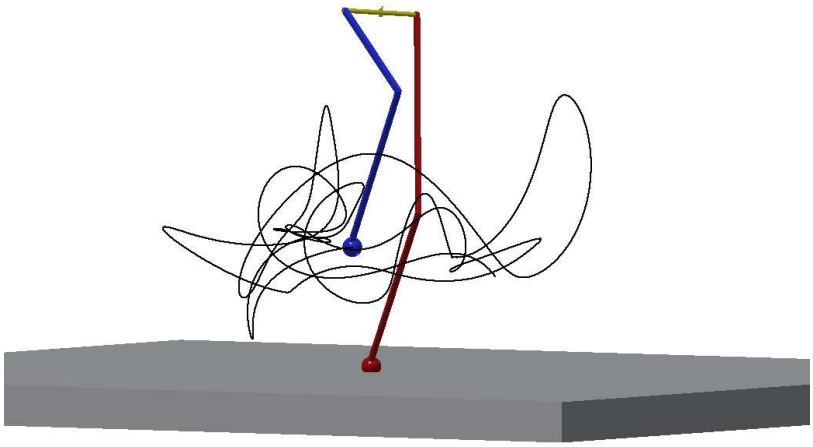

Figure 4.3. Complex motion paths simulated efficiently.

Figure 4.3 shows a case where the motion became complex even though the system was in equilibrium oscillation mode with no input actuation or disturbance. Note that even though the links are simple, behavior of complex pendulums may be extremely complex looking and non intuitive. The black like is the motion path of the blue foot in the 5 seconds. The details of such motions are analyzed in later sections. Simple simulations can become very complex when dealing with complex pendulums. A proper 3d observation tool is a necessary asset for digestion of such behavior.

4.3 Control Input

As discussed in the design section, for quick experimentation and lightweight circuitry, the initial control method for the robot was using manual IR radio transmitters to control the input current to the knee actuators. By using off the shelf toy components, these parts were very reliable and resilient.

We later moved to an arduino based IR control method directed by computer code. Even though this method was more accurate, the noise levels and signal reliability introduced new challenges. Additionally, low cost actuators don't always behave as instructed. To fix these issues, we used a combination of software filtering and slowed down the input data and complexity. Even though such basic input allowed the robot to achieve most required dynamic motions. They were all limited to one or two correct sequences before the changes became significant. For example, when directing the robot to ascend stairs, the motors and signal all work well the first time. Not because they are perfect but because the code accounts for that variance.

In order to have full long sequences of highly dynamic gates, the hardware, software, and electronics need major upgrades.. For better control of the robot, encoders and a feedback loop would be beneficial. For signal transmission, it's best to design a custom board to avoid inefficiencies and keep the transfer rate higher than the toy hardware. And on the software side, code optimization can reduce the load on the program running the code (currently data heavy and can only continuously work for about one minute before needing a few seconds of pause.

Lastly, other tech such as motion capture and machine learning algorithms may be used. And even though those methods may improve the functionality, they introduce new costs affecting both hardware simplicity and software calculation loads. Thus the proposed evolution path for reliable controls would be better system understanding and integration using simple, reliable, efficient hardware and software with seamless communication between subsystems.

4.4 Physics Simulation

4.4.1 Simulation Approach

From initial observations, it was clear that minor forces play a big role in the overall performance of the system. This platform cannot be properly simulated using simple robotic models. And if possible, those models don't present the intuitive insight that would allow better system design. In fact we did use those methods initially for the assumption of efficiency, yet proved to have their own downsides. Mainly due to being optimized for normal gravity cases and robot platforms. Therefore, a full physics simulation was developed. In order to accurately account for all forces and variables. A matrix model of the robot limbs is first constructed. This is then coupled to a time based calculation for all variables. The process is explained in detail in the next sections.

4.4.2 Matrices

Conventional dh parameters and robotics methods are used to construct a robot tree and assign frames to out joints. For the one leg system, the robot parameters are first initialized as follows. All remaining unset variables are set to start as zeros using the setupzeroes script. A few things to note include setting the initial frame on ground instead of on the robot. This allowed easier factoring of the buoyancy force and balloon behavior. It also causes a few more calculations steps later in the process. A tradeoff that worked well for our approach.

Table 4.1: initialization parameters for dh parameter and matrices setup

variable	***value***	***units***	***comment***
linkn	*5*	*-*	*Number of links*
l1	*femur*	*m*	*Link 1 length*
l2	*tibia*	*m*	*Link 2 lengths*
li	*[l1 l2]*	*m*	*Link lengths matrix*
thetah0	*pi/2+pi/4*	*rad*	*Hip joint angle initial*
thetak0	*-pi/2*	*rad*	*Knee joint angle initial*
thetaf0	*(pi/2-(thetah0+thetak0))*	*rad*	*Foot joint angle initial (vertical down)*
ji	*[thetah0 thetak0 thetaf0]*	*rad*	*Joint angle matrix*
angles(tc,:,j)	*[0 0 ji(1,j)]*	*rad*	*Joint angles around xyz axes*
kneeangle(tc,:)	*pi+thetak0*	*rad*	*Interior knee angle*
hx0	*0*	*m*	*Hip x initial*
hy0	*0*	*m*	*Hip y initial*
hz0	*l1*sin(thetah0)+l2*sin(thetah0 +thetak0)+1*	*m*	*Hip z initial*
positions(1,:,1)	*[hx0 hy0 hz0]*	*m*	*Hip initial position matrix*
masses	*[(Bm+Hem);0;footm;robot1m]*	*kg*	*Mass matrix used*

Following initialization, the parameters are set for dh table calculation. These parameters arethen set up as the following matrices.

$$
\begin{aligned}
a &= [positions(tc,1,1) \quad 0 \quad li(1,1) \quad li(1,2) \quad 0 \quad] \\
al &= [0 \quad (-pi/2) \quad 0 \quad 0 \quad 0 \quad] \\
d &= [positions(tc,3,1) \quad 0 \quad 0 \quad 0 \quad 0 \quad] \\
theta &= [0 \quad 0 \quad angles(tc,3,1) \quad angles(tc,3,2) \quad angles(tc,3,3)] \qquad (4.1)
\end{aligned}
$$

Using these parameters, each row of the dh table is calculated using the equation below. Where ii signifies the column numbers

$$dhl = [a(1,ii) \quad al(1,ii) \quad d(1,ii) \quad theta(1,ii)] \tag{4.2}$$

Note that ii is a looped variable from 1 to linkn. This adds all the rows to calculate the numerical dh table for our leg (not including theta variables in numerical output). Our example numerical output with the provided data would be as follows;

$$dh = 5\times4 \begin{matrix} 0 & 0 & 1.8536 & 0 \\ 0 & -1.5708 & 0 & 0 \\ 0.5000 & 0 & 0 & 2.3562 \\ 0.5000 & 0 & 0 & -0.7854 \\ 0 & 0 & 0 & -0.0000 \end{matrix} \tag{4.3}$$

With the dh table calculated, the Transform matrices are found. (ii = 1 to 5 loop)

$$ss = sin(dh(ii,4)) \tag{4.4}$$

$$ssa = sin(dh(ii,2)) \tag{4.5}$$

$$cc = cos(dh(ii,4)) \tag{4.6}$$

$$cca = cos(dh(ii,2)) \tag{4.7}$$

$R(:,:,ii) =$

$$\begin{bmatrix} cc & (-1)*ss*cca & ss*ssa & dh(ii,1)*cc \\ ss & cc*cca & (-1)*cc*ssa & dh(ii,1)*ss \\ 0 & ssa & cca & dh(ii,3) \\ 0 & 0 & 0 & 1 \end{bmatrix} \quad (4.8)$$

For each link, the transform T is found as

$$T(:,:,ii) = R(:,:,ii) \quad (4.9)$$

And the transform from base to link is found as

$$T(:,:,ii) = T(:,:,ii-1)*R(:,:,ii) \quad (4.10)$$

This yields numerical results of

```
>> R

R(:,:,1) =

    1.0000         0         0         0
         0    1.0000         0         0
         0         0    1.0000    1.8536
         0         0         0    1.0000

R(:,:,2) =

    1.0000         0         0         0
         0    0.0000    1.0000         0
         0   -1.0000    0.0000         0
         0         0         0    1.0000

R(:,:,3) =

   -0.7071   -0.7071         0   -0.3536
    0.7071   -0.7071         0    0.3536
         0         0    1.0000         0
         0         0         0    1.0000

R(:,:,4) =

    0.7071    0.7071         0    0.3536
   -0.7071    0.7071         0   -0.3536
         0         0    1.0000         0
         0         0         0    1.0000

R(:,:,5) =

    1.0000    0.0000         0         0
   -0.0000    1.0000         0         0
         0         0    1.0000         0
         0         0         0    1.0000
```

```
>> T

T(:,:,1) =

    1.0000         0         0         0
         0    1.0000         0         0
         0         0    1.0000    1.8536
         0         0         0    1.0000

T(:,:,2) =

    1.0000         0         0         0
         0    0.0000    1.0000         0
         0   -1.0000    0.0000    1.8536
         0         0         0    1.0000

T(:,:,3) =

   -0.7071   -0.7071         0   -0.3536
    0.0000   -0.0000    1.0000    0.0000
   -0.7071    0.7071    0.0000    1.5000
         0         0         0    1.0000

T(:,:,4) =

    0.0000   -1.0000         0   -0.3536
    0.0000    0.0000    1.0000    0.0000
   -1.0000   -0.0000    0.0000    1.0000
         0         0         0    1.0000

T(:,:,5) =

    0.0000   -1.0000         0   -0.3536
    0.0000    0.0000    1.0000    0.0000
   -1.0000   -0.0000    0.0000    1.0000
         0         0         0    1.0000
```

(4.11)

Using the calculated matrices, we can simply extract all joint positions and have the forward kinematics of the leg (ii = 1 to 5 loop).

$$jp(:,:,ii) = [T(1,4,ii) \quad T(2,4,ii) \quad T(3,4,ii)] \qquad (4.12)$$

The positions are found to be

$$positions(tc,:,1) = real(jp(:,:,2));$$

$$positions(tc,:,2) = real(jp(:,:,3));$$

$$positions(tc,:,3) = real(jp(:,:,4)); \quad (4.13)$$

$$hpos = transpose(positions(tc,:,1));$$

$$kpos = transpose(positions(tc,:,2));$$

$$fpos = transpose(positions(tc,:,3)); \quad (4.14)$$

With the numerical values shown at this instant

```
>> positions
positions(:,:,1) =
         0         0    1.8536

positions(:,:,2) =
   -0.3536    0.0000    1.5000

positions(:,:,3) =
   -0.3536    0.0000    1.0000
```

(4.15)

The frames are best shown in the figurea. Note that the additional frames are set for better calculations. The home frame is set in a point on ground due to ease of buoyancy adjustment, position calculation, and other dynamic and static modeling and calculation purposes.

To plot the robot, a rigid body tree is constructed in matlab first with specs for each body and joints set. Then, the robot configuration is set as follows.

$$Config = homeConfiguration(robot)$$

$$a1 = angles(tc,3,1)$$

$$a2 = angles(tc,3,2)$$

$$a3 = angles(tc,3,3)$$

$$configmatrix = [\ 0\ 0\ a1\ a2\ a3\ ]$$

$$Config(i).JointPosition = configmatrix(1,i) \tag{4.16}$$

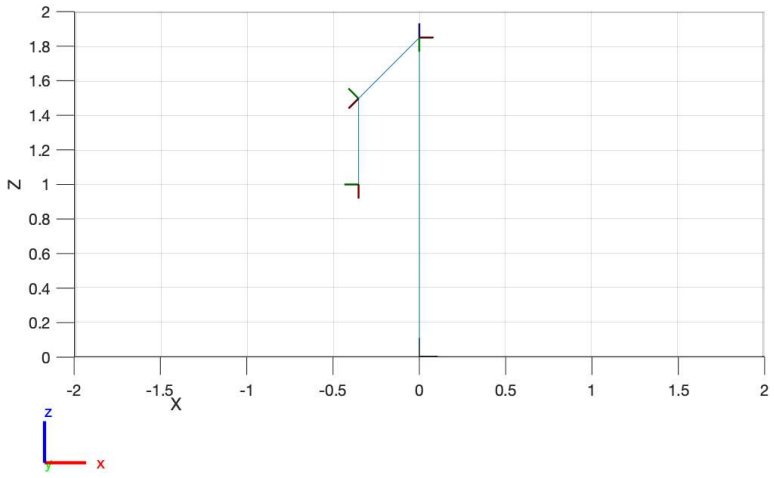

Figure 4.4: 2D view of a single leg of a robot with assigned matrices.

The posture of the robot is presented in the given calculated initial state. The frames are better visible in a 3d view shown below

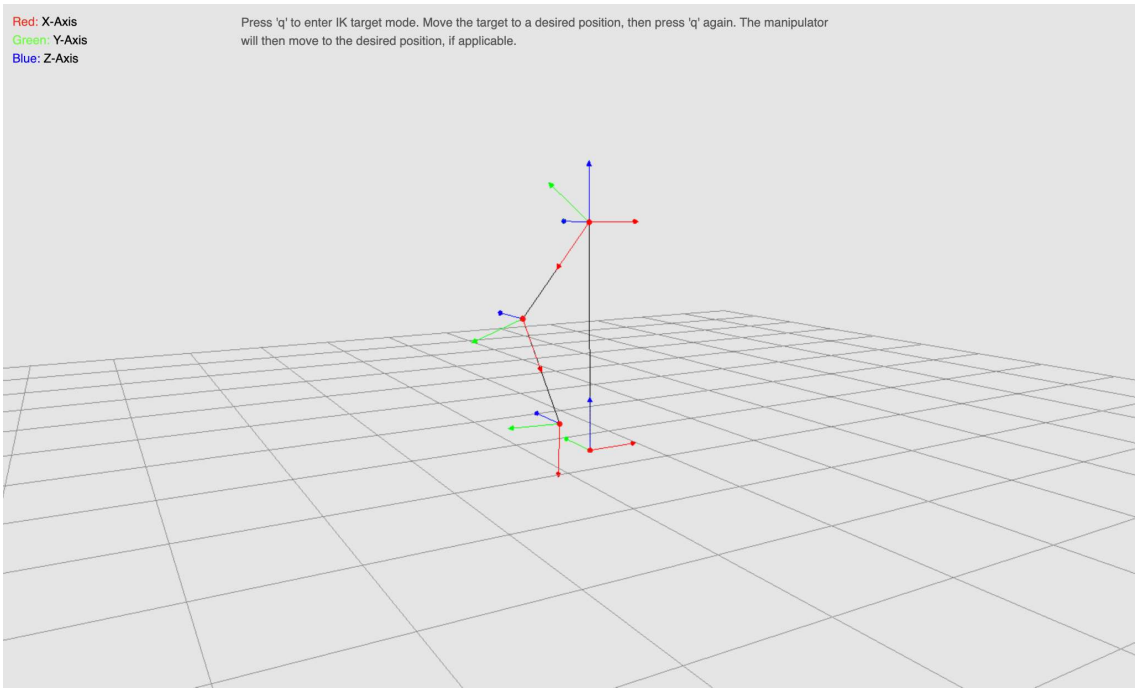

Figure 4.5: 3D view of a single leg of a robot with assigned matrices.

The presented matrices are calculated for the single leg robot. For balloon calculations, a separate calculation is used and new matrices are attached to the COB position of the balloon. Note that the first two frames remain constant.

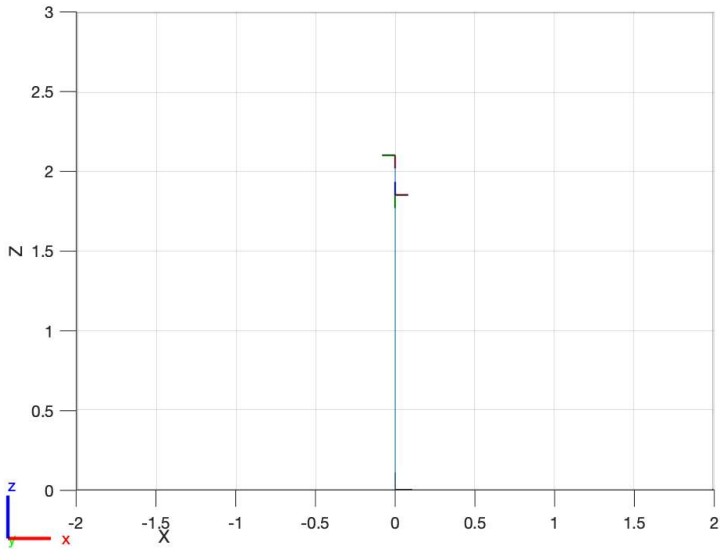

Figure 4.6: 2D view of balloon link of a robot with assigned matrices.

These two link trees fully model the one leg robot. For the two leg robot, the same method is used with three branches. The two legs will each have frames assigned with the only difference being the hip joints y position offset. With these frames fully defined, and with all the forces calculated, the overall dynamic and state of the robot can be calculated at each instant.

4.4.3 Software Architecture

The system does not use many sensors and various input systems, the controls and software architecture become quite simple. Even though the complexity in physics and gate generation persist. Figure 4.7 shows general software flow and Figure 4.8 presents details of calculations.

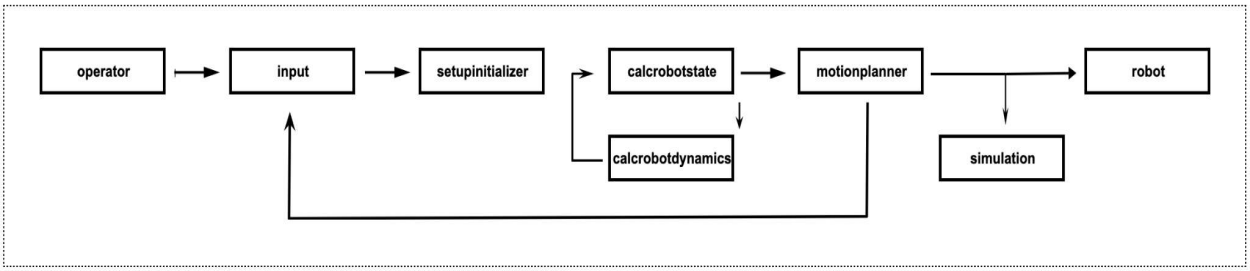

Figure 4.7: Overall software architecture control flow diagram.

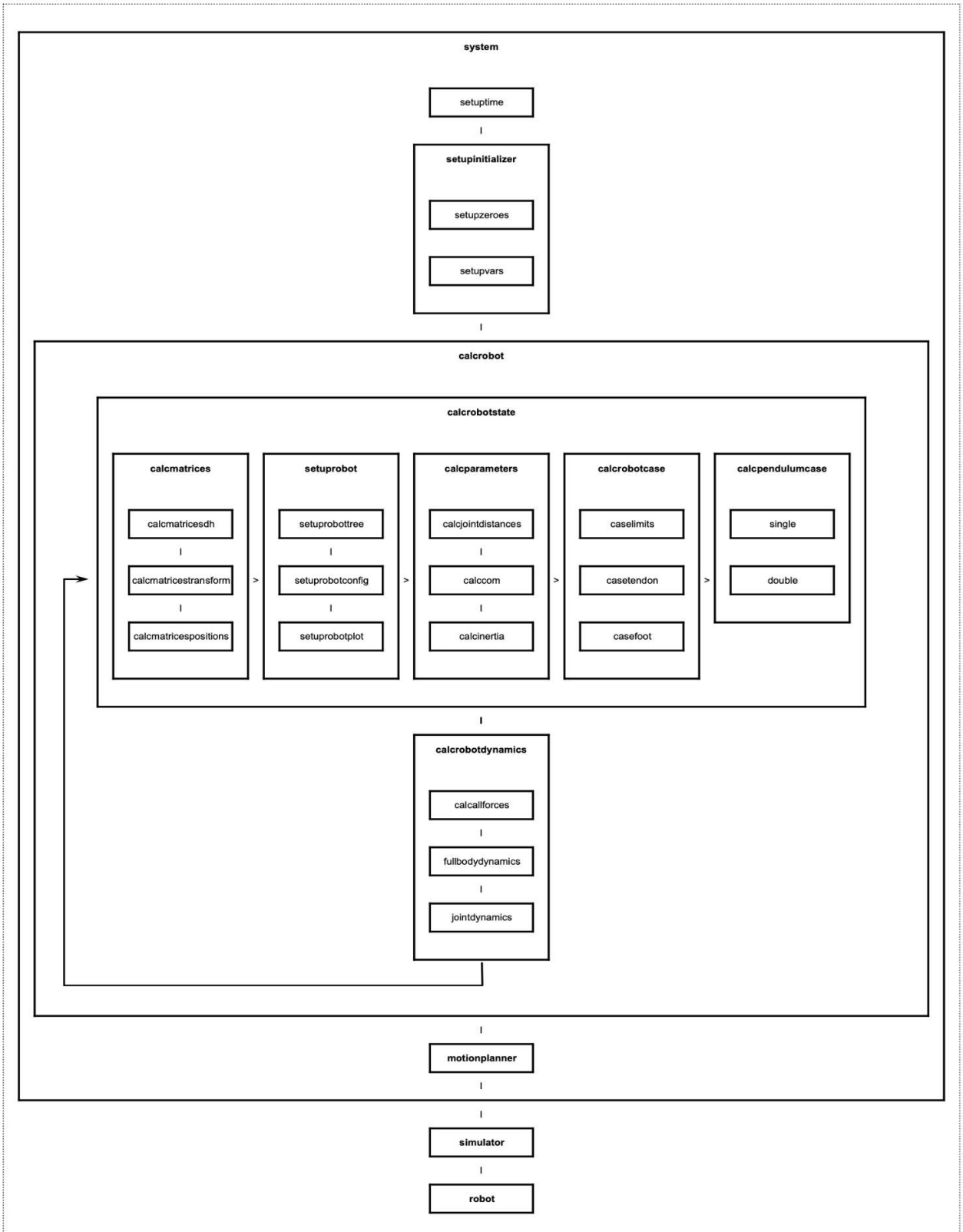

Figure 4.8: Flowchart of calculations

Figure 4.8 explained in in order is as follows:

1- Setup time and initialization.

2- Calculate matrices and robot state.

3- Calculate parameters and all cases.

4- Calculate all forces and dynamics.

5- Repeat 2,3,4 for each timeframe.

6- Send full data to the motion planner, simulator, and robot.

4.4.4 Data Input and Analysis

In the code, our data is either manually input for the knee controls, or by pre written scripts and motion planners and sequencers. It is filtered and cleaned and communicates input and actuation behavior with the rest of the code and robot.

Input series script makes manual and sequenced entry easy and auto translates from any type of time series input. Motion planner works with gate generators and feeds the desired data. Data processors filter and clean the signal. Based on calculation load or actuation timing and other limitations, they can discretize or smoothen discrete data. This allows both translation of super complex input into a manageable one, and the translation of low resolution incomplete input to smooth code that runs. The actuation calculators organize and calculate all actuator parameters and outputs based on actuator parameters and input data series.

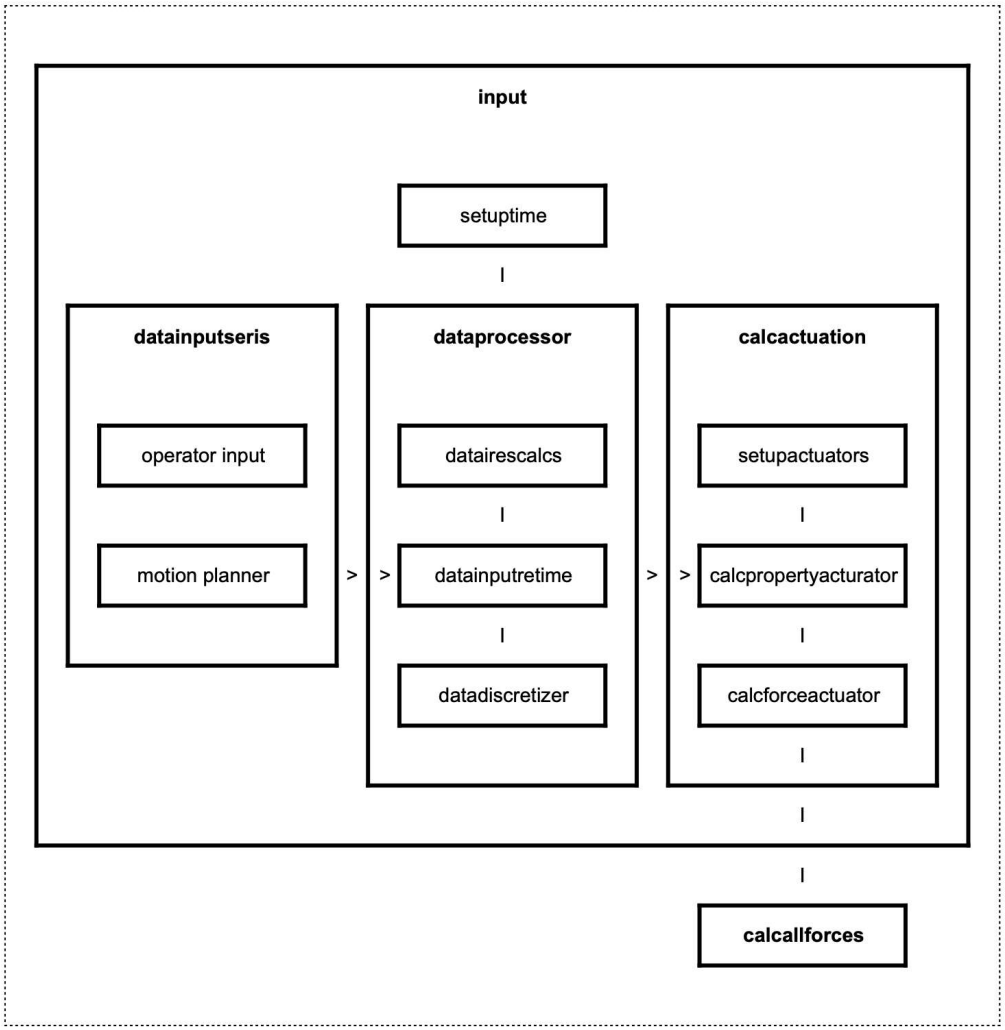

Figure 4.9: Data input and optimization software flow chart.

4.4.5 Simulation Set-up

The following chart shows the script running the matlab simulation from scratch. Although functional, this method became obsolete due to slow processing and lack of user friendly navigation and observation tools. And in most 3d cases, replaced by other simulators.

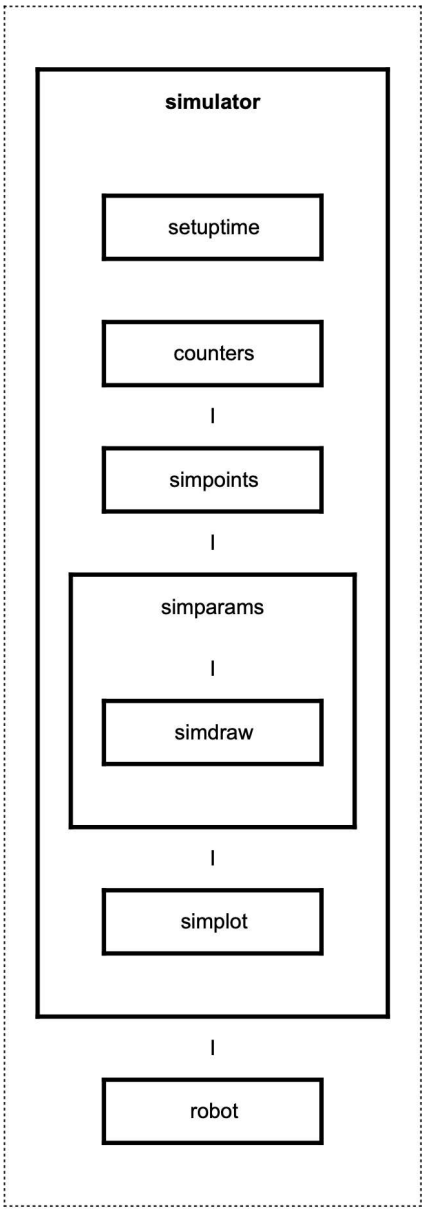

Figure 4.10: Simulation code flow chart.

CHAPTER 5

System Behavior

5.1 Actuation and Knee Behavior

5.1.1 Actuation

The actuation system uses a simple rc motor paired with a 100/1 gear reduction gearbox. The system is directly connected to a 3.7V lithium ion battery and circuitry which acts as a switch allowing a ratio of current to reach the motor. This setup provides enough speed to perform dynamic tasks and enough torque to perform them at high angles. This simpler approach was used due to the lower cost and lower weight associated with minimal components. The downside is lack of accurate positioning, which is not needed in most of our dynamic or control approaches, but becomes troublesome regarding repeatability. Actuator parameter are listed in the next table.

Table 5.1: Actuator parameters:

variable	***value***	***units***	***comment***
at	*[1;1]*	*-*	*type for each actuator*
aip	*[0 0; 0 0; 0 0; 0 0]*	*-*	*initial pos; vel; accel for each actuator*
dir	*[-1 0 1]*	*-*	*direction matrix [neg/ccw stop pos/cw]*
ires	*low*	*-*	*input resolution "low" "mid" "high"*
isr(act,tc)	*dil(act,tc)*	*-*	*Clean data input ratio*
icmax(act,1)	*5*	*-*	*Max control input magnitude*
isv(act,tc)	*isr(act,tc)*icmax(act,1)*	*-*	*clean input value*
posmax(act,1)	*pi/2*	*-*	*act angle max*
posmin(act,1)	*0*	*-*	*act angle min*
grat(act,1)	*100*	*-*	*actuator gear ratio*
mscm(act,1)	*200*pi*	*rad/s*	*Max motor speed*
velmax(act,1)	*2*pi*	*rad/s*	*Max act speed*
tormax(act,1)	*1.0*	*Nm*	*Max act torque*
atype(1,:)	*[5 100 200*pi 0 pi/2 1.0]*	*-*	*[icmax grat msacm mintheta maxtheta maxtor]*

All our actuation calculations follow a few initial assumptions. The first is that the high gear ratio prevents backdrivability. Thus the dynamic forces will not be exerted on the actuator. Second is we assume our tendon linkage system is perfect and without elasticity or tibia bending. Also, due to the tendon engagement parameter, we can position the robot in specific configurations that eliminate singularity and infinite torques acting on the actuators. And Lastly, by using press fit actuator holders around the tibia, in the case of error resulting in unwanted toques and jamming, the friction force will release first effectively loosening the tendon and saving the actuators.

With our assumptions and parameters known; actuator max acceleration is using the formula below. We assume minimal load going from max positive velocity to max negative velocity in dt time period. Actuator current draw is calculated afterwards.

$$accmax(act,1) = 2*velmax(act,1)/interval \quad (5.1)$$

$$actI(act,1) = tormax(act,1)/accmax(act,1) \quad (5.2)$$

For modeling and simulation purposes, the actuator initial parameters are set to 0. These include all parameter delta values and actuator position, velocity, acceleration, and torque parameters.

$$Isrdelt, isvdelt, posdelt, veldelt, accdelt, tordelt = 0 \quad (5.3)$$

$$\text{Actpos, actvel, actacc, acttor} = 0 \quad (5.4)$$

$$\text{aip} = [\ 0\ 0;\ 0\ 0;\ 0\ 0;\ 0\ 0] \quad (5.5)$$

Aip is the matrix holding actuator initial parameters. The parameters are later calculated using the equations below. All delta values are additionally calculated per dt.

$$actvel(act,tc) = isr(act,tc)*velmax(act,1) \quad (5.6)$$

$$actpos(act,tc) = actpos(act,tc-1)+actvel(act,tc)*dt \quad (5.7)$$

$$actacc(act,tc) = veldelt(act,tc)/dt \quad (5.8)$$

$$acttor(act,tc) = actacc(act,tc)*actI(act,1) \quad (5.9)$$

Using these parameters we construct the matrices defining actuation data which becomes

Parameter	**[value**	**sign**	**delta**	**minlim**	**maxlim**	**]**
ACTTINPUTNORM(act,:)	= [isr(act,tc)	sign(isr(act,tc))	isrdelt(act,tc)	-1	1	]
ACTTINPUT(act,:)	= [isv(act,tc)	sign(isv(act,tc))	isvdelt(act,tc)	-1*icmax(act,1)	icmax(act,1)	]
ACTTPOSITION(act,:)	= [actpos(act,tc)	sign(actpos(act,tc))	posdelt(act,tc)	posmin(act,1)	posmax(act,1)	]
ACTTVELOCITY(act,:)	= [actvel(act,tc)	sign(actvel(act,tc))	veldelt(act,tc)	-1*velmax(act,1)	velmax(act,1)	]
ACTTACCELERATION(act,:)	= [actacc(act,tc)	sign(actacc(act,tc))	accdelt(act,tc)	-1*accmax(act,1)	accmax(act,1)	]
ACTTTORQUE(act,:)	= [acttor(act,tc)	sign(acttor(act,tc))	tordelt(act,tc)	-1*tormax(act,1)	tormax(act,1)	]

(5.10)

Additionally, two variable recording actuation on/off state and range of motion case and validity are recorded. The actuator condition matrix is constructed.

ACTTCONDITION(act,:) = [time act actnum acton(act,tc) actrange(act,tc)]

(5.11)

All dthe data together produces the actuator output variable. A 3d matrix including all necessary and calculated data and parameters per actuator.

ACTTOUTPUT(:,:,tc) =

[ACTTCONDITION(act,:)

LINEHOLDER (zeroes)

ACTTINPUTNORM(act,:)

ACTTINPUT(act,:)

ACTTPOSITION(act,:)

ACTTVELOCITY(act,:)

ACTTACCELERATION(act,:)

ACTTTORQUE(act,:)] *(5.12)*

The actuator shaft is connected to a lever which interfaces with the tendon pulling the knee,

$$Mll = 0.01 \tag{5.13}$$

$$Tll = 0.01 \tag{5.14}$$

Mll is the motor lever length and Tll is the tendon connection distance with the knee joint, all lengths are in meters. When engaged, the tendon along with the actuator linkage produce a four bar linkage. Figures below show more details about the system.

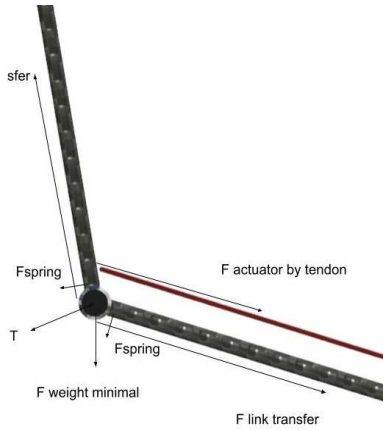

Figure 5.1: Knee CAD side view.

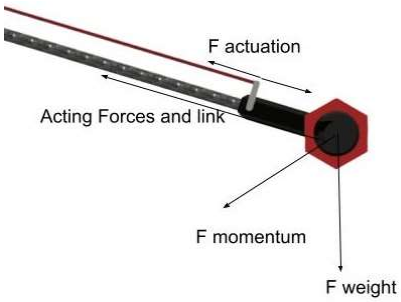

Figure 5.2: Lifted foot CAD side view.

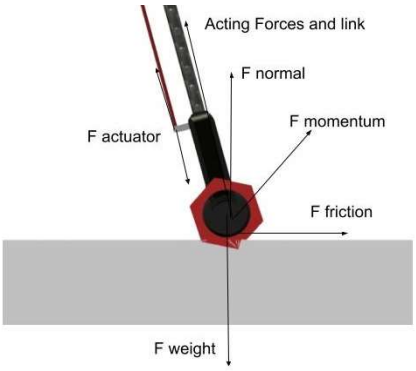

Figure 5.3: On ground foot CAD side view.

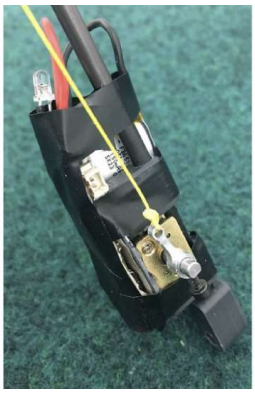

Figure 5.4: Foot assembly photo.

The tendon tension force on the tendon will be a function of the motors angle and tendon engagement. If the tendon is engaged, we can calculate this force with the equation below. Note that tendon engagement properties are discussed in the further sections.

$$Ftt(act,tc) = acttor(act,tc)*Mll*sin(actpos(act,tc)) \quad (5.15)$$

Motor tension force on the tendon is then applied to pull and close the knee joint. We then calculate the torque exerted on the knee joint from the actuator with engaged tendons as follows.

$$ktoract(act,tc) = Ftt(act,tc)*(sin(-1*thetak(tc))/Tll) \quad (5.16)$$

Note, given the high gear ratio and torque output of the actuator, as discussed initially, we omit the need for factoring backdrivability in our model. When the actuator is at a pi/2 angle (maximum effect on actuator), it will need a tendon force of 100N to be backdrived and none of the dynamic or knee forces come anything close to producing that tension in the tendon system.

5.1.2 Tendon Mechanism

As mentioned, the tendon mechanism creates a conditional four bar linkage system with the actuator. The specifics of manufacturing and materials are discussed in the previous sections. Torque on the knee Tk is calculated using the formula below

$$Tk=Ft*sin(teta)*Tdl \quad (5.17)$$

The tension force on the tendon is derived from the equation below

$$Ft*sin(teta) = At/Ldl \quad (5.18)$$

Where Ft is tendon tension force, Tk is knee torque, At is actuator torque, teta is actuator angle clockwise from vertical tibia from 0 position (same as clock). Tdl is the tendon to knee distance and Ldl is the tendon to actuator linkage length. Given:

$$Tdl = Ldl \quad (5.19)$$

We can conclude a 1 to 1 ratio and

$$At = Tk \tag{5.20}$$

Not that in order to properly model this system, proper definition of tendon engagement case and its calculation is crucial. Since the tendon has affixed length, we can calculate the tendon limit or max length as follows.

$$tendonlim(act,tc) = -1*actpos(act,tc) \tag{5.21}$$

When the tendon is disengaged, the distance between the two connections is lower than this limit and when properly engaged, it is equal. In the case of hyper engagement, it is built into the model to allow a 5% error and stop operations otherwise.

In addition to the actuator position, the overall robot posture affects this engagement as well. As seen in the schematic below. As the posture changes, the effect of gravity on knee closing and opening varies based on hip and knee angles. Additionally, different dynamic forces impact this condition as well. To measure this, a kneedesire variable is defined. To model if the tendon is fully engaged or not, we must quantify the knee desire, and with multiple dynamic forces throughout the robot, this is only possible by calculating all the other forces first. However, as a simplified approach, is comparing actuator position with knee angle. The tendon will only be engaged when the knee angle and actuator link angle are equal and the actuator has positive torque. The torque requirement of the actuator is crucial as the tendon may be at an extended position but without any tension.

One condition to note is the robot is designed to usually have the knees bent at 10 degrees to avoid unwanted impact shock, have better damping and smoother motion, and hold the actuator

and tendon properly engaged. However, in rare motion behaviors, the tendon is needed to be fully loosened. This is simply don't by actuator completely releasing from that offset angle.

5.1.3 Elasticity

As discussed, the spring used is a long lasting durable polymer power chain used for long duration high force orthodontics applications. As seen in the schematic below, due to the rolling nature of the knee joint the spring plays a big role in allowing the joint to passively open when the actuator is disengaged. The spring setup is shown in the knee design schematic.

The spring provides multiple benefits and use cases. First, given the tendon can only pull, it causes the knee to go back to position when the actuator angle changes and the knee joint opens. Second, it allows passive absorption of impacts and causes an overall filtering and smoothness of the forces acting on the robot and the knee joint. This spring force is not constant and increases as the knee closes, becoming a simple low force filter and dampener of force in straight leg conditions, and a high power explosive spring in full closing and release sequences which is especially crucial for jumping and fall damping.

The length of the spring changes as the double jointed knee mechanism rolls. And given the radii of the rolling elements and connection points of the spring, the spring force is calculated, and later converted to a torque around a simple rotary knee model. The table below presents the parameters used in this calculation.

Table 5.2: Spring parameters

variable	value	units	comment
thetak	angles(tc,2)	rad	Knee angle
Jrad	.003	m	Joint radius
k	1000	N/m	Spring constant

To calculate the force we first find the spring length with the knee fully open (collapsed inversely with minimal spring extension)

$$Sleni = 2*Jrad \tag{5.22}$$

The spring length based on knee angle is then calculated

$$Slen(act,tc) = 2*Jrad+(Jrad*pi*(1+((-1*thetak)/pi))) \tag{5.23}$$

Spring displacement, spring force, and final torque effect by the spring are calculated

$$Sdis(act,tc) = Slen(act,tc)-Sleni;\ \%\ spring\ displacement \tag{5.24}$$

$$Fs = k\,x \tag{5.25}$$

$$Fs(act,tc) = k*Sdis;\ \%\ spring\ force \tag{5.26}$$

$$kjreq = 2*Jrad;\ \%\ knee\ joint\ equivalent\ radius \tag{5.27}$$

$$ktorspring(act,tc) = Fs*kjreq\ \%\ torque\ on\ knee\ by\ spring \tag{5.28}$$

$$liftforcegram(act,tc) = ((ktorspring/tibia)/g)*k \tag{5.29}$$

This unique spring offers a high spring constant and lifetime and allows for the exertion of large controlled elastic forces in a very compact package.

5.1.4 Ground Contact

For the single leg version, the robot experiences two main states. First is when the robot is completely in air with no external disturbances. In this case, the foot does not contact the ground. In the second case we have the foot in contact with the ground. This introduces the normal force and ground friction which play a significant role in the robots dynamics. Additionally, we must factor in the transition times between these cases. When the foot touches the ground we set an impact case of 1 and when the foot touches the ground we set that as -1. These are summarized in the table.

Table 5.3 1 leg robot foot contact parameters

Variable	***Possibility 1***	***Possibility 2***
fontact	*0*	*1*
fimpact	*-*	*[1 -1] (hitt, lifoff ground)*

For the bipedal version, we have four contact conditions including; both feet no contact, both contact, only left contact, and only right contact.

Table 5.4: 2 leg robot foot contact parameters

Variable	***Possibility 1***	***Possibility 2***	***Possibility 3***	***Possibility 4***
fontact	*[0 0]*	*[1 1]*	*[1 0]*	*[0 1]*
fimpact	*-*	*[1 -1]* *(both feet* *hitt, lifoff ground)*	*[1 -1]* *(Right foot* *hitt, lifoff ground)*	*[1 -1]* *(Left foot* *hitt, lifoff ground)*

For simpler and more accurate modeling, we assume the ground is always rigid and the collision instantly reduces the foot velocity in the z direction to 0 when hitting ground. This does not cause a sudden infinite force and impulse.

The knee joint is always slightly bent, and no matter the angle of contact, the center of rotation and mass will not instantaneously stop. Instead they will be dampened by the bending of the knee and spring force. And given the knee is not in a straight position, the hip joint will always have an offset from the tibia axis and thus, we will never experience sudden impulse and always have full fluid gradual force transfer. Fall damping is better observed in the supplementary attached video files.

5.2 Dynamic Cases Discussion

To properly categorize the dynamic behavior of this system, aside from force analysis, identification of sub system motion and dynamic categorization is needed. The general approach to humanoid walking has evolved through the years. Although, it's generally agreed that human bipedal walking is an oscillatory motion at which muscles resist the body from falling as the legs go through loops of swinging and catching. Energy is stored in the tendons and as one leg is being swung, the other acts as a base. It takes energy to stand, and if we could turn a human off, it would collapse to the ground. It's similar in the case of humanoid robots. Balance takes energy. And moving is a complex constellation of forces and motions together if done elegantly. We can list all the control methods used and all the best algorithms. Non work for this system. For this system, stability is cheap and default. Closing the knees takes energy. Falling is expensive when

standing, and cheap when falling. This non intuitive motion is organized in this section as sub-motions and systems.

5.2.1 1 Leg Robot Dynamic Cases

5.2.1.1 No Foot Ground Contact

The single leg robot experiences two main dynamic state categories. First is no foot ground contact. At this state, the robot falls down. We refer to this overall motion as “body landing motion”. If the body is jumping or ascending, we refer to it as “body rising motion”. But how is this quantified with respect to the whole body motion and component motions? We can treat the whole system as a normal moving body. The sub systems introduce the complexity.

Regardless of state, the robot desires to move to a posture at which the feet are dangling down and the balloon is on top. The knee is opening as the top and bottom masses try to alight vertically to cancel out the body rotation. This is the first main concept in the dynamics of this system. For reference, we refer to this motion as the “straightening motion”. Refer to the pendulum equilibrium condition section for a visual explanation.

When knee actuation is introduced, the system becomes capable of closing and opening the knee dynamically. Due to the rotary architecture of the joints. This input also affects the momentums. The hip joint is underactuated and free to rotate. The leg system will start to behave similar to a swing hanging from the balloon. The energy input to the system seems confusing until it is compared to a person swinging in a sewing and moving its feet to ascend and control this swing.

This oscillatory motion, with correct understanding, timing, and forces is the basics of controlling the dynamic state of this robotic system. The exact details of the oscillations are discussed in depth in the pendulums section. In short, in this non ground contact state the

oscillation may be controlled to allow for a controlled landing position of the foot. This position may be in from, under, or behind the location of the robot's COB, causing a follow up straightening motion. We refer to this foot placement determining oscillatory swinging motion as "foot placement delta x".nThe knee motion can also adjust the landing poster and knee angle, this changes the body height upon impact. We refer to this alteration as "foot placement delta z". In this state, air resistance forces play a significant role and moving the legs is easy why altering the balloon path takes more force.

5.2.1.2 Foot Ground Contact

Once the foot touches the ground, the normal and friction forces play a major role. First, the robot no longer falls down. Instead, the foot stays down and the rest of the body and balloon move to an upright position by the "straightening motion". Second, ground friction stabilizes the foot contact position preventing free sliding.

Motion of the knee can now result in two different motions. One, lifting the leg and moving back to no ground contact state. We refer to this as "foot lifting motion". Second, if the feet remain on the ground, the momentum and motion of the knee moves the balloon component and causes an inverted swinging motion. As if you were a bubble wrapped in flesh swinging on an inverted swing on the bottom of the ocean :) exactly the inverse of the swing.

In this state, the knee input allows the COB to shift both vertically and horizontally using the oscillatory motion. We refer to the vertical COB displacement motion "body placement delta z". Swinging can also determine the point where the feet can lift off and transition into a non contact state, the x position of the body fights off the straightening motion and creates an overall desired momentum in the forward or backward direction. This is referred to as the "body

placement delta x". Additionally, aside from the straightening motion, we refer to the process of the feet and COB getting closer or farther as "body length motion". These motions create the building blocks of systems control strategies and motion planning.

Table 5.5: Single leg robot reference motions

Robot	***Foot contact***	***Reference motion***	***Motion details***
1 leg	*No contact*	*body landing motion*	*Whole robot falls down (-z)*
1 leg	*No contact*	*Body rising motion*	*Whole robot rises up (+z)*
1 leg	*Both*	*Body length motion*	*COB & feet change distance (+-z for one or both)*
1 leg	*Both*	*Straightening motion*	*COB & COR vertically align (Pitch rotate to 0)*
1 leg	*No contact*	*Foot placement delta x*	*Foot placement vs COB (+-x)*
1 leg	*No contact*	*Foot placement delta z*	*Foot touchdown timing (+-z)*
1 leg	*Contact*	*Foot lifting delta x*	*Foot swing positioning (+-x)*
1 leg	*Contact*	*Foot lifting delta z*	*Foot swing timing (+-z)*
1 leg	*Contact*	*Body placement delta x*	*COB changes position (+-x)*
1 leg	*Contact*	*Body placement delta z*	*COB changes height (+-z)*

These references are not exclusive and are often paired and happening together. These motions are best observed in the supplemental videos. A few extra details remain regarding the single leg motion categorization. First, the leg may lift off, or push off the ground. Lift off is achieved by closing the knee quickly. Push off is achieved by releasing a closed knee and using stored spring energy and buoyancy potential to create an upward momentum. This is mainly used to jump.

Given the singular active DOF, the single leg roots motion is very limited and reliant on timing. In the pendulums section, these motions are further analyzed and later used for motion planning. Lastly, the single leg dynamics dont allow for control in the y direction. This being

said, there may be fast swings which create a small radial torque and roll and yaw twist in the robot. To be able to harness these minute changes, a different system design is needed and with our current system, the one leg version may only properly locomote in the sagittal plane of x and z directions.

5.2.2 2 Leg Robot Dynamic Cases

The bipedal robot uses a similar body and identical legs as the one leg system. The main major change is that the balloon is attached in between the two legs and now the hip joints have a small distance from each other as shown in the figure 2.2.

This offset is later shown to assist the system in complex motion and turning strategies. Aside from that, having two legs now allows the robot to have a third main dynamic case of one leg in contact with ground and the other lifted. These details are explored in the following sub sections. The majority of the motions discussed in the one leg section still apply, although with further details and sub motions. And some new ones are added. These new motions offer complex motion in 3d space and are better categorized and observed as complex pendulum combinations.

5.2.2.1 No Foot Ground Contact

In this case the robot is falling. The main difference from the previous one leg case is the possibility of the two legs to have independent swings. These swings, when in sync behave similar to the one leg case and when independent can alter the 3d orientation of the system along with component momentums. An example of this alteration is two opposite leg swings creating a yaw twist which aerially turns the robot. The same method was experimented with for the robot

NABi and discussed in detail in publication [23]. The other main difference is the possibility of having different feet contact the ground at different positions and times. With this difference, the robot will land into a one foot ground contact dynamic state.

5.2.2.2 One Foot Ground Contact

This is the main state used in walking. While the foot in contact behaves similar to the case in the one leg system (aside from hip offset). The lifter leg can now be able to swing freeling and change the state of the robot's posture and motion. The sum of these swings create complex movement and turning motions. While the lifter foot mainly controls the swing and momentum in the x direction, the in-contact foot controls the swinging legs height and ground contact location and timing. This control is the basics behind bipedal walking gait generation for Ballu.

One important metric here is buoyancy force to foot weight ratio. Based on this, when in a one leg contact state, the robot may remain stable, or fall back to a two leg contact case. Aside from this ratio, non contact foot’s height and position play a role and alter the motion of the body about the contact foot's pivot point. At every state, the position of COR, COB, Foot1, Foot2, and all the forces determines the stable case. With a simple knee adjustment, the robot may be controlled and moved into a desired 3d twist motion. Some very unique motions can be achieve by correct understanding of this concept. We explore this in detail in the pendulums section.

5.2.2.3 Two Foot Ground Contact

While both feet are on the ground, in sync motion behaves like the one leg case and off sync motion changes the orientation and position of the hip joint axis and body. Depending on this orientation and force delta differences, interesting and complex foot lift up or jumping gates may

be achieved. Examples include body shifting and dancing in x, y, and z directions and motions such as side stepping and side hopping.

For every knee angle combination, the body will move to a stable posture position. That, and all the postures during the path to that new desired posture are achievable with correct positioning of the knee angles without even lifting a foot. Note that the solution might have multiple answers and possible stable configurations. Also, as discussed, the knee joint has a nonlinear force profile and using this nonlinearity along with positioning and timing, the robot can get into a multitude of static, dynamic, lift off, step starting, or gate initiating postures. The figure below shows just how two simple legs can result in these posturing states. All these explanations are better implemented and shown in motion and in motion planning sections when we use them for desired motion.

One important consideration with regards to two foot on ground placement is the architecture of hip joints and the resistance towards turning. In most cases, this rigid 1 DOF hip joint alignment keeps the robot from performing undesirable spins and maintains stability, reducing unwanted yaw motions. Tests on this concept are attached in the supplemental videos.

5.3 Pendulum Categorization

The previous section introduces the concept of legs swinging. This is due to the two link rotary joint architecture. A mass attached to any link rotating about a rotary joint freely acts as a pendulum. BALLU's motion is best observed as a dynamic sentence made of words consisting of pendulum letters. Simply put, a combination of pendulums build and control the robot.

5.3.1 Single

Consider a balloon single link system. Holding the balloon up, the leg is a simple pendulum, and having the foot anchored, the body behaves like a simple pendulum. Ballu has double linked legs, although when the knee joint is locked, the system behaves like a simple single pendulum when the foot is not in contact with the ground as shown.

Figure 5.5: Single pendulum case.

We consider the hip joint as the base, the feet as the weight, and the distance from hip to foot as pendulum link length. This simple pendulum will follow a x position value vs time graph of a simple sine wave with a link length and gravity dependent period. The system oscillates between states of max potential energy and high momentum kinetic energy.

$$T=2*pi*sqrt(L/g) \qquad (5.30)$$

Note that this period is an approximation for smaller oscillations and very slightly changes for larger oscillations.

5.3.2 Inverted Single

The same system with a locked knee, becomes an inverted pendulum when the foot is in contact with the ground and the balloon can freely move. Note that for simplicity, we omit foot sliding possibility in this explanation even though it is included in the calculations. This inverted pendulum behaves like a normal pendulum, except buoyancy replaces weight. Aside from that, air resistance dampens the motion significantly.

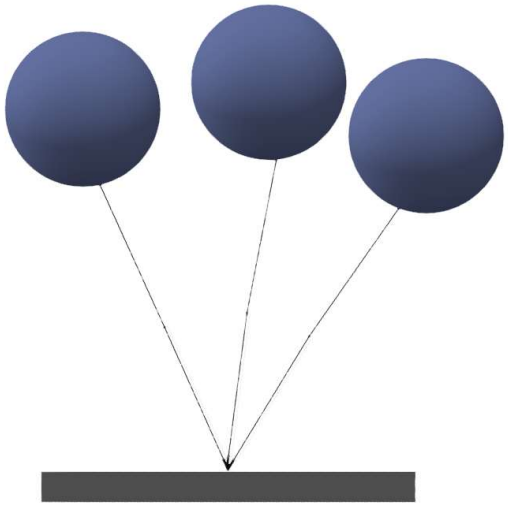

Figure 5.6: Inverted single pendulum case.

There are two main differences between the inverted and normal system. First, different forces. This is due to the change in acceleration when comparing weight and buoyancy force. We calculate the upward acceleration due to buoyancy to be 16.33 m/ss vs the -9.81 m/ss for normal gravity.

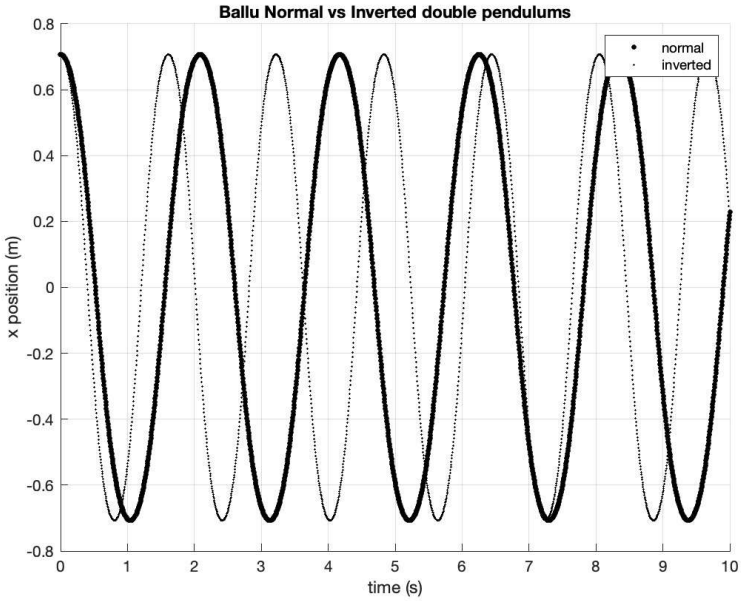

Figure 5.7: Single vs inverted single pendulum case x position plot.

This change alters the motions period and does not impact the oscillation amplitude. The second change is the introduction of a large atmospheric resistive air drag force on the balloon which is not present on the feet due to their low surface area.

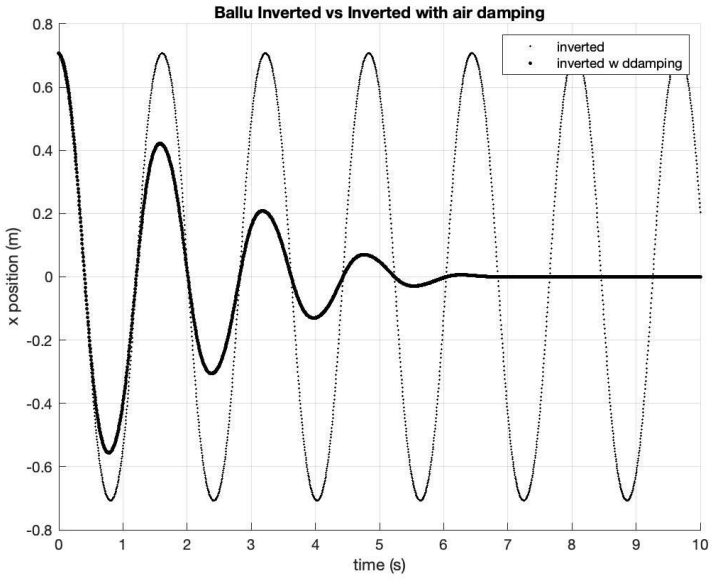

Figure 5.8: Pendulum damping effect.

This introduces a major damping effect which stops the balloon from oscillating after a few oscillations.

5.3.3 Double

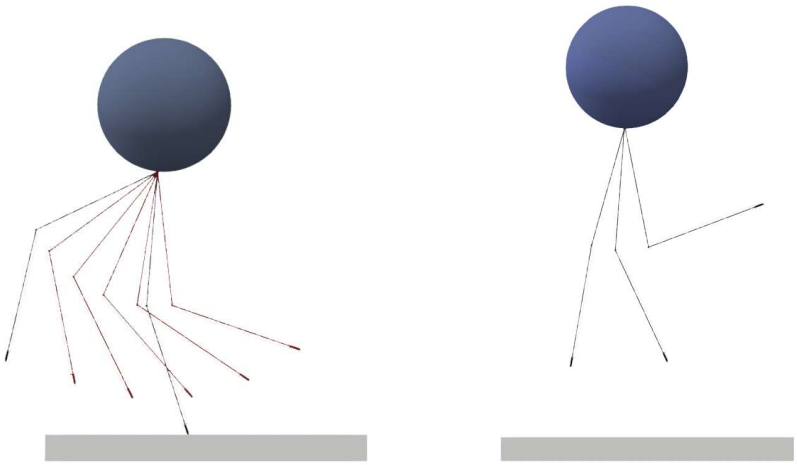

Figure 5.9: Normal double pendulum case. a. with support leg on ground (Left). b. Without support leg on ground (Right)

Now consider a double link leg, with no major mass in the knee and the knee as a passive rotary unactuated joint. In this case, the leg becomes a double pendulum. Since Ballu does not have a fully free passive knee joint, the model needs to be edited for behavior to account for any external input. The figure below compares the motion of the knee joint and foot joint in a normal double pendulum case given the initial angle conditions.

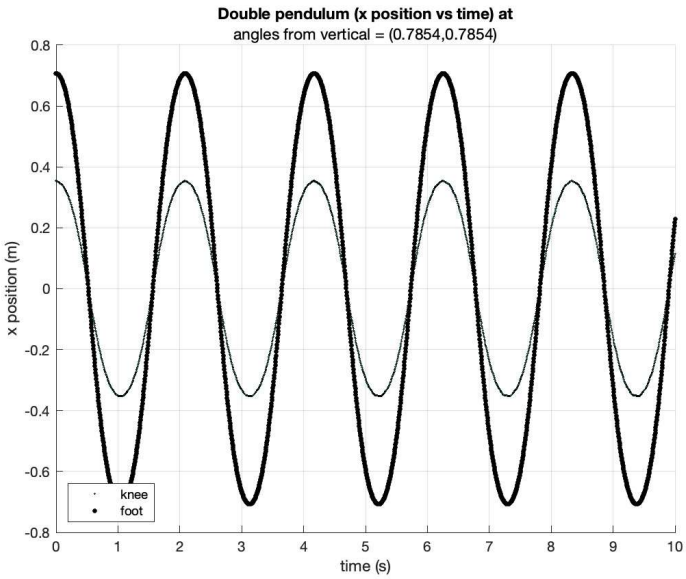

Figure 5.10: Double pendulum case.

Although the figure seems simple and very similar to the single pendulum case, this motion can get very complicated very quickly by simply only changing the initial conditions and angles. The table below shows the alterations in motions given combinations of initial link angles. The knee joint remains passive and unactuated and frictionless for these observations.

Table 5.6: Double pendulum initial conditions vs behavior

Hip ang	*Knee angle = hip-pi*	*Knee angle = hip-3pi/4*	*Knee angle = hip-pi/2*	*Knee angle = hip-pi/4*	*Knee angle = hip*
0	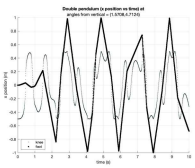	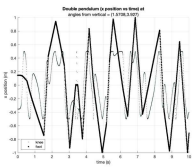	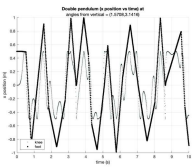	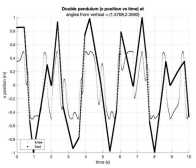	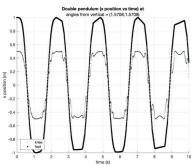
pi/4	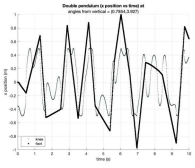	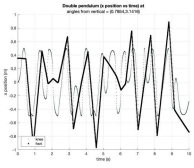	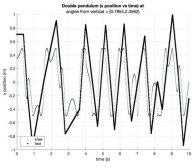	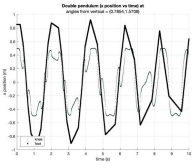	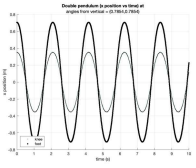
pi/2	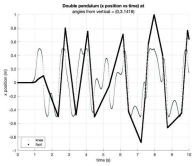	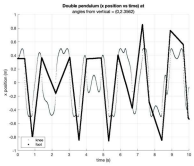	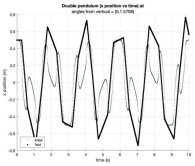	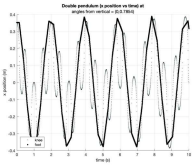	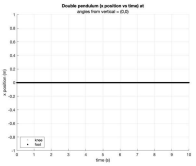
3pi/4	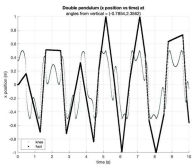	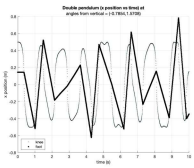	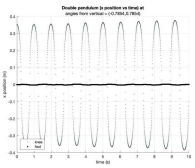	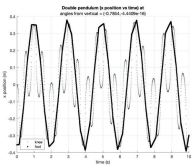	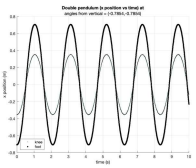
pi	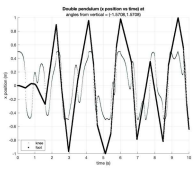	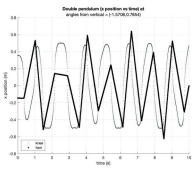	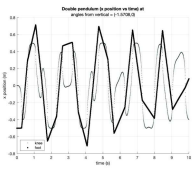	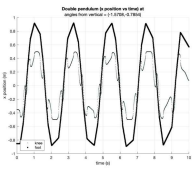	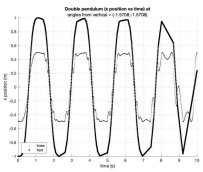

As complex as these motions seem, the total oscillation is rarely interacted with and for control purposes, we are mainly interested in steps and oscillations under one period. Note that even in an unactuated case with no tendon engagement, the robot leg is not modeled as a perfect pendulum system. This is the result of the knee spring assisting the knee opening and resisting it closing and all the other details involved.

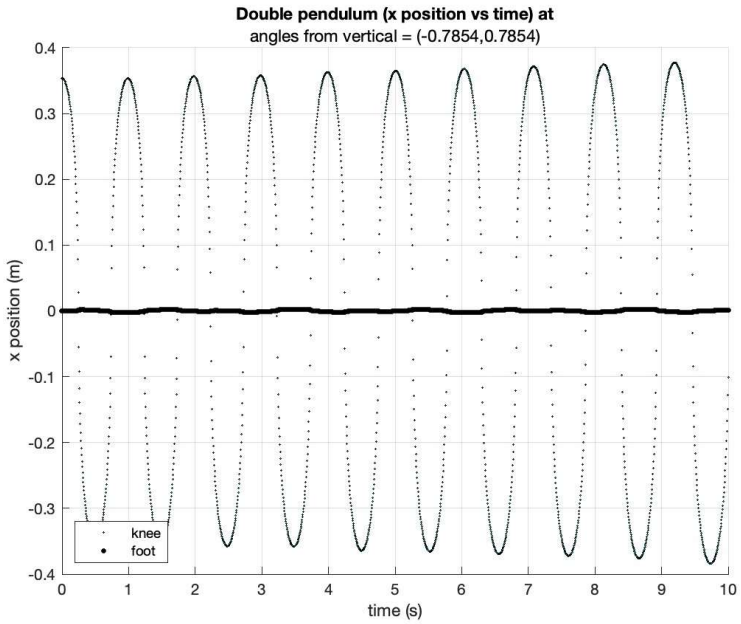

Figure 5.11: Double pendulum motion where lower mass is stable and middle mass is semi stable and oscillating back and forth. Of the cases, this one is my favorite. Like flying between stars, n like the sun blazing in space n v orbit it.

5.3.4 Length Varying Double

When the actuator controls the knee, the system no longer behaves like a double pendulum. Instead it can be modeled in two ways. First is to model it as a simple double pendulum at every instant separately given the calculated dynamics. Second is to model the system as a length varying complex single pendulum, where the link length (hip to foot distance) is a function of knee angle. A Key change here is that when the tendon is engaged, the knee joint does not freely turn. Both methods result in numerical answers, yet when observed from an energy standpoint, we can observe the varying link length changes the period. And the energy changes vary the swing. For a simple oscillation, the following graphs show the effect of opening and closing the knee during oscillation. We observe the following graph which includes the knee forces for a simple closing and opening motion from t=0 to t=2 s.

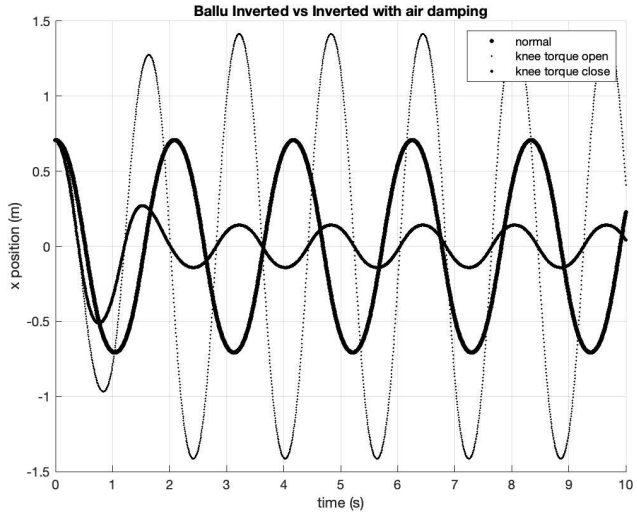

Figure 5.12: Double pendulum vs. double pendulum with knee torque opening it, vs double pendulum with knee torque closing it.

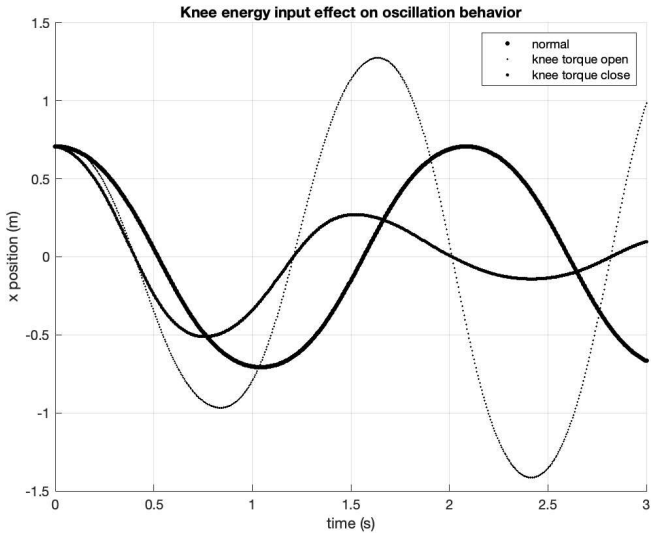

Figure 5.13: Zoomed in view of figure 5.8 with tmax=3s. Note how this energy delta affects motion in a predictive manner

The knee opening input increases the distance between the feet and hip joint and thus the oscillation amplitude increases. Until the input is stopped and normal progression continues. Closing has the opposite effect and reduces the amplitude. There are also changes in oscillation period. By using a combination of these during the non contact phase of the robot's foot, we can control and adjust step placement.

We can study all details about complex pendulums and observe their chaotic motion, although, if we look past the distractions of the motion, we see a very balanced energy dance is happening.

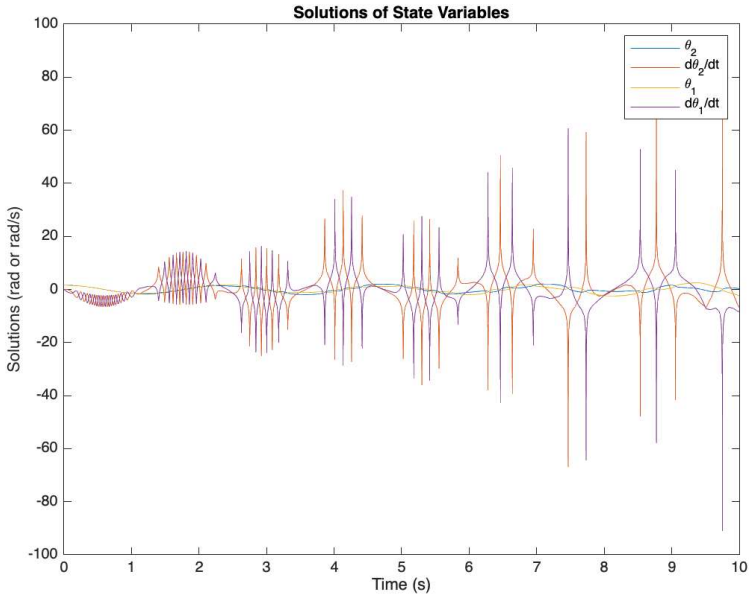

Figure 5.14:Double pendulum solution of state variables. Notice how the derivatives increase in magnitude and yet always cancel eachother out.

5.3.5 Inverted Double

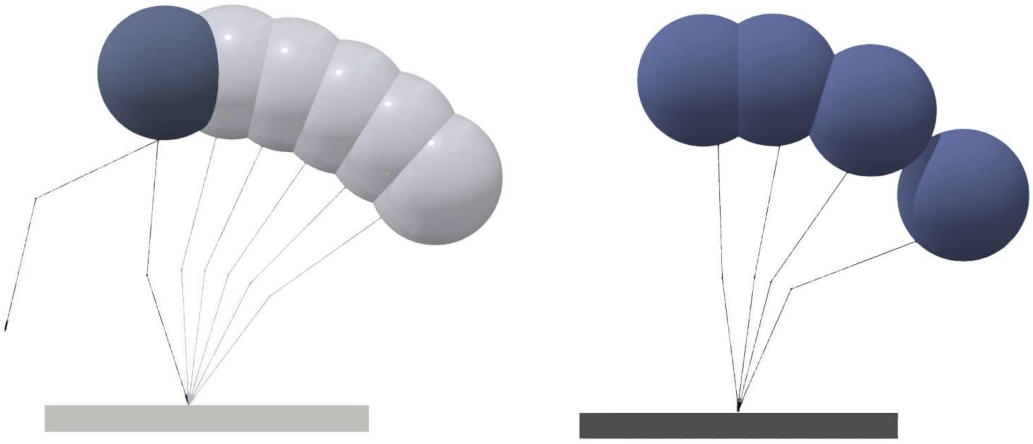

Figure 5.15: Inverted double pendulum motion of BALLU about a base foot.

The inverse of the double pendulum case holds true in similar fashion to the inverted single pendulum. All the behavior will be similar to the normal double pendulum case with the addition of damping and the change from gravity dominated pull to buoyancy dominated.

5.3.6 Length Varying Inverted Double

In the normal case, the foot can adjust quickly, but in this case, the balloon will move slower and if the motion is quick, it may interfere with the normal oscillation and cause unwanted or complex forces that twist and change the balloon hip connection orientation.

5.3.7 A Complex Quadruple Pendulum

The six cases discussed above explain the motion of one leg. In a bipedal system, we have two legs. A combination of pendulums is present. When no ground contact, the pendulums affect each other through the forces exerted on the link connecting the hip joints. With both feet contacting, there will be a complex motion and no clean pendulum oscillatory motion.
The interesting case involves one foot ground contact and the other lifted. Considering the contact foot leg an inverted double pendulum, the no contact leg becomes a double pendulum, attached to the end of an inverted double pendulum. A strange but elegant 4 ink pendulum with a y offset is shown in the figure. As a reminder, even though the system and geometry looks very much like human walking, the forces are totally different.

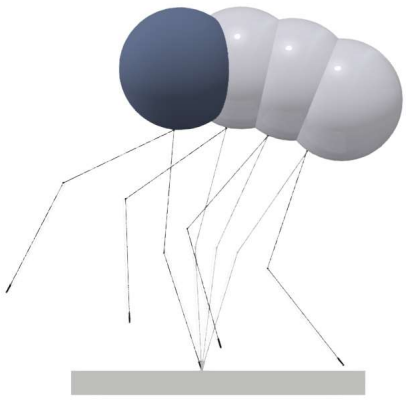

Figure 5.16: Double combination of one normal and one inverted double pendulum during walking.

We assume ground is an anchor, the hip is a mass with buoyancy force, and the free foot a mass with weight. The motion of the oscillation of such a system would be nothing but modern abstract wild art. Note that this complex quadruple pendulum does not behave in an easy to predict manner , hence for motion planning operations we observe it one leg at a time, or we calculate the whole system. As discussed in the previous sections, We can mainly use the contact foot leg as means to adjust the no contact foot's height, and the no contact foot swing as means to set its position for contact. Together, we can use this system for taking accurate steps with these two degrees of freedom. A last case of swing with no foot landing may be used to create twists. Further discussed in the turning strategies section.

5.3.8 A Complex Quintuple Pendulum Tree

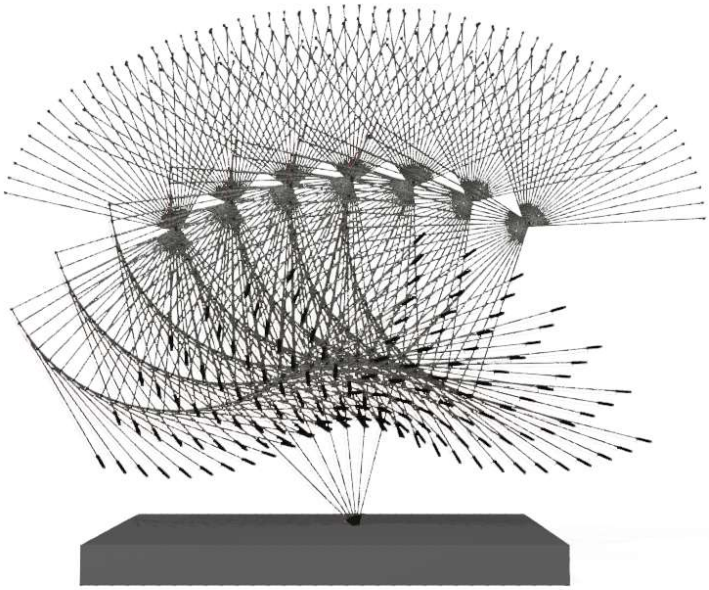

Figure 5.17: BALLU possibility pendulum tree around an anchored foot rotation about one axis.

None of the cases presented discuss the oscillations of the balloon itself around the hip joint. Given the offset from COB to hip joint, any momentum will cause the balloon to oscillate as well. In the figure, the balloon is shown as a link from hip to COB for simplicity purposes. This motion is dampened by air drag and minimized by the major upward buoyancy force. Although small, the effects of this oscillatory behavior are calculated in the overall calculations.

We can still calculate the forces at the hip joint and adjust for this delta. To do this, we create a new matrix for the balloon cob itself and adjust the forces from that frame to the hip frame. This is further shown in the matrices section. Overall with this addition, and an expanded human mind, the whole system may be observed as a complex quintuple pendulum tree.

5.3.9 Pendulum Transition Metric

With all these cases, and with the overall locomotion dependent on these oscillatory motions. In order to achieve smooth motion, not only is it crucial to avoid chaotic sub motions, but it's necessary to define a metric that allows the system to transition between sections efficiently and smoothly. As seen, even a simple initial condition changes the total behavior. Effectively, knee actuation is our only input, yet the timing of this input determines the system output due to complex oscillations and nonlinearity. By sacrificing very accurate foot placement, we can achieve better overall locomotion and walking. Given a known motion desire, and multiple possible solution paths, the pendulum transition metric (PTM) is defined with the following equations for every solution path :

$$Mcobdelta = Mcob(t+dt)-Mcob(t) \tag{5.30}$$

$$Mcordelta = Mcor(t+dt)-Mcor(t) \tag{5.31}$$

$$PTM = Mcordelta - Mcobdelta \tag{5.32}$$

Where Mcob(t) is the momentum about cob at time t and likewise for cor point. The lowest PTM is desired as it limits unwanted robot body twists and impulses while walking. Path planning and dynamic motion selection if discussed in detail in the motion planning section.

This is a good metric to use to limit unwanted body rotations while performing simple motions, but in highly dynamic states, this method of optimization doesn't always work. Even though the mentioned categorizations provide a good initial outlook, their shortcoming is our method of observation. Pendulums don't always act in 2D space. And even though simple ones

may behave predictably in 3d space, complex ones can be very very very wild and seemingly chaotic. And that is exactly what we aim to understand and use to our advantage for new locomotion techniques. The next section discusses 3d pendulum cases, combination pendulums and their equilibrium states. Note that only conditions applying to BALLU are mentioned.

CHAPTER 6

Motion

6.1 Motion Planning

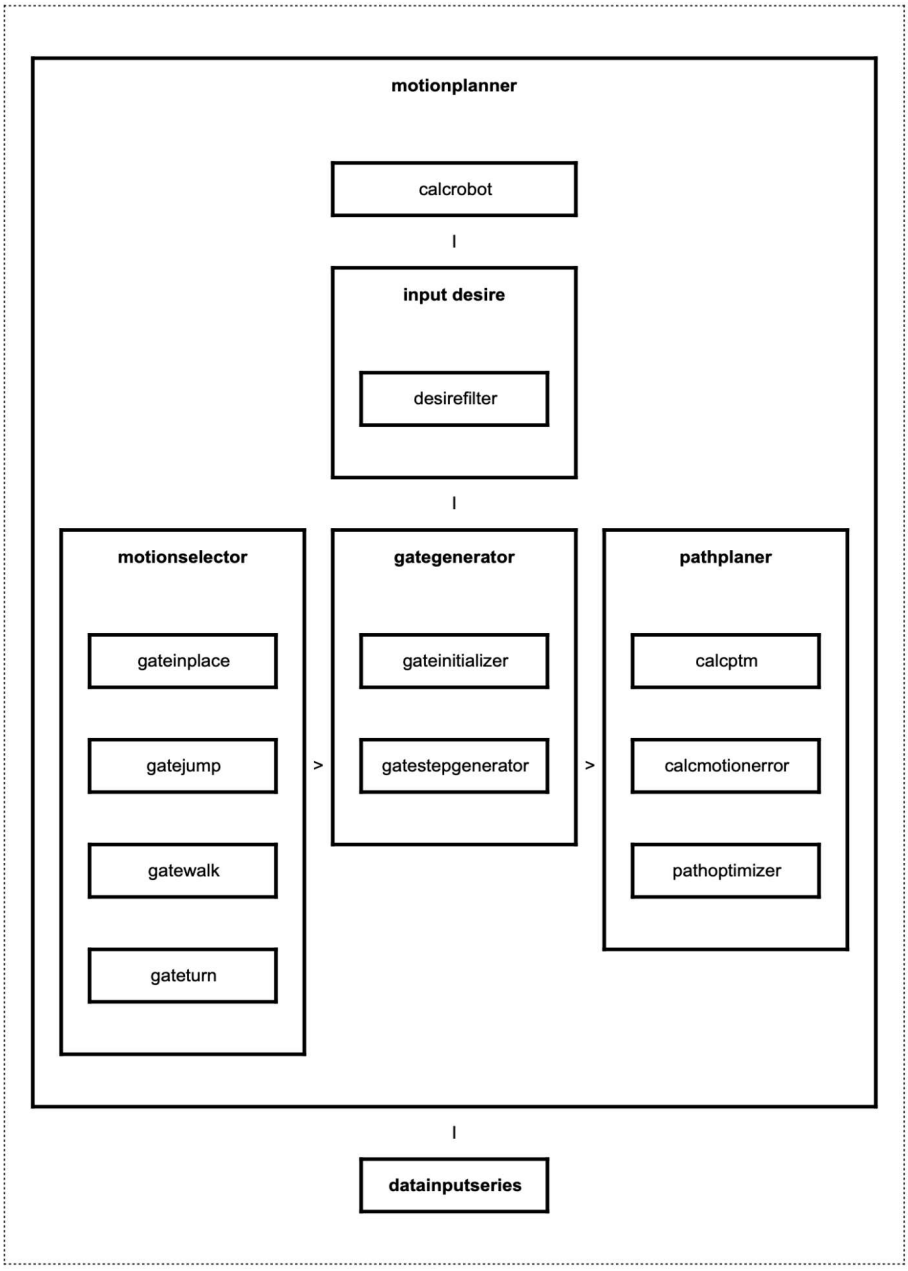

Figure 6.1 Motion planner flowchart.

As observed in the flowchart, a combination of processes lead to proper motion planning. Based on the desired motion, the optimum method will differ. Each type of motion is further discussed in its subsequent section.

6.2 Single Leg Robot Motion

6.2.1 In Place Motion

The single leg may be actuated to pull the balloon down or push it up. By correct actuation timing the leg may also be able to oscillate and push the body forward and back, building up the initiation sequence for motion.

6.2.2 Jumping

Depending on the ratios of buoyancy and mass forces, different motions may be possible. For the single leg robot, given correct actuation input, and timing, the robot has experimentally been able to jump up and forward. These experiments are attached in video form. The physics of this motion is quite simple and will be fully discussed for the bipedal case.

6.2.3 Walking

Walking is undefined by the single leg, the single leg may use small hops to take steps or drag itself forward and back. Both of these motions were possible in simulation and testing.

6.3 Bipedal Motion

6.3.1 In Place Motion

These motions include posing, dancing, and body shift for different sequences.

This section includes single steps, body motion, turning, and dancing. There are two main cases for in place motion. The first case involves both feet staying on the ground while the second case discusses one feet off the ground.

With both feet touching the ground, the robot can stay static, landing, actuating one leg, or actuating both legs. When falling from a height, the robot will land and recover to its original balanced posture. BALLU can easily land and recover when dropped from any height. This is due to the light design, the buoyancy in the body, the compliance in the knees, and the slow terminal velocity as it falls. In specific tests, the robot has been dropped multiple times from heights of more than 20m and has safely recovered back to the upright position.

Fig. 6.2: BALLU prototype being kicked (Left). The prototype being thrown from a building (Right). In both cases, the user is safe, and the robot recovers to its balanced position unharmed.

Fig. 6.3: The robot landing with legs highlighted for clarity (Top). Passive model falling and recovering (Bottom-Sequence left to right).

Note that all landing cases use buoyancy and knee spring to have a fully passive fall recovery. The general equation for finding the terminal velocity of a falling object is given below.

$$v_{Terminal} = \sqrt{\frac{2*m*g}{A*C*\rho}} \qquad (6.1)$$

This equation is derived from eq(2) and the variables stay the same. This equation is derived by setting the drag force equal to the weight of the object. Although in our case, it is necessary to include the buoyancy force. Therefore, the terminal velocity of the robot is approximated using the equation below.

$$v_{Terminal} = \sqrt{\frac{2*(m*g-F_{Bouyancy})}{A*C*\rho}} \quad (6.2)$$

Terminal velocity is calculated with the effect of buoyancy. Clearly, the falling speed reduces as the buoyancy force increases. The variables are similar to the previous equation. With landing velocity and mass known, within a specific landing time, we can calculate the force needed for the robot to fully recover without collapsing. The robot will collapse if the body (hip joint area) hits the feet. That distance is 0.9 m. It is known that impact velocity equals terminal velocity and the stopping velocity is 0 m/s. The required acceleration can be calculated using eq(6).

$$v_{final}{}^2 = v_{Terminal}{}^2 + 2ax \quad (6.3)$$

Where the velocities are known, a is the acceleration required (assuming constant acceleration for simplicity), and x is the distance discussed above.

$$F = ma = (m\, v/t) \quad (6.4)$$

With known acceleration and mass, force is solvable. Although the mass does not include the mass of the feet as they hit the ground. Thus the maximum force required is only provided by the buoyancy and knee springs. Note that the knee springs also help absorb the initial shock of landing that would otherwise propagate through the whole robot.

The next case of in place motion is when both feet are actuated together while they still touch the ground. In this case, the knees are closed and opened. While the knees are closing, the body comes down and when the knees open, the body goes back up. If the buoyancy force could lift the legs, this motion would be simple and the body would move up and down in a straight line.

With the actuation component attached to the ankle section. The knee angle will affect the position of the body. The figure below shows this.

Fig. 6.4: For this prototype, the effect of bending the knee is shown.

As the knees are bending more, the horizontal position of the hip connection is moving forward with respect to feet. If the legs are actuated identically, the body's motion will stay in its original sagittal plane. But, if the actuation of the legs are different, the body will also lean to the side.

Aside from that, if this actuation is done at a high speed, the body will have an initial oscillation which will be dampened by joint frictions and air resistance. These motions control the body's position. This positioning capability can also air other motions such as jumping, hopping, and walking. If used correctly, the oscillation can also give the robot character in its motion.

6.3.2 Jumping

In short, humans bend their knees, lower their center of mass, and then push with their feet to jump. BALLU uses a similar strategy, along with some different ones. Keep in mind that humans use a large number of muscles, tendons, nerves, and a sophisticated control algorithm to jump. In the case of BALLU, each leg has only one DOF. In the case of jumping feet, if both feet jump together, the robot will effectively separate from the ground and perform a jump. The remaining cases are discussed for the single DOF knee actuated robot. This embodiment is designed to hop, jump to small heights, and jump to higher heights. The details of each motion is described in the sections below.

Regarding hopping; The buoyant force is held constant. It cannot lift the robot. Although with enough momentum, it can momentarily lift the robot. By putting the robot in a squat position and then releasing the body, the buoyant component starts pulling the legs to the extended standing position. Although it will also have a certain velocity while moving up. The momentum will cause the whole robot to perform a hopping motion. Going to the squat position is done by actuating and bending the knees. The elastic power chains pull the knee back to its extended position. This pulling force will aid the hopping motion by pushing against the ground and body with a small force. The figure below shows the hopping sequence.

Fig. 6.5: The hopping sequence is shown (Sequence left to right).

Hopping is a key locomotion technique when the effect of gravity is lowered (by buoyancy in this case. For humans it is much easier to hop rather than walk underwater. Similarly, underwater creatures use hopping motions for locomotions. Another case to further highlight this point is astronauts hopping motion on the moon, when the effect of gravity is much lower than earth.

6.3.3 Walking

Tested are oscillatory symmetrically repeating steps with various amplitude and speeds. For momentum considerations, the software is designed to gradually increase step size to maturity and have a few selected lead up steps. In the gait sequence code this is referred to as the adaptcycle. (as observed in plots).

The walking cycles proved to be reliable and follow planned paths in testing for small, medium, and large step cycles.

For all sequences shown below and in the following sections, this experimental setup was used: matlab code generated gate, and sends data to robot through a chain consisting of an arduino, a custom circuit, a IR transmitter, and the IR receiver and chip on board the feet. As shown in the figure.

Figure 6.6: Experimental setup.

The table below summarizes the experiment parameters.

Table 6.1: Experiment setup parameters

Robot platform:	BALLU Biped
Robot force input:	Current control actuation, Knee torque (Left & Right)
Coding Platform:	MATLAB
Simulation Platform:	MATLAB, Autodesk
Electronics:	Arduino uno, custom circuit, IR transmitter
Control type:	Open loop
Observation type:	Human observer, Mounted camera (no feedback control, just recording)
Input variable:	Current, Voltage
Input resolution:	[-1 0 1], [-5…0…5] 0.25 steps
Input refresh rate:	100-20 Hz

The sequence shown below presents the simple walking gate.

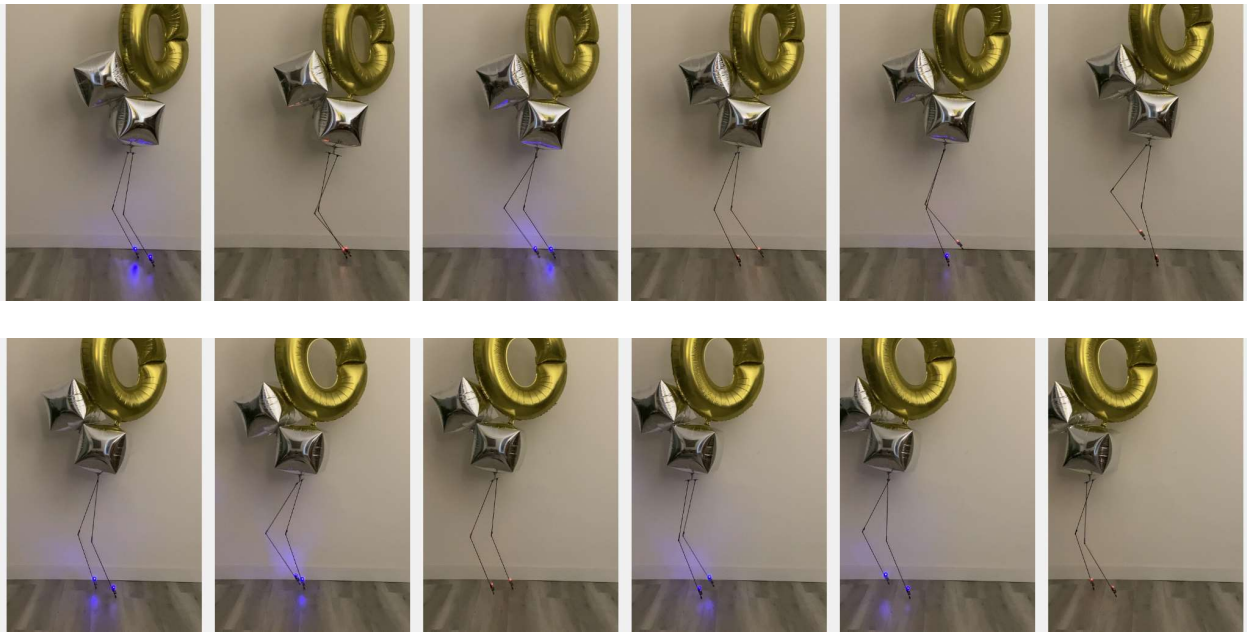

Figure 6.7: Normal walking gait testing. (frames start from top left, to top right and then bottom left to bottom right)

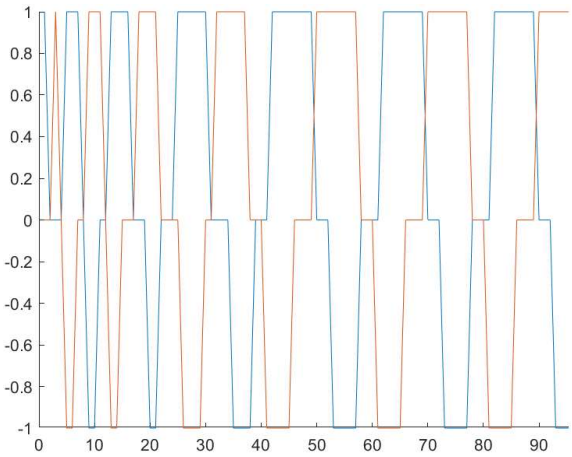

Fig. 6.8: Input motor signals plot for the normal walking gait for the two legs. (y axis is on and off and x axis is number of .05s time increments)

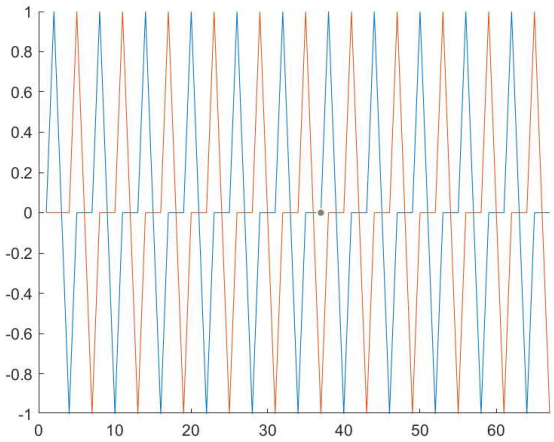

Fig. 6.9: Input motor signals plot for a smaller step walking gait walking gait for the two legs. (y axis is on and off and x axis is number of .05s time increments)

By changing the step size and timing, we can also have gaits with larger step sizes as presented in the next figure.

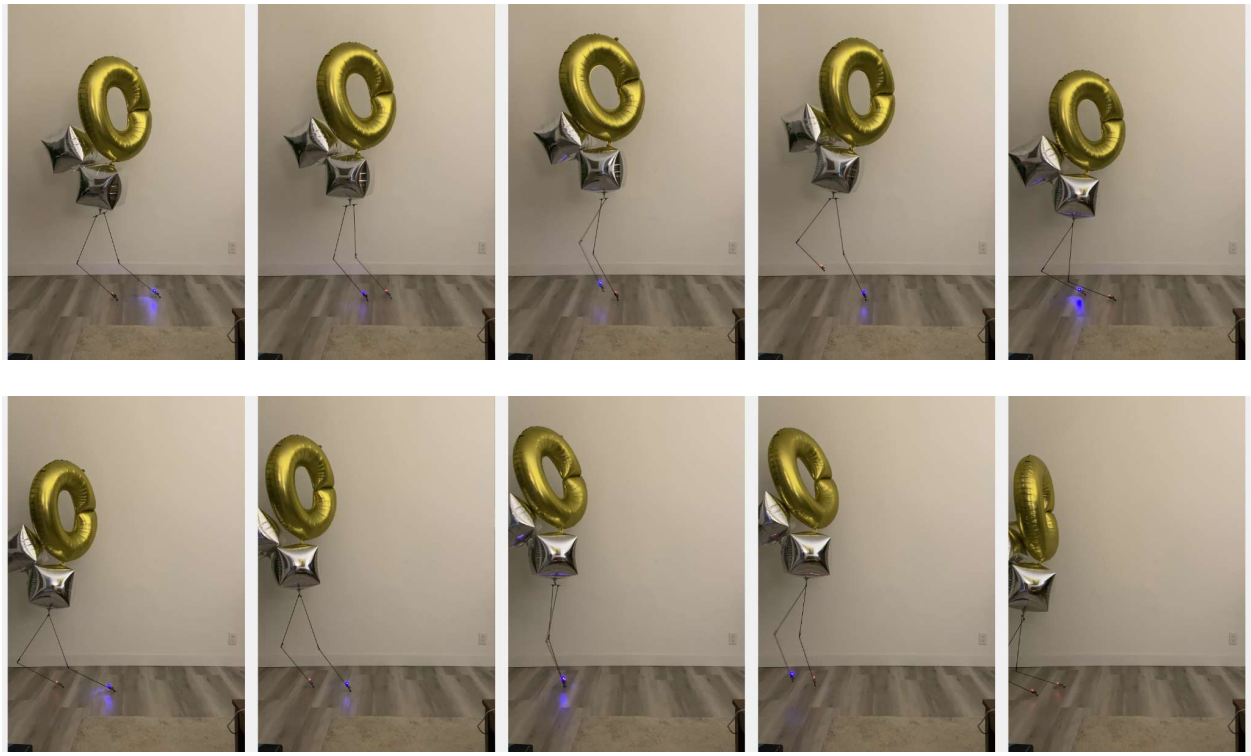

Figure 6.10: Large step walking gait testing. (frames start from top left, to top right and then bottom left to bottom right)

We minimize sudden impulse inputs to the system. To do this, the control software

simultaneously calculates the motion profile and momentum profile of the system for each pendulum combination type. And then selects the transition point at which the impulse is minimum. For example, while taking steps in the bipedal robot, both the swinging leg, and the supporting leg can individually control foot step placement.

Case 1 : swing leg swings, and swing legs knee opens to enable swinging foot ground contact.

Case 2 : swing leg swings, and support legs knee closes to enable swing foot ground contact.

In case one, a sudden knee opening alters the posture, and in case two a body height adjustment. These two change the COR in different ways. It is desired to have the choice with the minimum dynamic cost. That is a combination of these cases together.

There is no need to perform each action immediately as

First, this combination ratio is measured by the following calculation.

$$Pathdelta = desired\ state - current\ state \tag{6.5}$$

Using the mechanics of the robot, we can also achieve a backwards step. First, the tendon is fully disengaged and the legs are straightened out, and the sequence begins. This is possible due to the knee spring force offset initially present. The sequence can be observed in the next figure.

Figure 6.11: Backwards step testing. (frames start from top left, to top right and then bottom left to bottom right)

6.3.4 Turning

Multiple turning methods are tested. The first one is a large step mass shift turning. This is done by lifting one leg and causing a mass offset, then allowing the robot to slowly fall and reorient. The sequence is shown in the next figure.

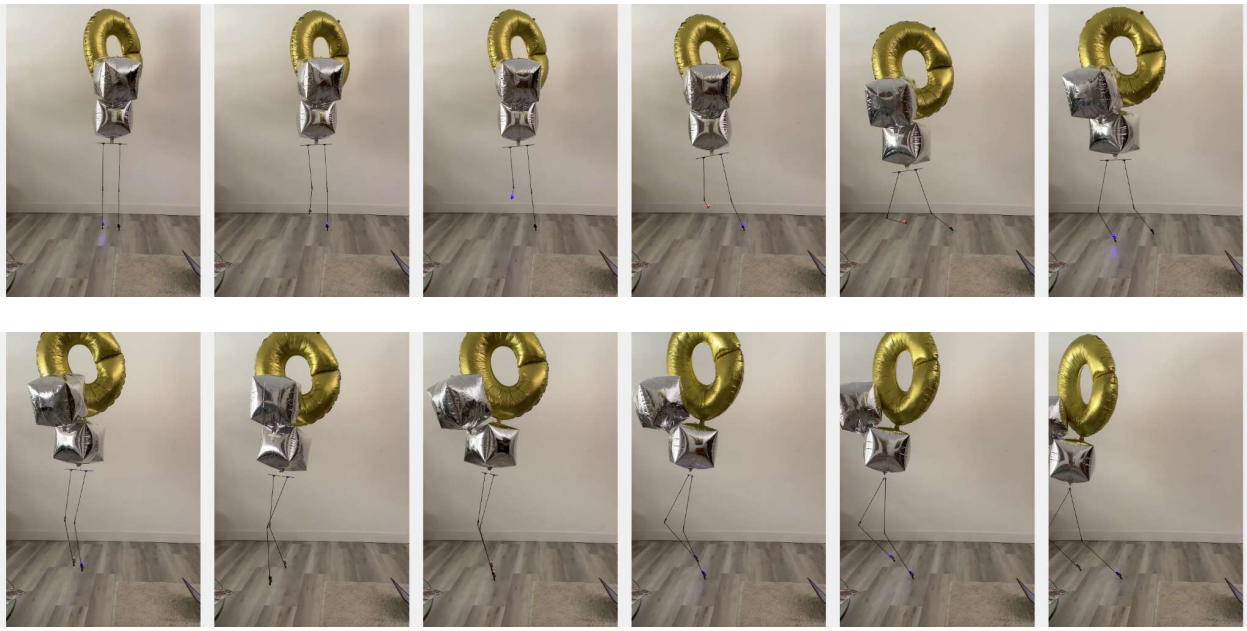

Figure 6.12: Mass shift turning testing. (frames start from top left, to top right and then bottom left to bottom right)

The next method is turning using small unequal steps. With correct step timing, this is easily achievable as shown.

Figure 6.13: Small step turning testing. (frames start from top left, to top right and then bottom left to bottom right)

The next turning method tested, is one using variable actuation in the knees to produce a rotational moment. This is done without the need to take extra steps and presented in the next figure.

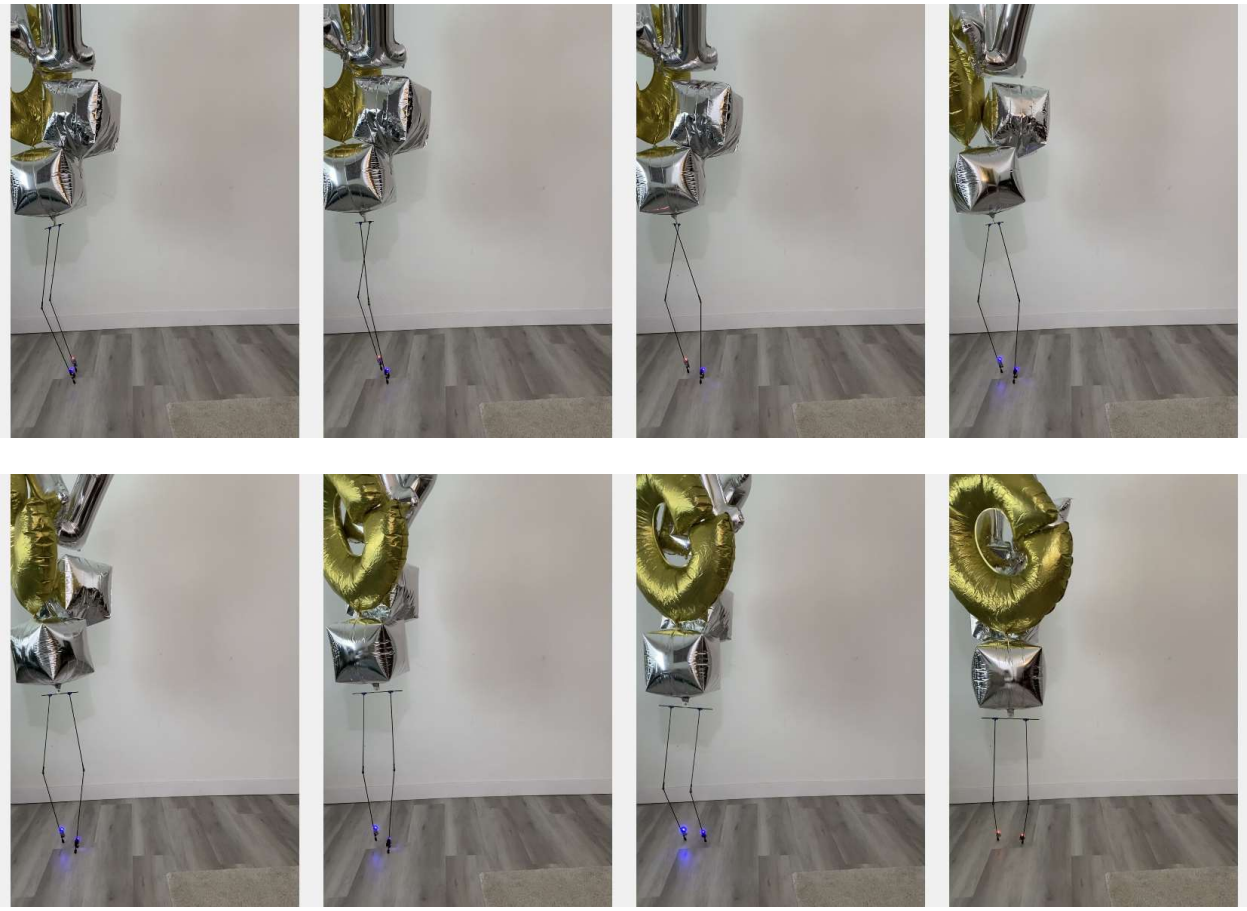

Figure 6.14: Momentum turning testing. (frames start from top left, to top right and then bottom left to bottom right)

The next turning method is torque assisted turning which is discussed in its own section.

6.3.5 Obstacles, stairs, and rough terrain

The robot can easily walk down stairs using a modified walking gait. It can also go over obstacles and actual stairs by simply lifting and placing each leg as shown in the next figure.

Figure 6.15: Ascending stairs. (frames start from top left, to top right and then bottom left to bottom right)

6.4 Novel Motion and Deviations

6.4.1 Sky Jump

SkyJump gives the robot the ability to jump and ascend to very high altitudes. It can potentially allow the robot to fly. This is all done by using air resistance. Imagine if we could claw and climb the atmosphere, like a cliff. The idea is similar to climbing, but instead of fully supporting the weight, we are using a smaller force in a larger range and a longer time. Here is the clarification; because of air resistance, parachutes lower our terminal velocity and allow a safe landing. Imagine attaching a ladder to a parachute and telling a person that is on the ground to start climbing this

lowering ladder. As long as the person climbs the ladder faster than our ladder is lowering, the person will be ascending.

This concept can be turned into a technology which can ascend a mass (robot, human, vehicle …) to an altitude using air resistance. In the case of BALLU, the robot will need a winch to connect its body (buoyant component) to the legs. To jump, first the body will start to rise (using the buoyancy from helium) to an altitude much higher than the required jump height. This is done while the legs are still on the ground. Then, the body and legs are quickly pulled together. The body will descent as the legs ascent. When they meet, the robot will be at the required height. The mass of the legs are much higher than the body, although the body has a large surface area and the legs have a very small surface area. This will assist the height of the jump. The figure below shows the steps of this process.

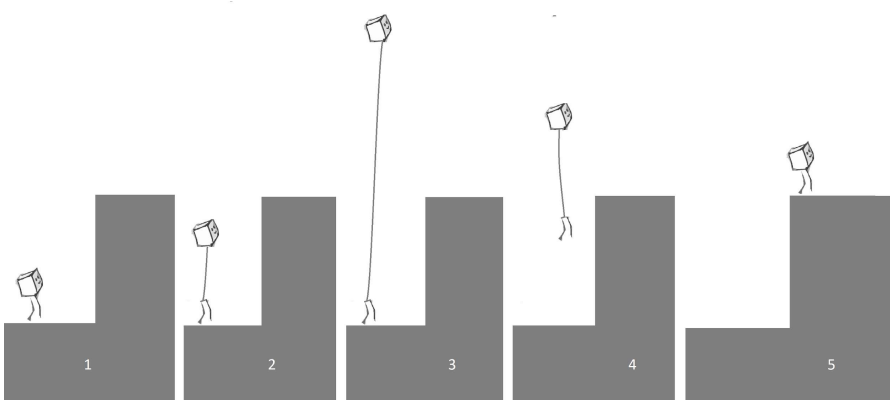

Fig. 6.16: A potential use of SkyJump technology is shown.

A high speed motor, or a sudden release of energy can be used to pull the body and the legs together. For other uses, the legs can be replaced by any mass. The body can be replaced by a parachute or other high surface area component which can initially rise up by buoyancy, a drone, being blasted up, or any other technology. Same process could be used to slow down a mass before

landing from a high velocity fall. Also, if the process is repeated at a fast rate, it can lead to the possibility of flight using air resistance. More on skyjump is discussed in our paper [44].

6.4.2 Torque Assisted in Place Turning

Following our analysis of the complex desire state of the spring, we see how the torque variance and pivot point geometrically change the motion of the system. The concept is understood by considering non-linear and non-one dimensional pendulum equilibrium conditions, and best observed through the simulation with 3d point path recording.

However, to explain, consider the robot with one leg contacting the ground (support leg). While the other leg is swinging, the body experiences two main opposite forces from the buoyancy (upward), and from the swinging foot's weight (downward). Each of these forces creates a moment about the balancing legs contact point. As the orientation of the body changes, depending on the ratio and position of these forces, these two moments may add to cause a net rotation to either direction or cancel eachother out.

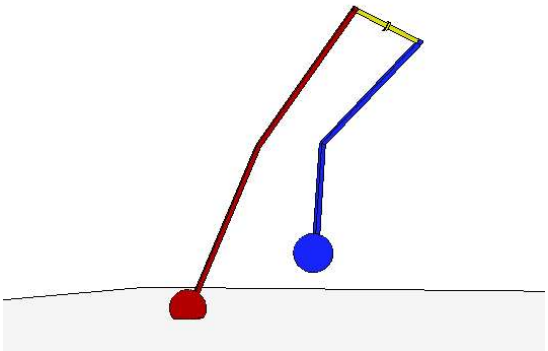

Figure 6.17: Robot positioning with one support leg and body offset angle.

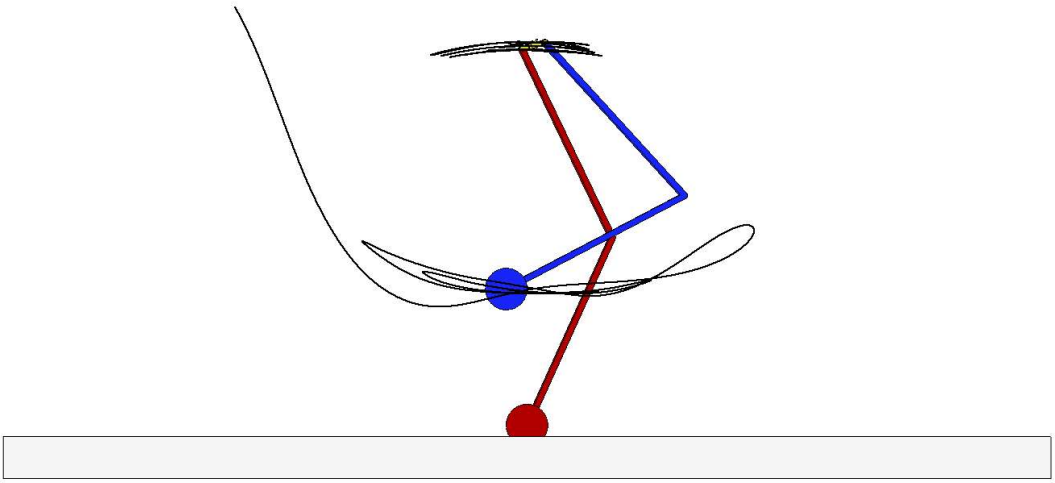

Figure 6.18: Robot positioning with one support leg and one swinging leg side view (leg motion marked and tracked).

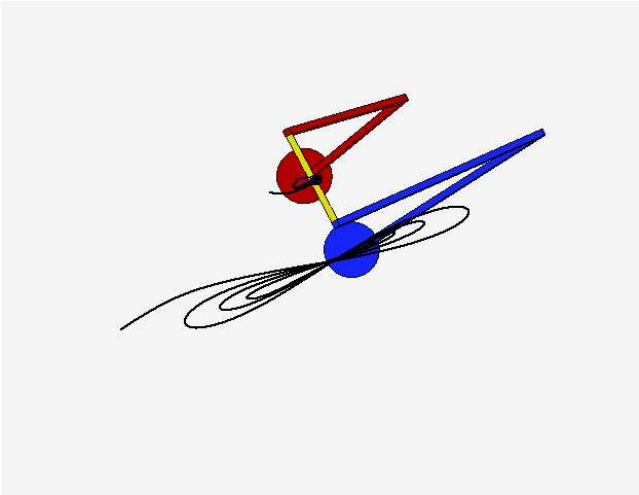

Figure 6.19: Robot positioning with one support leg and one swinging leg top view (leg motion marked and tracked). In a simple oscillation, the twisting about the base foot will cancel out as shown in the tracked swing path.

The figure shows this state. In short, given the robot's geometry and joint architecture, the system will have a lowest energy cost motion when the knees are actuated. In some specific cases, the robot can experience a dynamic twist instead of a leg swing. This means the body rotates but the

mass points won't move much. Testing this method is shown in the next figure. This phenomena makes for a new elegant method for turning without using traditional methods and is a topic of future research.

Figure 6.20: Torque assisted turning testing. (frames start from top left, to top right and then bottom left to bottom right)

CHAPTER 7

Conclusion

7.1 Results

Experimentation results and simulations follow the same behavior. The motion is categorized through its cases and pendulum classifications. The data along with testing, point towards the direction of system reliability and control accuracy. To get to optimal levels and experiment with faster dynamic gates and smaller unwanted disturbances, its crucial to make some changes. These are further discussed in limitations, potential and future work sections. The goal and contribution of this research has been to Organization and classification of behavior understanding, and proposing novel unique methods of movement and locomotion for a buoyancy assisted biped robot.

7.2 Limitations

Any advantage comes along with some disadvantages and limitations. This section discusses the current limitations of this technology. Due to the lightweight design, it takes a small force to disturb the state of the robot. One of the main disturbances affecting the motion is wind. The robot can only function in a windy environment if it is equipped with active balancing technology such as propellers to compensate for the disturbances. Or the robot has a method of decreasing surface area and increasing joint stiffness which are future topics. In addition to the disturbance issue, the robot cannot currently generate large forces to do certain tasks. It cannot be equipped with the actuation power needed. Carrying heavy objects is also a limitation.

Although carrying sensors and cameras is possible and one of the uses of the robot. Note that heavy objects may be stored and placed in the feet. The only locomotion strategy that can move a larger mass on the feet is the single DOF jumping feet strategy. These objects are not limited to stay in the feet region. For example certain sensors can have the sensing component on the body of the robot while the heavy components are stored in the feet.

7.3 Future work

Some avenues of future research and improvements include; Faster fluid locomotion through oscillation gait planning, Software improvements, Hardware improvements, modularity and system integration work.

The robot can also be equipped with a camera and microphone to transfer video and sound. Thus people can control the robot remotely. For example this can be used to have video calls with the added dimension of locomotion. This being said, the robot is currently only capable of walking at a slow pace. Although many robots are present at a certain location, all the information and personalization of one robot may be transferred to another robot at a more convenient location. With this method the robots can be teleported and used for specific tasks given their schedule and location. This can be specifically beneficial for audience targeted advertisements.

As briefly stated, some functionalities of the robot may be controlled from the environment rather than being on the robot. These include processing, projection, and actuation. BALLU is a lightweight robot that is greatly affected by air resistance and outside forces. We can turn this disadvantage to an advantage by using these outside disturbances to further stabilize and control

the robot. In a closed environment, we can use air vortices to hit the robot. Air vortices can travel through air without losing much of their energy. By directing them in a controlled manner toward the robot, it is possible to push or adjust the robot's location and motion as required. To do this properly, these vortices have to be generated and directed from accurately positioned robotic gimbals that are installed within the environment.

When operating multiple robots at an area, managing, fixing, and refilling the robots is necessary. One method of arrival and departure of the robots from an exhibit is using a ceiling mount conveyor. The robots are initially stuck to the conveyor. Then the legs are released to land without the body. The body is then detached from the conveyor and winched down to connect back to the legs. The opposite is done for the departure and storage of the robots. The figure below illustrates this scenario.

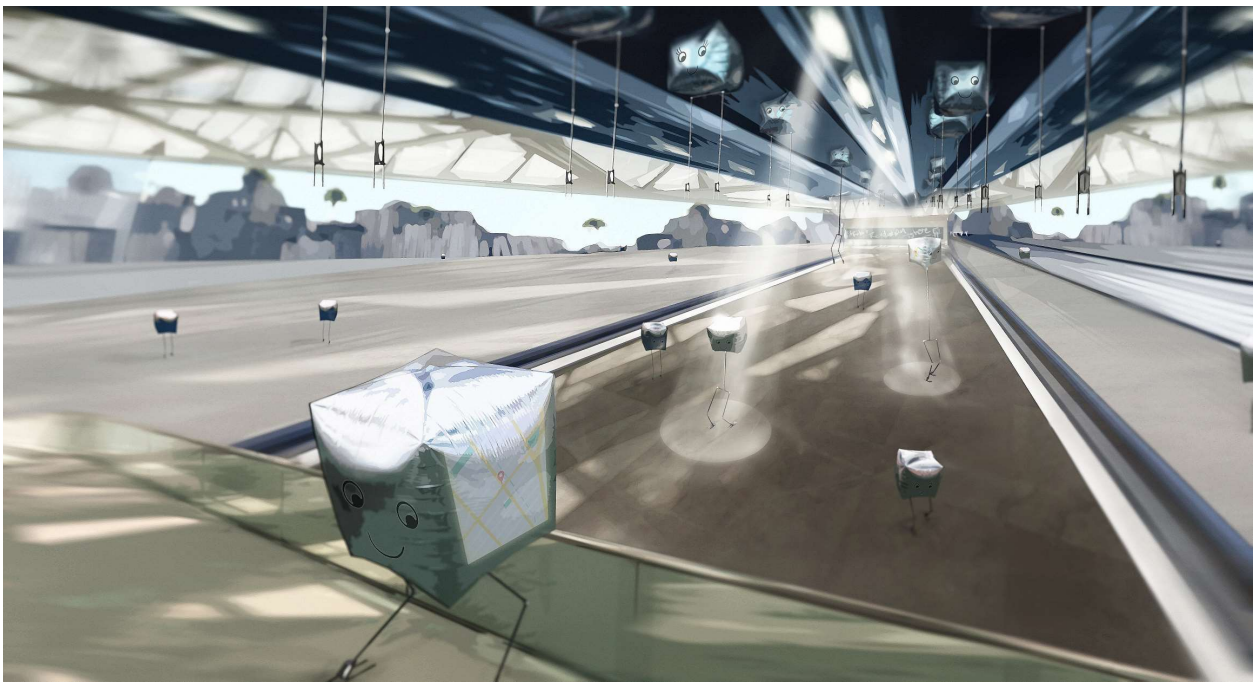

Figure 7.1: The arrival and retrieval of robots from a ceiling mount conveyor system is shown.

This technology shows potential in multiple directions. Yet the most important advantage of this buoyancy assisted lightweight robot is its safety while in operation. Due to the soft body and the light weight, the robot will not damage any human. It is also stable and won't fall on anyone. Additionally, the passive and elastic properties of the joints allows for additional safety. By being passive and elastic, the legs could adjust when hitting an object. The trajectory of the motion will change, but the robot and the object (which can be a human) will not be damaged. A human scale version of BALLU is so safe to operate that even a small child can comfortably interact with the technology.

This technology can take many different forms in addition to the bipedal design discussed. Some of these designs are discussed below. The first alteration to this design can be a scaling change. To be ideal for different tasks, the size of the robot can be changed. For example in an expo environment, smaller robots can act as guides interacting with individuals while larger scale robots can act as moving information stands and billboards.

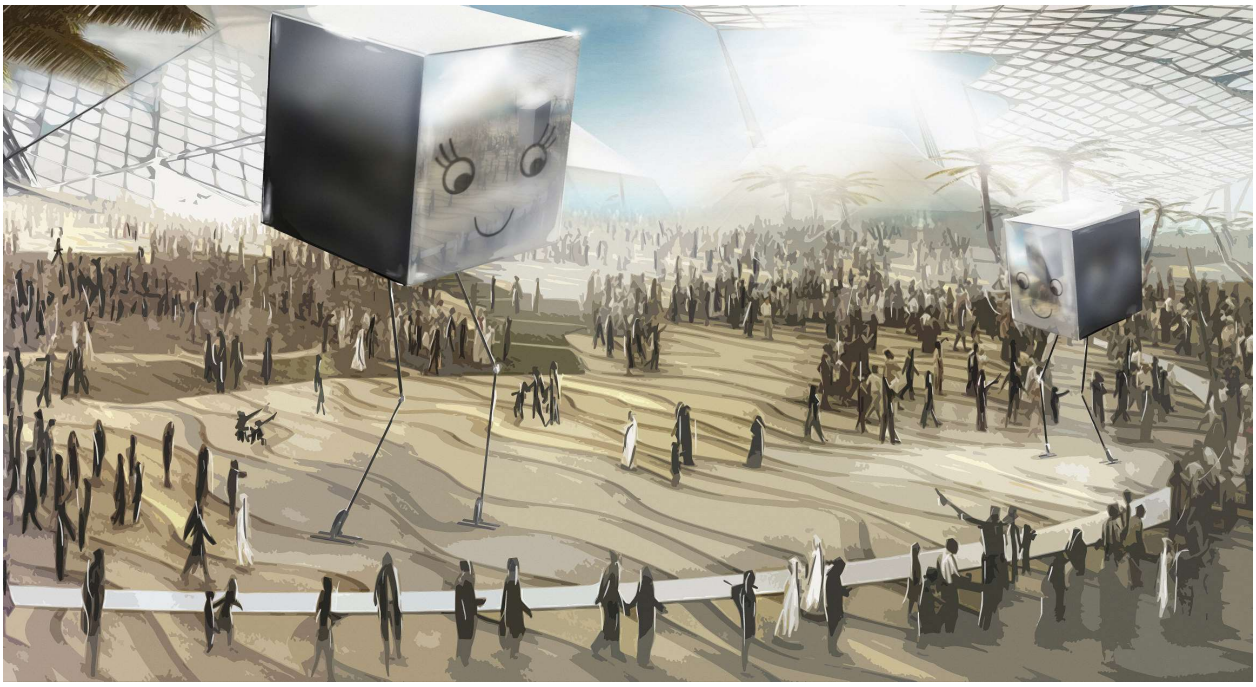

Figure 7.2: Render of biped large scale BALLU walking amongst people.

In addition to overall scaling, the shape of the body and the ratio of body to leg can lead to possible new functionalities. Changing the number and size of legs will also lead to some interesting uses. For example a robot with only one leg is able to hop and move. This can be an additional robot, and it can show that the bipedal design can partially function with only one leg. Decreasing legs will limit the motion. However, increasing the number of legs allows for better stability and a wider range of motion. One example is a quadruped BALLU.

The addition of the two new feet limits the motion of the body and aids the stability.
Early non-actuated prototypes show that this setup can be potentially useful for very rough terrains and climbing tasks. The figure compared mountain goats on a cliff to the quadruped version of BALLU. These robots may be actuated using the legs, or remotely using air vortices.

7.4 Potential

Due to the new design architecture, BALLU has extra limitations, but it also has some new capabilities and potential that other robots do not possess. The first one is that the robot passively balances using buoyancy. It can walk on a tightrope, remain balanced on a skateboard, surfboard, or any other task requiring such balancing. This may look as an entertainment purpose, but it is also useful when a higher vantage point is needed in sensing operations. In certain scenarios, the lightweight design allows for easier climbing of cliffs and walls. The positioning of the feet is key in these scenarios. Some other interesting functionalities relate to walking strategies. Also, as

long as the feet are buoyant enough to stay above water, the robot can walk on water. In addition to these functionalities, the balloons can be designed to accommodate different needs.

Figure 7.3: A sketch.

BALLU is a lightweight, ultra safe, stable, low cost robot with natural motion. It can be used in various scales and formats. It can be used in applications from entertainment, to rough terrain remote exploration, and testing in hazardous environments. This platform can be used as a transportable display and recording device for a multitude of uses. And again, it is the only robot that never falls and can jump off a tall building and continue walking. This being said, the robot currently functions best indoors. These functionalities will also require many future improvements to function perfectly. Afterall, the functionalities can only increase and improve in time. In summary, the realization of this playful balloon bot idea is just a step. The creation of BALLU is a step in the path of creating technologies that allows us to understand dynamic systems better, and use them to our advantage in specific desired areas of interest. And to create an exciting future.

BIBLIOGRAPHY

1. Needham, Joseph (1991). Science and Civilisation in China: Volume 2, History of Scientific Thought. Cambridge University Press. ISBN 978-0-521-05800-1.

2. Hero of Alexandria; Bennet Woodcroft (trans.) (1851). Temple Doors opened by Fire on an Altar. Pneumatics of Hero of Alexandria. London: Taylor Walton and Maberly (online edition from University of Rochester, Rochester, NY). Retrieved on 2008-04-23.

3. Moran, Michael E. (December 2006). "The da Vinci robot". Journal of Endourology. 20 (12): 986–90. doi:10.1089/end.2006.20.986. PMID 17206888. ... the date of the design and possible construction of this robot was 1495 ... It is now known that da Vinci's robot would have had the outer appearance of a Germanic knight."

4. US, Christoph Salge,The Conversation. "Asimov's Laws Won't Stop Robots from Harming Humans, So We've Developed a Better Solution". Scientific American. Retrieved 2021-11-04.

5. "Humanoid History -WABOT-". www.humanoid.waseda.ac.jp. Archived from the original on 1 September 2017. Retrieved 3 May 2018.

6. "Electric Dreams - Marc Raibert". robosapiens.mit.edu. Archived from the original on 8 May 2005. Retrieved 3 May 2018.

7. Raibert, Marc H. Legged robots that balance. MIT press, 1986.

8. Raibert, Marc. "Dynamic legged robots for rough terrain." 2010 10th IEEE-RAS International Conference on Humanoid Robots. IEEE, 2010.

9. Guizzo, Erico. "By leaps and bounds: An exclusive look at how boston dynamics is redefining robot agility." IEEE Spectrum 56.12 (2019): 34-39.

10. "Honda | ASIMO | ロボット開発の歴史". honda.co.jp. Archived from the original on 2005-12-29. Retrieved 2005-11-15.

11. "Aldebaran Robotics". Archived from the original on 2010-06-14. Retrieved 2012-10-18.

12. "Darwin-OP - ROBOTS: Your Guide to the World of Robotics". robots.ieee.org. Retrieved 2021-11-05.

13. "Say Hello to Robonaut2, NASA's Android Space Explorer of the Future". Popular Science. 5 February 2010. Archived from the original on 2010-02-07.

14. Park, Ill-Woo, et al. "Mechanical design of the humanoid robot platform, HUBO." Advanced Robotics 21.11 (2007): 1305-1322.

15. Han, Jeakweon, and Dennis Hong. "Development of a full-sized bipedal humanoid robot utilizing spring assisted parallel four-bar linkages with synchronized actuation." International design engineering technical conferences and computers and information in engineering conference. Vol. 54839. 2011.

16. Krotkov, Eric, et al. "The DARPA robotics challenge finals: Results and perspectives." The DARPA robotics challenge finals: Humanoid robots to the rescue (2018): 1-26.

17. Atkeson, Christopher G., et al. "What happened at the DARPA robotics challenge finals." The DARPA robotics challenge finals: Humanoid robots to the rescue (2018): 667-684.

18. Pratt, Jerry. "DARPA Robotics Challenge (DRC) Using Human-Machine Teamwork to Perform Disaster Response with a Humanoid Robot." Florida Institute for Human and Machine Cognition Inc. Pensacola United States (2017).

19. Knabe, Coleman, et al. "Design of a series elastic humanoid for the DARPA Robotics Challenge." 2015 IEEE-RAS 15th International Conference on Humanoid Robots (Humanoids). IEEE, 2015.

20. Lahr, Derek, et al. "Early developments of a parallelly actuated humanoid, SAFFiR." International Design Engineering Technical Conferences and Computers and Information in Engineering Conference. Vol. 55942. American Society of Mechanical Engineers, 2013.

21. Ghassemi, Sepehr, et al. "Feasibility study of a novel biped NABiRoS: Non anthropomorphic bipedal robotic system." 2016 IEEE-RAS 16th International Conference on Humanoid Robots (Humanoids). IEEE, 2016.

22. Yu, Jeffrey, et al. "Investigation of a non-anthropomorphic bipedal robot with stability, agility, and simplicity." 2016 13th International Conference on Ubiquitous Robots and Ambient Intelligence (URAI). IEEE, 2016.

23. Yu, Jeffrey, et al. "Exploration of turning strategies for an unconventional non-anthropomorphic bipedal robot." International Design Engineering Technical Conferences and Computers and Information in Engineering Conference. Vol. 58189. American Society of Mechanical Engineers, 2017.

24. Ghassemi, Sepehr, and Dennis Hong. "Investigation of a novel continuously rotating knee mechanism for legged robots." 2018 15th International Conference on Ubiquitous Robots (UR). IEEE, 2018.

25. Raibert, Marc H., and Jessica K. Hodgins. "Animation of dynamic legged locomotion." Proceedings of the 18th annual conference on Computer graphics and interactive techniques. 1991.

26. Marc H Raibert, H Benjamin Brown Jr, and Michael Chepponis. “Experiments in balance with a 3D one-legged hopping machine.” The International Journal of Robotics Research, 3(2):75–92, 1984

27. RMcn Alexander. “Mechanics of bipedal locomotion.”Perspectives in experi-mental biology,1:493–504, 1976.

28. Jose A Cobano, Joaquin Estremera, and P Gonzalez De Santos. ”Robotics and Autonomous Systems,56(9):751–761, 2008.

29. John J Craig.Introduction to robotics. Pearson Educacion, 2006

30. Yukai Gong and Jessy W Grizzle. “Zero dynamics, pendulum models, and angularmomentum in feedback control of bipedal locomotion.”Journal of DynamicSystems, Measurement, and Control,144(12):121006, 2022.

31. Hugh Herr and Marko Popovic. Angular momentum in human walking. The Journal of Experimental Biology, 211(4):467–481, 2008.

32. Jeakweon Han and Dennis Hong. Development of a full-sized bipedal humanoid robot utilizing spring assisted parallel four-bar linkages with synchronized actuation. In International Design Engineering Technical Conferences and Computers and Information in Engineering Conference, pages 799–806, 2011.

33. Shuuji Kajita, Fumio Kanehiro, Kenji Kaneko, Kiyoshi Fujiwara, Kensuke Harada, Kazuhito Yokoi, and Hirohisa Hirukawa. “Biped walking pattern generation by using preview control of zero-moment point.” In ICRA, volume 3, pp.1620–1626, 2003.

34. Thomas A McMahon and George C Cheng. “The mechanics of running: how does stiffness couple with speed?”Journal of biomechanics,23:65–78, 1990.

35. Jerry E Pratt and Sergey V Drakunov. “Derivation and application of a conserved orbital energy for the inverted pendulum bipedal walking model.” InProceedings2007 IEEE International Conference on Robotics and Automation, pp. 4653–4660. IEEE, 2007.

36. Gill A Pratt and Matthew M Williamson. “Series elastic actuators.” In Intelligent Robots and Systems 95.’Human Robot Interaction and Cooperative Robots’, Proceedings. 1995 IEEE/RSJ International Conference on, volume 1, pp. 399–406.IEEE, 1995.

37. Jeffrey Chen Yu.Control Implementation of Dynamic Locomotion on Compliant, Underactuated, Force-Controlled Legged Robots with Non-Anthropomorphic Design University of California, Los Angeles, 2020.

38. A. W. Winkler, F. Farshidian, D. Pardo, M. Neunert, and J. Buchli. Fast trajectory 136 optimization for legged robots using vertex-based zmp constraints. IEEE Robotics and Automation Letters, 2(4):2201–2208, Oct 2017.

39. Luis Sentis and Oussama Khatib. A whole-body control framework for humanoids operating in human environments. In Proceedings 2006 IEEE International Conference on Robotics and Automation, 2006. ICRA 2006., pages 2641–2648. IEEE, 2006.

40. Derek Lahr, Viktor Orekhov, Bryce Lee, and Dennis Hong. Early developments of a parallelly actuated humanoid, saffir. In ASME 2013 international design engineering technical conferences and computers and information in engineering conference, pages V06BT07A054–V06BT07A054. American Society of Mechanical Engineers, 2013.

41. Evan Ackerman. Agility robotics introduces cassie, a dynamic and talented robot delivery ostrich, 2017.

42. Ghassemi, Sepehr, and Dennis Hong. "Feasibility study of a novel robotic system BALLU: Buoyancy assisted lightweight legged unit." 2016 IEEE-RAS 16th International Conference on Humanoid Robots (Humanoids). IEEE, 2016.

43. Ghassemi, Sepehr, et al. "Feasibility study of a novel biped NABiRoS: Non anthropomorphic bipedal robotic system." 2016 IEEE-RAS 16th International Conference on Humanoid Robots (Humanoids). IEEE, 2016.

44. Lin, Xuan, et al. "Feasibility Study of an Aerial Lifting Device Using Aerodynamic Drag for Ascent." International Design Engineering Technical Conferences and Computers and Information in Engineering Conference. Vol. 59247. American Society of Mechanical Engineers, 2019.

45. Maekawa, Azumi, Ryuma Niiyama, and Shunji Yamanaka. "Aerial-biped: A new physical expression by the biped robot using a quadrotor." ACM SIGGRAPH 2018 Emerging Technologies. 2018. 1-2.

46. Kim, Kyunam, et al. "A bipedal walking robot that can fly, slackline, and skateboard." Science Robotics 6.59 (2021): eabf8136.

47. Zhang, Chi, et al. "Biologically inspired jumping robots: A comprehensive review." Robotics and Autonomous Systems 124 (2020): 103362.

48. Salagame, Adarsh, et al. "A Letter on Progress Made on Husky Carbon: A Legged-Aerial, Multi-modal Platform." arXiv preprint arXiv:2207.12254 (2022).

49. Yamada, Yasuyuki, and Taro Nakamura. "Gerwalk: Lightweight mobile robot with buoyant balloon body and bamboo rimless wheel." 2018 IEEE International Conference on Robotics and Biomimetics (ROBIO). IEEE, 2018.

50. Song, Seung Hwan, and Hyouk Ryeol Choi. "Design, Control and Implementation of Torus-Type Omniorientational Blimp With Tilting Actuators." IEEE Access 9 (2021): 147985-147993.

51. Rodriguez-Barroso, Alejandro, and Roque Saltaren. "Cable-Driven Robot to Simulate the Buoyancy Force for Improving the Performance of Underwater Robots." International Conference on Cable-Driven Parallel Robots. Cham: Springer International Publishing, 2021.

52. Chen, Yang, et al. "Sideways crab-walking is faster and more efficient than forward walking for a hexapod robot." Bioinspiration & Biomimetics 17.4 (2022): 046001.

53. Matsumoto, Osamu, Shuuji Kajita, and Kiyoshi Komoriya. "Flexible locomotion control of a self-contained biped leg-wheeled system." Intelligent Robots and Systems, 2002. IEEE/RSJ International Conference on. Vol. 3. IEEE, 2002.

54. Jeans, J. Blake, and Dennis Hong. "IMPASS: Intelligent mobility platform with active spoke system." Robotics and Automation, 2009. ICRA'09. IEEE International Conference on. IEEE, 2009.

55. Tadakuma, Kenjiro, et al. "Mechanical design of the wheel-leg hybrid mobile robot to realize a large wheel diameter." Intelligent Robots and Systems (IROS), 2010 IEEE/RS International Conference on. IEEE, 2010.

56. Shih, Ching-Long. "Ascending and descending stairs for a biped robot." IEEE Transactions on Systems, Man, and Cybernetics-Part A: Systems and Humans 29.3 (1999): 255-268.

57. Kajita, Shuuji, Hirohisa Hirukawa, Kensuke Harada, and Kazuhito Yokoi. Introduction to Humanoid Robotics, Springer-Verlag, Berlin, 2005.

58. J. Buchli, M. Kalakrishnan, M. Mistry, P. Pastor and S. Schaal, "Compliant quadruped locomotion over rough terrain," Intelligent Robots and Systems, 2009. IROS 2009. IEEE/RSJ International Conference on, St. Louis, MO, 2009, pp. 814-820.

59. Kuindersma, Scott, et al. "Optimization-based locomotion planning, estimation, and control design for the atlas humanoid robot." Autonomous Robots 40.3 (2016): 429-455.

60. Stumpf, Alexander, et al. "Supervised footstep planning for humanoid robots in rough terrain tasks using a black box walking controller." Humanoid Robots (Humanoids), 2014 14th IEEE-RAS International Conference on. IEEE, 2014.

61. K. Hirai, M. Hirose, Y. Haikawa and T. Takenaka, "The development of Honda humanoid robot," Robotics and Automation, 1998. Proceedings. 1998 IEEE International Conference on, Leuven, 1998, pp. 1321-1326 vol.2.

62. S. Lohmeier, T. Buschmann and H. Ulbrich, "Humanoid robot LOLA," Robotics and Automation, 2009. ICRA '09. IEEE International Conference on, Kobe, 2009, pp. 775-780.

63. K. Kaneko et al., "Humanoid robot HRP-4 -Humanoid robotics platform with lightweight and slim body," Intelligent Robots and Systems (IROS), 2011 IEEE/RSJ International Conference on, San Francisco, CA, 2011, pp. 4400-4407.

64. E. Guizzo and E. Ackerman, "The rise of the robot worker," in IEEE Spectrum, vol. 49, no. 10, pp. 34-41,October 2012.

65. Zielinska, Teresa, and Andrzej Chmielniak. "Biologically Inspired Motion Synthesis Method of Two-legged Robot with Compliant Feet." Robotica 29.07 (2011): pp. 1049-057.

66. K. Takahashi, M. Noda, D. N. Nenchev, Y. Tsumaki and A. Sekiguchi, "Static Walk of a Humanoid Robot Based on the Singularity-Consistent Method," Intelligent Robots and Systems, 2006 IEEE/RSJ International Conference on, Beijing, 2006, pp. 5484-5489.

67. S. Kajita, F. Kanehiro, K. Kaneko, K. Yokoi and H. Hirukawa, "The 3D linear inverted pendulum mode: a simple modeling for a biped walking pattern generation," Intelligent Robots and Systems, 2001. Proceedings. 2001 IEEE/RSJ International Conference on, Maui, HI, 2001, pp. 239-246 vol.1.